



THESIS  
2  
(1996)



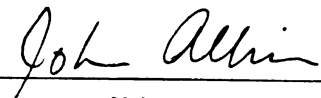
This is to certify that the  
thesis entitled  
A Study of the Gas Phase Ion-Molecule  
Chemistry of Glycerol

presented by

Guy Kirby Smith

has been accepted towards fulfillment  
of the requirements for

Masters degree in Chemistry

  
Major professor

Date 12-20-95

**LIBRARY**  
**Michigan State**  
**University**

**PLACE IN RETURN BOX to remove this checkout from your record.**  
**TO AVOID FINES return on or before date due.**

<b>DATE DUE</b>	<b>DATE DUE</b>	<b>DATE DUE</b>
_____	_____	_____
_____	_____	_____
_____	_____	_____
_____	_____	_____
_____	_____	_____
_____	_____	_____
_____	_____	_____

**MSU is An Affirmative Action/Equal Opportunity Institution**

c:\cir\datedue.pm3-p.1

**A STUDY OF THE GAS PHASE  
ION-MOLECULE CHEMISTRY  
OF GLYCEROL**

**BY GUY KIRBY SMITH**

**A THESIS**

**Submitted to  
Michigan State University  
in partial fulfillment of the requirement  
for the degree of**

**MASTER OF SCIENCE**

**Department of Chemistry**

**1995**

## **ABSTRACT**

### **A STUDY OF THE GAS PHASE ION-MOLECULE CHEMISTRY OF GLYCEROL**

**By**

**Guy K. Smith**

In an effort to understand the origin and formation of the background ion detected in Fast Atom Bombardment mass spectrometry, a study of the gas phase ion-molecule chemistry of glycerol was completed. The ion-molecule reactions of both the positive and negative ions of glycerol with neutral glycerol were determined. The studies were conducted using the technique of Ion Cyclotron Resonance mass spectrometry.

The existence of gas phase glycerol dimers was proven. The evidence for even larger gas phase glycerol clusters is examined. The dominant ion-molecule reactions found for the fragment ions of glycerol are the formation of a fragment ion-glycerol cluster. Some of the fragment ion-glycerol clusters cluster with an additional glycerol. The studies of the negative ions of glycerol confirm these results.

Several ion-molecule reactions for both the positive ions and negative ions of glycerol were detected. The fragmentation mechanisms of both the positive ions and the negative ions of glycerol are proposed.

## **DEDICATION**

**This Thesis is dedicated to my mother, Annabelle Cherry Smith, for only her continual support has made this long journey possible. She gave me the courage and ambition to persevere.**

## **ACKNOWLEDGMENTS**

I would like to extend a very special thanks to Dr. John Allison for all his guidance, time and especially his patience. The experience that I have gained in the Allison group is a useful resource that I will use to further my academic and professional careers.

I would also like to thank Dr. Ledford, Dr. Pinnivia, Dr. Jackson and Dr. Stille for serving on my committee. Their comments were most helpful.

I would like to thank Marty Rabb, Ron Haas, Scott Sanderson, and Tom Clark for their invaluable assistance in completing this research. I would also like to thank Russell Geyer, Dick Minke and Sam Jackson for making this research possible.

The Ion Cyclotron Resonance Mass Spectrometer, "Bruno", is still working.

# TABLE OF CONTENTS

	<b>Page #</b>
<b>List of Tables</b>	vii
<b>List of Figures</b>	viii
<b>Chapter One: Fast Atom Bombardment</b>	1
Introduction	1
The Mechanisms of Ion Formation in FAB	4
FAB Studies of Glycerol	15
References	25
<b>Chapter Two: The Results of the Positive Ion Studies of Glycerol</b>	27
Proof of the Existence of Glycerol Dimers	32
Evidence for the Existence of Gas Phase Glycerol Clusters	33
The Source of the Glycerol Clusters	36
The Origin, Structure and Chemistry of the Fragment Ions of Glycerol	38
The High Mass Ions of Glycerol	47
Proton Transfers from the Fragment Ions	55
Conclusions	57
References	59
<b>Chapter Three: The Studies of the Negative Ions of Glycerol</b>	61
The Formation of the Negative Ions	61
The Negative Ion ICR Mass Spectrum of Glycerol	63
A Comparison of the Negative Ion Mass Spectra of Glycerol and Ethylene Glycol	67

The High Mass Anions of Glycerol	71
The Evidence for the Existence of Glycerol Clusters	73
A Comparison of FAB and EI Mass Spectra of Glycerol	74
Mass-to-Charge Ratio Verification	75
References	76
<b>Chapter Four: The Experimental Section</b>	<b>77</b>
The Theory of Ion Cyclotron Resonance Spectrometry	77
Introduction	77
Ion Motion in an ICR	78
Ions in Resonance	82
Double Resonance Experiments	83
The Marginal Oscillator	85
Chemicals used in the Experiments	88
References	89
<b>Chapter Five: The Appendix</b>	<b>90</b>
Detailed Description of the ICR components	90
The Procedure for a Typical ICR Experiment with Glycerol	94
Positive Ion Spectra	94
Negative Ion Spectra	95

## LIST OF TABLES

<b>Chapter One: The Introduction</b>	<b>Page #</b>
Table 1.1: Molecular Weights of Compounds Produced from Glycerol by Ar Atom Bombardment	18
 <b>Chapter Two: The Results of the Positive Ion Studies of Glycerol</b>	
Table 2.1: The Relative Intensities of the Low Mass Positive Ions of Glycerol	29
Table 2.2: The Positive Ions of Glycerol and Glycerol-d <sub>5</sub>	30
Table 2.3: Relative Intensities of the ICR Spectra of Glycerol	36
Table 2.4: The High Mass Ions in the ICR Mass Spectrum of Glycerol	53
 <b>Chapter Three: The Studies of the Negative Ions of Glycerol</b>	
Table 3.1: The Compositions of the Fragment Anions of Glycerol	63

## LIST OF FIGURES

<b>Chapter One: Fast Atom Bombardment</b>	<b>Page #</b>
Figure 1.1- The Sputtering of Glycerol by Fast Ar Atom Bombardment	3
Figure 1.2- A Schematic Diagram of the Fast Atom Gun on the JEOL HX-110	5
Figure 1.3- The FAB Mass Spectrum of Tryglycine (MW of 189) Dissolved in a Glycerol Matrix	7
Figure 1.4- The Glycerol-Vacuum Interface	8
Figure 1.5- a) The Gas Phase FAB Spectrum of Glycerol b) The EI Spectrum of Glycerol at 70 eV c) The Partial FAB Spectrum of Glycerol	11
Figure 1.6- A Comparison of the OH <sup>-</sup> Negative Chemical Ionization Mass Spectra of Irradiated and Unirradiated Glycerol	17
Figure 1.7- The Neutral Compounds Formed by the Coupling of Glycerol Derived Free Radicals	20
Figure 1.8- The FAB Spectra of Glycerol Taken at 1 Minute Intervals Until All of the Glycerol is Consumed	23
<b>Chapter Two: The Results of the Positive Ion Studies of Glycerol</b>	
Figure 2.1- A Comparison of the ICR Mass Spectrum with an EI Mass Spectrum of Glycerol	28
Figure 2.2- The Proton Transferred Structures of the Methanol Dimer: Computer drawings of the calculated equilibrium geometries of the ionized methanol dimers at MP2/6-31G**	34
Figure 2.3- A Comparison of the ICR Mass Spectrum with the Glycerol Sample in a Capillary Tube vs. Glycerol Evaporated from the ICR Cell Walls	37
Figure 2.4- The Fragmentation Pathways of the Protonated Glycerol Molecule	39
Figure 2.5- The Dehydration of Protonated Glycerol	40
Figure 2.6- The Possible Structures of the C <sub>3</sub> H <sub>7</sub> O <sub>2</sub> <sup>+</sup> Ion	41

Figure 2.7- The Possible Structures of the $C_3H_5O^+$ Ion	43
Figure 2.8- The Structures of the $C_2H_5O^+$ Ion	45
Figure 2.9- The Structures of the $C_2H_3O^+$ Ion	46
Figure 2.10- The Fragmentation of Glycerol by Alpha Cleavage	48
Figure 2.11- The Formation of the $C_2H_3O^+$ Ion from the $C_2H_5O_2^+$ Ion	49
Figure 2.12- The Formation Mechanisms for the $m/z = 62$ and 74 Ions	50
Figure 2.13- Two Formation Mechanisms for the $m/z = 44$ Ion	51
Figure 2.14- The High Mass Ions of Glycerol	52
Figure 2.15- The Relative Intensity of the Cluster Ions of Methanol vs. $n$ , the number of Methanols in the Cluster	58
<b>Chapter Three: The Negative Ion Studies of Glycerol</b>	
Figure 3.1- The Low Mass Anions of Glycerol	64
Figure 3.2- Proposed Structures for the $(C_3H_5O_3)^-$ Ions	66
Figure 3.3- The Proposed Concerted Loss Fragmentation Mechanism	68
Figure 3.4- The Proposed Formation Mechanism for the $m/z = 47$ Anion	69
Figure 3.5- The Formation Mechanism of the $m/z = 45$ Ion	70
Figure 3.6- The High Mass Anions of Glycerol	72
<b>Chapter 4: The Experimental Section</b>	
Figure 4.1- The Path of a Positive Ion in a Uniform Magnetic Field	78
Figure 4.2- The ICR Cell	80
Figure 4.3- The Cycloidal Path of a Drifting Ion in the ICR Cell	81
Figure 4.4- Ion in Resonance in the ICR Cell	83
Figure 4.5- A Typical ICR Double Resonance Spectrum	84

<b>Figure 4.6- The Equivalent Circuit of the LC Tank Circuit used in the Marginal Oscillator Detector</b>	<b>85</b>
<b>Figure 4.7- Block Diagram of the Marginal Oscillator</b>	<b>86</b>
<b>Figure 4.8- The Block Diagram of the Ion Cyclotron Resonance Spectrometer at Michigan State University</b>	<b>87</b>
<b>Chapter Five: The Appendix</b>	
<b>Figure 5.1- The Sample Inlet to the ICR</b>	<b>94</b>

# **Chapter One:**

## **Fast Atom Bombardment**

### **Introduction**

Sputtering is a phenomenon that can be used to generate gas phase ions from solids. Sputtering was first reported by Grove in 1853.<sup>1</sup> Grove observed that gaseous ions eroded the cathode in a gas discharge source. J. J. Thomson observed sputtering in 1910.<sup>2</sup> Thomson experimented with "Kanalstrahlen" (an ion beam) striking a metal plate. Secondary rays (ions and particles) were emitted in all directions. Only a small fraction of the secondary rays were charged. The sputtering phenomenon can be simply described. When a solid is bombarded by high energy (2-10 kilo electron volts (KeV)) particles some of the solid is vaporized.<sup>3</sup> A small fraction (approximately 1%) of the vaporized material appears is in the form of positive and negative ions.<sup>4</sup>

When sputtering is mated with analysis of the secondary ions by mass spectrometry, the method of analysis is called Secondary Ion Mass Spectrometry (SIMS). The SIMS technique is used to analyze the surfaces of solids. SIMS can also be used to analyze non-volatile organic compounds. The organic analyte is applied as a monolayer to a metal target.<sup>5</sup> The monolayer is bombarded with fast ions and a mass spectrum is obtained. Since the sample exists as a monolayer, only approximately  $1 \times 10^{12}$  molecules can be deposited in the area bombarded by the ion beam.<sup>5</sup> The small number of molecules in the target area results in a short sample lifetime. Sample lifetimes as short as several seconds have been reported.<sup>3</sup> Reducing the current of the bombarding

ions improves the sample lifetime but a reduction in ion intensity results. The application of SIMS to solid organic analytes is called Organic or Molecular SIMS.

The sputtering phenomenon depends on the transfer of momentum from the impinging particle to the atoms of the solid. The impact of the fast ion causes a collision cascade which desorbs atoms and ions from the solid analyte. See Figure 1.1. The beam of fast argon atoms (Ar) strikes the glycerol (G) matrix ejecting neutral glycerol molecules, protonated glycerol molecules  $(G+H)^+$  and fragment ions from glycerol ( $G_F^+$ ). The sputtering yield is the number of molecules sputtered per incident particle. The sputtering yield generally increases with the energy and mass of the bombarding atoms or ions.<sup>4</sup> The sputtering yield is also a function of the angle of incidence.<sup>4</sup> Since the energy and angle of incidence of the bombarding particles can be controlled, a focused beam of particles can be used to probe the surface composition of a solid.

A fast neutral atom impinging on a solid analyte can also sputter ions into the gas phase.<sup>4</sup> The advantage to using fast atoms instead of fast ions is that the possibility of charging of the solid analyte is eliminated. Charging of the analyte can interfere with the collection of the sputtered ions by distorting the electric fields in the source of a sector mass spectrometer. Fast atoms are also not slowed or deflected by the electric fields in the source of any mass spectrometer.<sup>4</sup>

During Organic SIMS experiments, Barber et al.<sup>3</sup> observed that low vapor pressure oils and liquids (pumping fluids, Apiezon oils, Santovac 5, Convalex 10 and siloxanes) gave SIMS spectra which lasted for hours. These low vapor pressure liquids were common contaminants detected in Organic SIMS.<sup>3</sup> These observations led to the idea of using low vapor pressure viscous fluids as solvents in solutions of nonvolatile organic molecules. The solutions were found to give long lasting and stable SIMS spectra.<sup>3</sup>

Barber et al.<sup>3</sup> dissolved the analytes in glycerol. These glycerol-analyte solutions were applied to a metal target and bombarded with fast atoms.<sup>3</sup> The fast atoms deposit

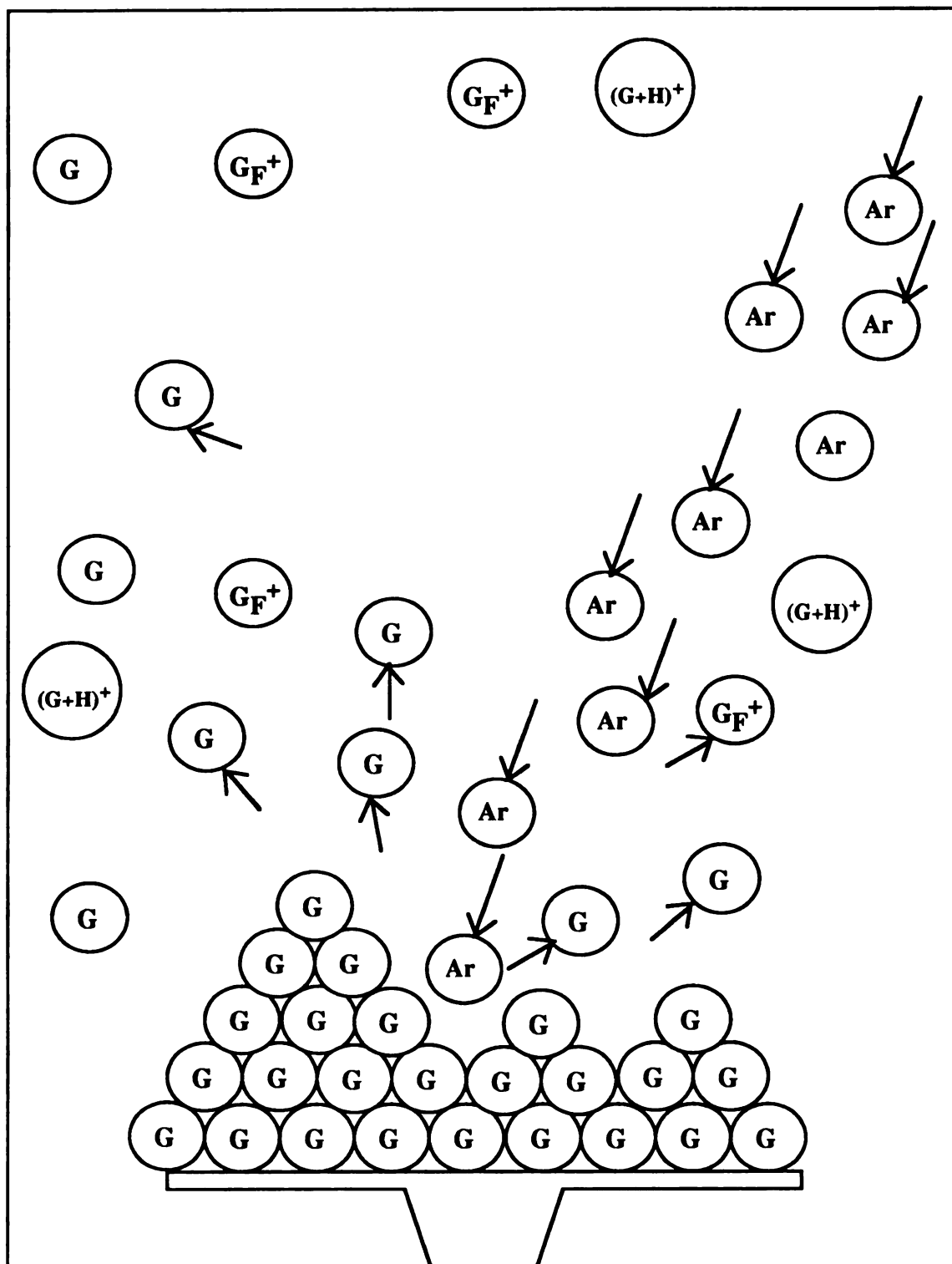


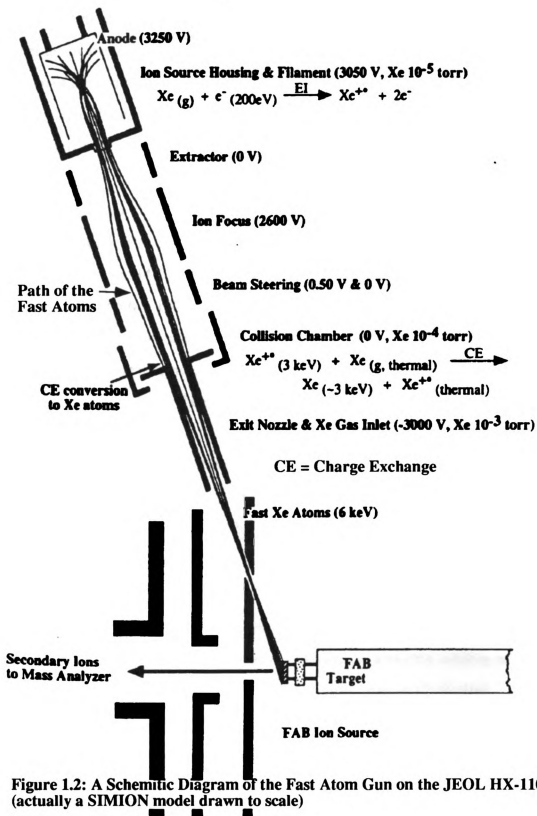
**Figure 1.1: The Sputtering of Glycerol by Fast Ar Atom Bombardment**

their energy initially in the glycerol matrix since the impacting atom is much more likely to strike glycerol molecules than analyte molecules. The energy is then transferred to the dissolved analyte by collision between the glycerol and the analyte molecules. The ions generated from the analyte-glycerol solution include protonated analyte molecules and some fragment ions from the analyte. These ions can be detected for a much longer time than the ions from a pure analyte monolayer. In this document, fast atom bombardment (FAB) is defined as the bombardment of a liquid sample by fast atoms. Glycerol is the most commonly used matrix in fast atom bombardment.

Glycerol has several properties that make it an excellent FAB matrix. The ability of glycerol to dissolve many polar organic analytes is its first useful property. If the analyte is not dissolved in the FAB matrix, few analyte ions are observed.<sup>6</sup> The second useful property of glycerol is its low vapor pressure. Glycerol does not evaporate rapidly in a vacuum. The vapor pressure of glycerol at room temperature is approximately one millitorr.<sup>7</sup> The high viscosity of glycerol helps prevent the glycerol solution from draining from the metal target. Glycerol has a dielectric constant of 42.5 Debyes.<sup>8</sup> This dielectric constant is large enough to completely dissolve 1:1 electrolytes and gives glycerol similar acid-base chemistry to that of water.<sup>9</sup> This allows the pH of the glycerol-analyte solution to be manipulated to enhance FAB's sensitivity for certain analytes. The last important property of glycerol is its low reactivity with the analyte molecules. This property assures that the FAB mass spectra contains mostly ions from the glycerol and the analyte with as few ions from reaction products as possible.

### **The Mechanisms of Ion Formation in FAB**

Figure 1.2 is a diagram of a typical fast atom bombardment source.<sup>6</sup> The fast atoms exit the FAB gun with a kinetic energy of 2 to 10 KeV and impact the glycerol and analyte solution that is applied to the stainless steel target. The heavier noble gases



(argon and xenon) are the fast atoms typically used. The heavier the bombarding atom, the higher the momentum of the atom becomes. The sputtering yield increases as the momentum of the bombarding atom becomes larger. The fast atom beam impacts the target at an angle of approximately 64 degrees from the normal.<sup>10</sup> This angle allows more of the secondary ions generated in the source to be detected by the mass spectrometer.

A typical liquid SIMS (FAB) spectrum of a low molecular weight analyte is shown in Figure 1.3.<sup>6</sup> The fragment ions of the triglycine analyte are detected at  $m/z = 30, 76, 87, 115, 133$  and  $145$ . The protonated triglycine molecule (triglycine has a MW of 189) is detected at  $m/z = 190$ . The molecular ion of triglycine is not very abundant. Ions from the glycerol matrix are detected at nearly every  $m/z$  value. The more intense ions from the glycerol matrix are the fragment ions at  $m/z = 45, 57$  and  $75$ , the protonated glycerol molecule ( $m/z = 93$ ) and the proton bound glycerol dimer ( $m/z = 185$ ).

The basic question to be answered for fast atom bombardment is **"Where and how are the secondary ions detected in the FAB experiments formed?"** The wide variety of analytes and matrices that can be used in FAB tends to confuse the answer to the question. The exact mechanisms of the formation of the secondary ions is not known. In many FAB experiments, the secondary ions may be formed by several distinct mechanisms.

Figure 1.4 shows the glycerol solution on a metal target being bombarded by the fast atom beam. The fast atoms pass through a gaseous layer above the solution before impacting the glycerol-analyte mixture. This gaseous layer consists of glycerol molecules evaporating from the surface of the solution as well as glycerol molecules desorbed into the gas phase by the impact of the fast atoms. The solution is a mixture of the glycerol matrix and the analyte and is much thicker than a monolayer.<sup>9</sup> The solution layer may be more than 100 angstroms thick.<sup>9</sup> The matrix and analyte molecules are

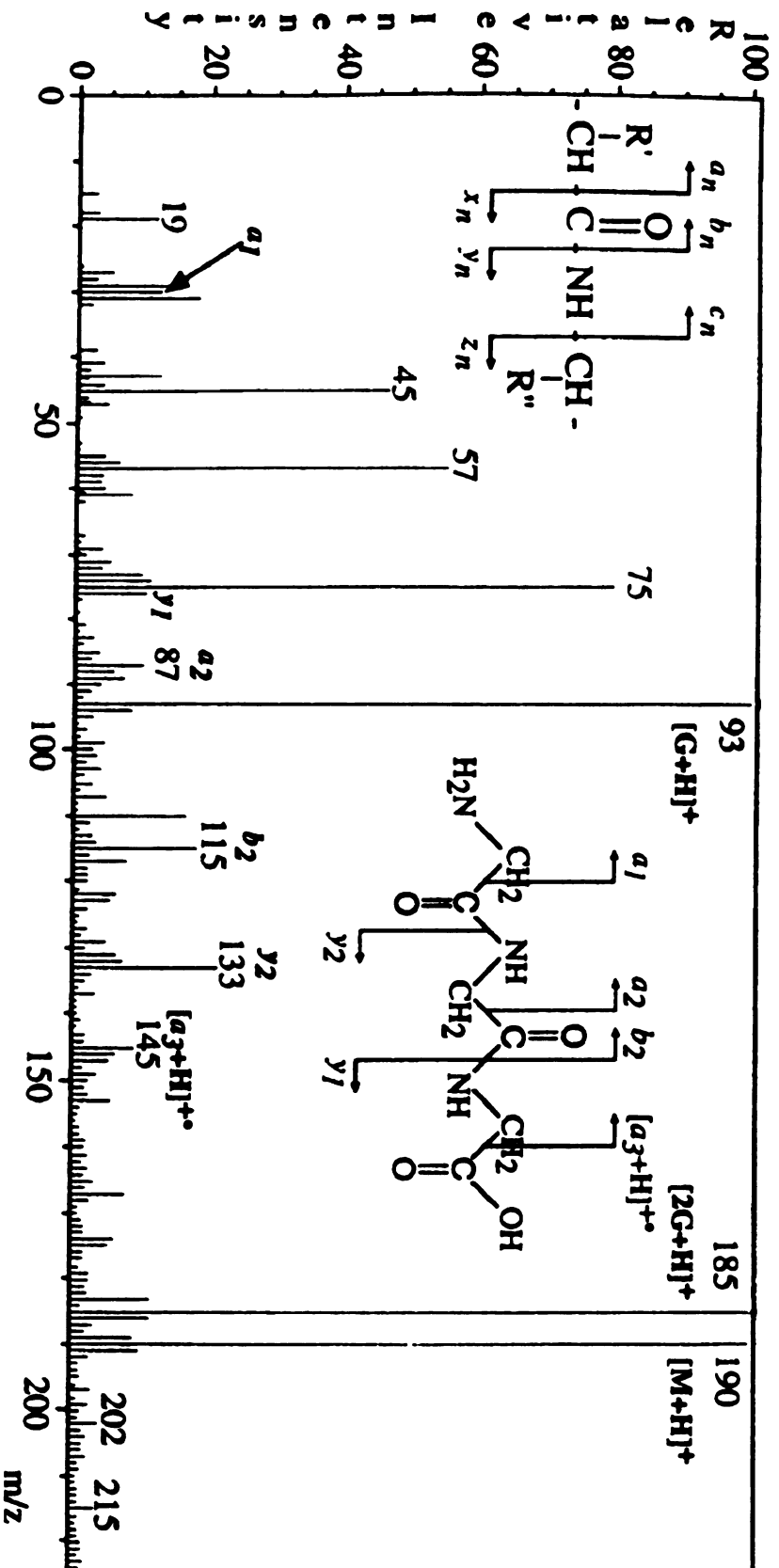
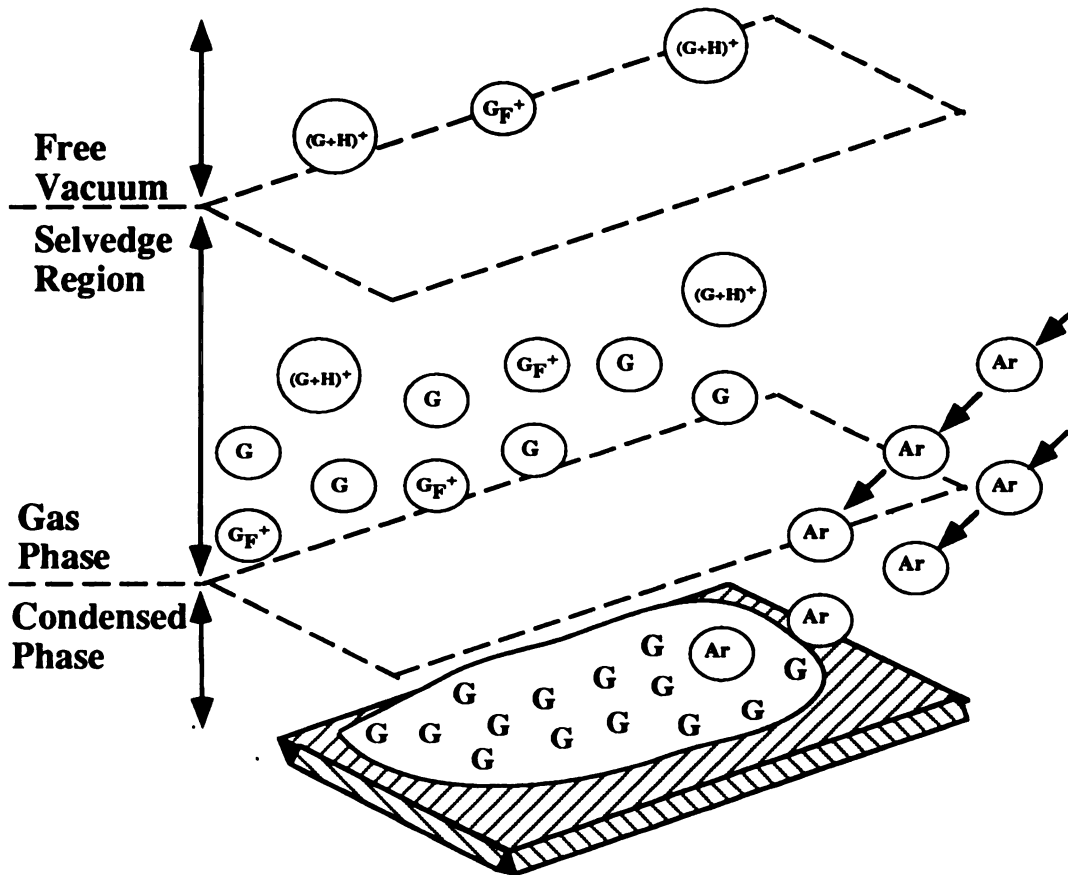


Figure 1.3: The FAB Mass Spectrum of Triglycine (MW of 189) Dissolved in a Glycerol Matrix



**Figure 1.4: The Glycerol-Vacuum Interface**

desorbed into the gas phase by the impact and the heating of the solution as the energy of the fast atom is dissipated. The ions formed are detected by the mass spectrometer.

It is generally accepted that three distinct types of molecular ions can be produced by particle bombardment of molecules at interfaces.<sup>11</sup> The first type of molecular ions result from direct desorption of precharged compounds. The second type of molecular ions are the even electron ions formed by the clustering of the analyte molecules with inorganic cations and anions. The last type of molecular ions are radical cations and anions. In addition to the molecular ions formed in FAB, fragment ions of the analyte and the matrix are also generated.

The ions generated by FAB could be formed by one or by a combination of up to four basic mechanisms. The first possible mechanism is the ionization of gas phase molecules directly by the impact of the fast atoms. The fast atoms exit the gun and first pass through a gaseous region above the glycerol-analyte solution as shown in Figure 1.4. Fast atoms with energies of up to 10 KeV possess sufficient energy to ionize and even fragment neutral molecules. The ionization step is shown in Equation 1. Morelas<sup>12</sup> measured the cross section for the ionization of glycerol by 10 KeV xenon atoms to be 20 Å<sup>2</sup>.



The large cross section for the ionization of glycerol leads to the conclusion that gas phase ionization is surprisingly efficient<sup>9</sup>. However, the ionization of gas phase neutral molecules is not the dominant mechanism of ion formation in FAB.

The vapor pressure of glycerol at 25 °C is approximately one millitorr. This pressure is 100 to 1000 times the pressure of the FAB source. In addition to the evaporating glycerol more glycerol is added to the gaseous layer by the impact of the fast atoms. Each fast atom that impacts the solution is estimated to add 1000 glycerol and

analyte molecules to the gas phase.<sup>13</sup> The gas pressure above the solution of a typical open FAB source has been estimated to be  $10^{-5}$  to  $10^{-4}$  torr.<sup>9</sup> Despite the efficient ionization of the gas phase molecules it is probable that most of the ions detected in FAB are not formed in the gas phase. The gas phase glycerol has approximately  $3.2 \times 10^{12}$  molecules/cm<sup>3</sup> versus the  $8.25 \times 10^{21}$  molecules/cm<sup>3</sup> of the liquid phase.<sup>14</sup> The high energy fast atoms are also efficient in ionizing molecules in the liquid phase.<sup>9</sup> Assuming the ionization efficiencies are equal in the gas phase and the liquid phase a fast atom would have to travel through 10 meters of the gas phase to have an equal number of collisions as occur in a 100 Angstrom path in the liquid phase. Experimental evidence for the gas phase ionization not being the dominant mechanism in FAB comes from comparing the FAB spectra of gaseous glycerol to the FAB spectra generated by bombarding neat glycerol. Bojeson et al.<sup>15</sup> ionized gas phase glycerol using a fast atom beam that did not strike any liquid glycerol. The FAB spectrum of gas phase glycerol is shown in Figure 1.5.<sup>15</sup>

The gas phase FAB mass spectrum of glycerol has the base peak representing the  $m/z = 61$  ion. The gas phase FAB spectrum of glycerol resembles its electron impact mass spectrum. The  $m/z = 61$  ion has low relative intensity in the FAB spectrum of liquid glycerol. The  $m/z = 93$  (G+H)<sup>+</sup> ion makes up the base peak in the FAB spectra of liquid glycerol and ions consisting of (G<sub>n</sub>+H)<sup>+</sup> can be detected for n values as large as 15 or more.<sup>3</sup> The peak representing the  $m/z = 93$  ion has a low relative intensity in the gas phase FAB spectrum of glycerol. Most of the ions formed in FAB do not originate from direct gas phase ionization.<sup>9</sup>

A second possible mechanism is that the ions exist in the glycerol and analyte solution and are merely desorbed into the gas phase by the impact of the fast atoms. In this mechanism the fast atoms merely supply the energy needed to desorb the ions into the gas phase. Evidence in support of this mechanism is found in the FAB spectra of

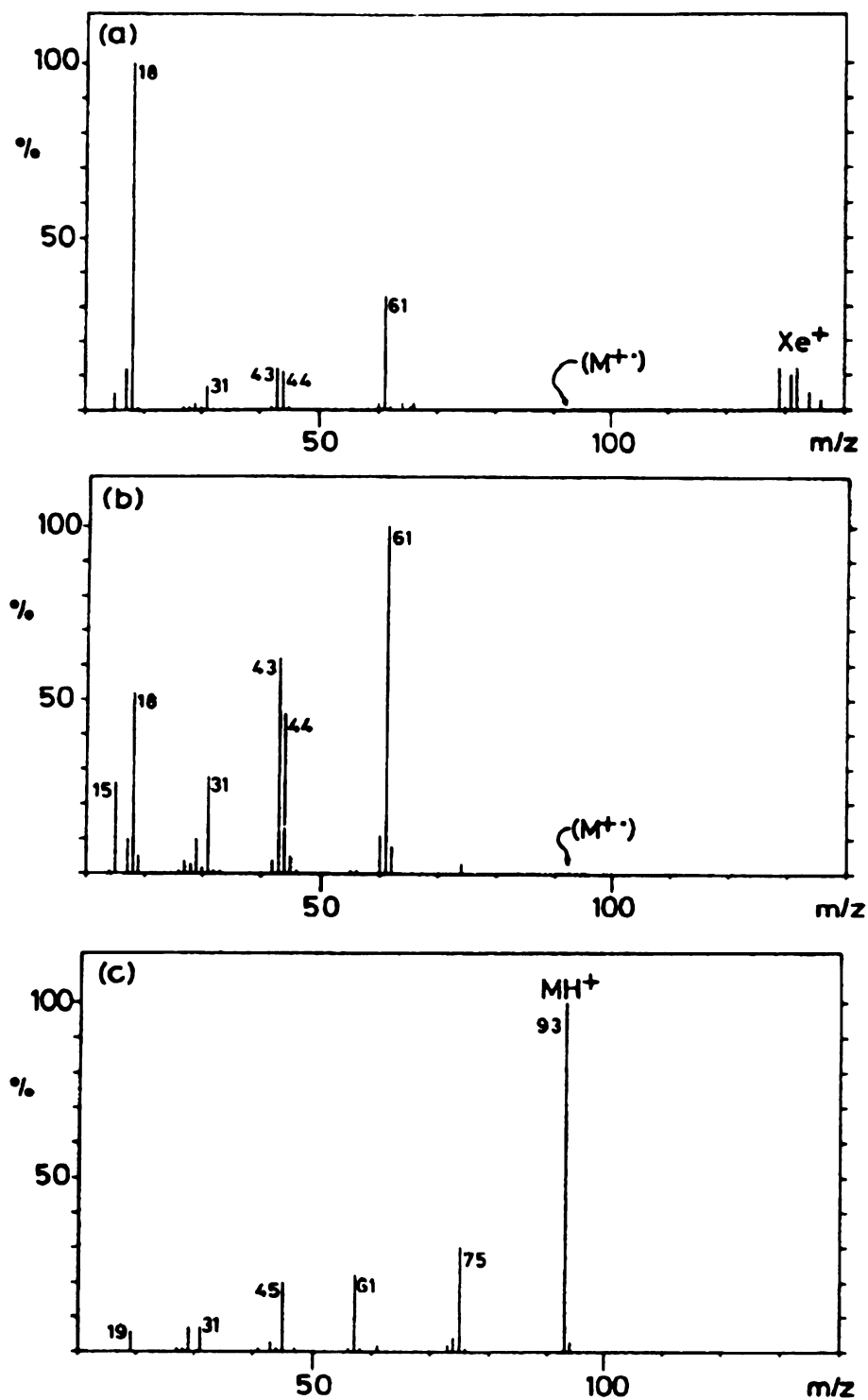


**Figure 1.5: a) The Gas Phase FAB Spectrum of Glycerol  
b) The EI Spectrum of Glycerol at 70 eV  
c) The Partial FAB Spectrum of Glycerol**

salt-glycerol mixtures. In the case of sodium chloride, sodium ions are detected in positive ion FAB spectra and chloride anions are detected in negative ion FAB spectra.<sup>16</sup>

Glycerol has a dielectric constant of 42.5 Debyes. The dielectric constant of glycerol is high enough to completely dissociate 1:1 electrolytes.<sup>8</sup> Sodium chloride is completely dissociated in the glycerol matrix. If the sodium chloride is completely dissociated, then the sodium cations and chloride anions that are detected in the FAB experiment are not formed by the fast atoms impacting solid sodium chloride. The ions are desorbed from the solution by the impact of the fast atoms.

The addition of acids to the glycerol matrix is a common method to improve the quality of the FAB mass spectra of polypeptides. The basic principle is to increase the concentration of protonated polypeptides in solution so that more protonated molecules  $(M+H)^+$  would be desorbed by the fast atoms' impacts. However the increase in the relative intensity of the protonated polypeptide ions,  $(M+H)^+$ , detected in the FAB spectra is often small.<sup>17</sup>

If the preexisting ions in the solution are desorbed directly into the gas phase in FAB, the addition of a salt or an acid to the matrix should increase the total ion current of the mass spectra. Sunner et al.<sup>18</sup> found that the addition of salts and HCl to the glycerol matrix did not increase the total ion current. The salts and HCl added did change the relative intensities of the ions such as protonated glycerol  $(G+H)^+$  and sodiated glycerol  $(G+Na)^+$  that are detected. Sunner attributes the lack of an increase in the total ion current to three effects.<sup>18</sup> The ion/ion recombination in the gas phase may limit the total number of ions reaching the mass spectrometer. As the number of ions desorbed increases the ion/ ion recombination may become more efficient. A second effect is caused by the solvation shell of glycerol molecules around the charged species. The solvation shell reduces the concentration of the charged species near the solution/vacuum interface. This redistributes the analyte ions deeper into the matrix. The third effect is the increase in the matrix's surface tension as the glycerol evaporates. Kriger et al.<sup>19</sup>

demonstrated the increased surface tension causes an efficient transport of ions away from the area of the solution being irradiated.

The detection of protonated or sodiated molecules in the FAB spectrum of an acid or salt containing solution does not prove that the ions are desorbed from the solution. The FAB spectrum of NaCl solutions contains peaks representing sodium cations and chloride anions. These sodium cations could form sodiated molecules by gas phase ion-molecule reactions with the neutral molecules.

Preexisting ions may be readily desorbed for analytes such as salts or organic acids. However, the FAB spectrum of glycerol contains lower mass ions with  $m/z$  values of 31, 45, 61 and 75, in addition to the protonated glycerol molecule ( $m/z = 93$ ).<sup>15</sup> The lower mass ions detected in the FAB spectrum of glycerol are not ions that are known to exist in liquid glycerol. Some of the low mass ions detected in the FAB spectrum of glycerol are fragment ions detected in the EI mass spectrum of glycerol. Most of the ions detected in the FAB spectra of glycerol are not preexisting ions directly desorbed from the liquid glycerol.

The third possible mechanism in FAB ionization is that the ions are formed in and then desorbed from the liquid phase by the impact of the fast atoms. The impact of the fast atom on the solution causes a "collision cascade" which desorbs many neutral molecules into the gas phase. The impact of the fast atoms forms the ions directly in the collision cascade where the ions are immediately desorbed.

When a fast atom strikes the glycerol, the momentum is transferred from the fast atom to the glycerol molecules. A series of violent collisions between the fast atom and the glycerol molecules along the impact track form a collision cascade. The collision cascade is shown in Figure 1.1. The momentum transfer is so great that up to 1000 neutral glycerol molecules are ejected into the gas phase per fast atom impact.<sup>20</sup> The vast majority of glycerol molecules ejected are intact and neutral. However, ions and fragment ions of glycerol are also formed in the collision cascade.

Most of the ions initially formed in FAB are formed in the liquid phase due to the high number density of liquid glycerol ( $8.25 \times 10^{21}$  molecules/cm.<sup>3</sup>). The ionization cross sections for gas phase and liquid phase glycerol by fast atoms are not significantly different.<sup>9</sup> Fast atoms, with kinetic energies of up to 10 KeV, are capable of ionizing neutrals in condensed phases.

Ions formed in the glycerol liquid are desorbed into the "selvedge" region above the surface. Ion-molecule reactions in the gaseous "selvedge" region modify the ions detected in the FAB spectra.

The nature of the interface between the glycerol and the vacuum is not clear. The initial collision cascade releases neutral molecules into the gas phase creating a localized high pressure gas region called the "selvedge" region.<sup>9</sup> The density change in the selvedge region could be very sharp as in conventional liquid/gas interfaces or could be a more gradual change. One model of the FAB selvedge is that the ions are initially formed and desorbed in the collision cascade. These ions are both the fragment ions and the molecular ions. The glycerol molecules are then desorbed more gradually by a near thermal process of evaporation. The selvedge region cools rapidly due to the energy required to break the hydrogen bonds between the glycerol molecules before the glycerol molecules can evaporate. Heat is also conducted away into the matrix. The ions that are already desorbed form clusters with the gas phase neutral molecules. The extent of gas phase ion-molecule chemistry that occurs in the selvedge region remains to be determined.

Experimental support for the occurrence of ion-molecule reactions in FAB is that some analytes with gas phase proton affinities lower than the matrix do not have a protonated molecule in their positive ion FAB spectrum. A good example is the lack of a protonated molecule,  $(M+H)^+$ , in the FAB spectra of monosaccharides in diethanolamine and triethanolamine matrices.<sup>21</sup> This effect can be so pronounced as to eliminate the protonated molecule of an only slightly less basic analyte in a glycerol matrix. An

example of this is the FAB spectrum of a cyclic monosaccharide in glycerol. The protonated molecule of the cyclic monosaccharide  $(M+H)^+$  cannot be detected even though the gas phase basicities of glycerol and the cyclic monosaccharide are very similar.<sup>22</sup> The gas phase basicities, not the liquid phase basicities, determines how easily each of the compounds in the mixture are detected as a protonated molecule.

If gas phase ion-molecule reactions are the source of the ions detected in FAB, the fragment ions should protonate the neutral molecules. The dominant positive ions detected in FAB are the protonated glycerol and protonated analyte molecules. Some of the fragment ions must have a lower proton affinity than the glycerol and so react to form the  $(G+H)^+$  ion. The analytes which can be detected as a protonated molecule  $(M+H)^+$  will have proton affinities that are greater than that of the fragment ions. These ideas explain why some analytes with proton affinities lower than that of glycerol have a strong protonated molecule in their positive ion FAB spectra.

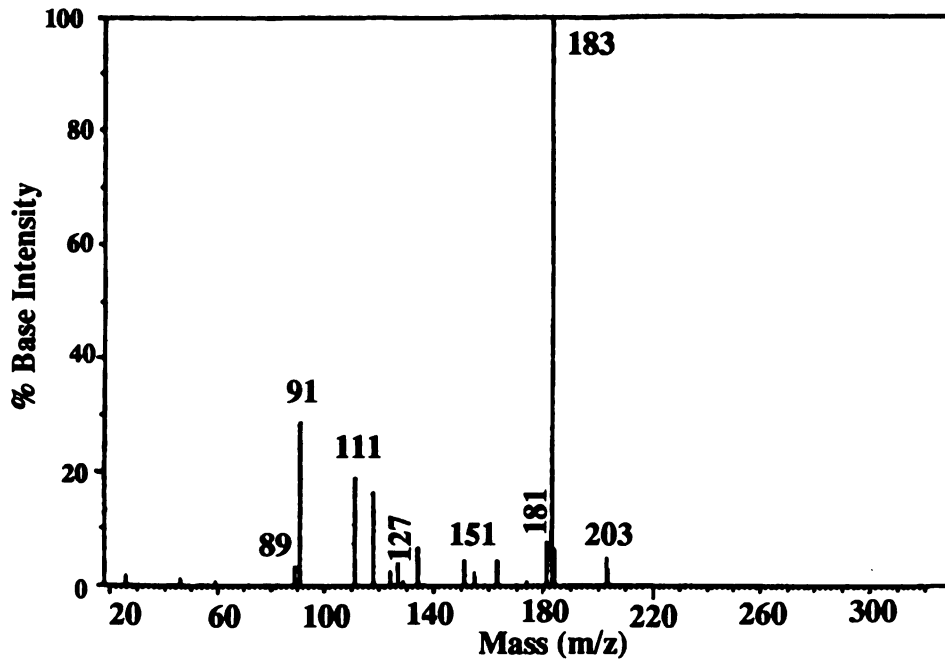
The fast atom bombardment mass spectrometry of some crown ethers determined that the relative intensity of the peak representing the  $(M+H)^+$  ion depends on the source pressure.<sup>23</sup> The  $(M+H)^+$  ions pressure dependence is a property of an ion formed in an ion-molecule reaction. The experimental evidence is strong for ion-molecule reactions modifying the ions detected in FAB.

## FAB Studies of Glycerol

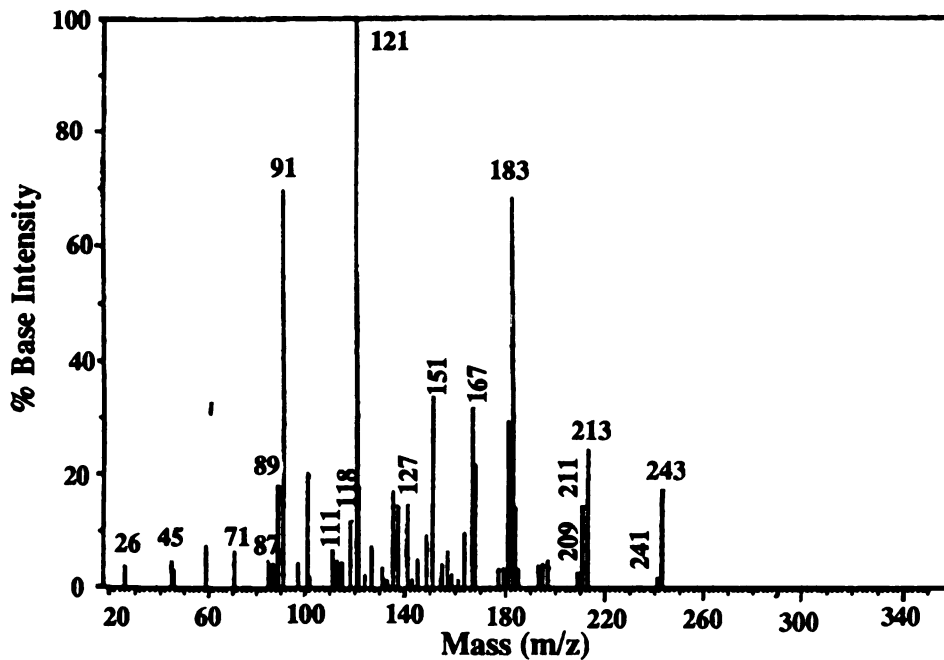
F. H. Field performed a FAB experiment in which pure glycerol was bombarded with 5 KeV positive Ar fast atoms until the glycerol sample was completely consumed.<sup>24</sup> As the time of irradiation increases, the  $(G_n+H)^+$  ions disappear and a new set of ions is detected. After all of the glycerol was consumed, a semisolid mass with crystalline material immersed in a clear liquid remained on the probe tip. Field explained his results

as a combination of glycerol evaporation which is accelerated by the fast atom bombardment and a change in the chemical composition of the glycerol.

The irradiated glycerol was dissolved in water and a Negative Ion Chemical Ionization (NICI) study using  $\text{OH}^-$  ions as the reagent ions was performed.<sup>24</sup> A comparison of the negative chemical ionization spectra of unirradiated glycerol and the irradiated glycerol is shown in Figure 1.6.<sup>24</sup> The much larger number of ions detected in NICI spectra of the irradiated glycerol indicates the presence of many compounds in addition to glycerol. Field compared the NICI mass spectra of unirradiated glycerol and irradiated glycerol to identify the new compounds. The anions with  $m/z$  values of 89, 111, 121, 127, 151, 167, 181, 197, 211, 213 and 243 are assigned by Field to be  $(\text{M}-\text{H})^-$  anions of new compounds. The NICI of most organic compounds (using  $\text{OH}^-$  as the reagent ion) forms  $(\text{M}-\text{H})^-$  anions. Field lists in Table 1.1 the molecular weights of the proposed compounds formed by the Ar fast atom bombardment of glycerol. A typical FAB mass spectra of glycerol was compared with ions the NICI mass spectra. The FAB mass spectra of compounds in a protic matrix contains peaks for the  $(\text{M}+\text{H})^+$  ions. Table 1.1 has a list of the  $(\text{M}+\text{H})^+$  ions detected in the FAB mass spectra of glycerol. These ions lend support to be view that fast atom bombardment produces new chemical species. Field attributes the formation to the new compounds in glycerol to radiation induced reactions which differ from both conventional radiation chemistry and hot atom chemistry.<sup>24</sup>



OH<sup>-</sup> NICI Mass Spectrum of Unirradiated Glycerol



OH<sup>-</sup> NICI Mass Spectrum of Irradiated Glycerol  
(11.8 Min. irradiation)

Figure 1.6: A Comparison of the OH<sup>-</sup> Negative Chemical Ionization Mass Spectrum of Irradiated and Unirradiated Glycerol

**Table 1.1: Molecular Weights of Compounds Produced from Glycerol by Ar Atom Bombardment**

FAB (M+H) <sup>+</sup>	MW (M)	OH <sup>-</sup> NICI (M-H) <sup>-</sup>
	90	89
113	112	111
123	122	121
129	128	127
153	152	151
	168	167
183	182	181
	198	197
	212	211
	214	213
	244	243

The FAB spectrum of pure glycerol contains ions at nearly every mass up to and beyond 2000 Daltons.<sup>25</sup> These "background" ions may originate from products of radiation chemistry occurring in the matrix. The impact of very high energy (10 MeV) particles and ions with solids is known to ionize, fragment and to produce free radicals from the solid. Gross et al.<sup>25</sup> postulate that fast atoms with energies of up to 10 KeV are energetic enough to cause reactions in the glycerol matrix similar to those observed in solids in the radiation chemistry of high energy particles and ions.

Gross et al.<sup>25</sup> studied the origin and structure of these glycerol-derived "background" ions using tandem mass spectrometry. Gross et al. group the "background" ions into four categories by the ions' origin. These categories are: (1) matrix-derived free radical coupling products, (2) thermal decomposition products of the coupling products, (3) small neutral molecules formed by addition of or loss of a H atom by a free radical, and (4) aggregates of glycerol with the preceding 3 categories of products. The ions detected include protonated (positive) ions or deprotonated (negative) ions formed from the neutral products of the radiation chemistry.

During fast atom bombardment, free radicals are formed from glycerol molecules. The large amount of momentum transferred to the radicals in their formation prevents their immediate recombination.<sup>25</sup> These free radicals couple with other free radicals to form new covalent molecules (See Figure 1.7). The newly-formed covalent molecules may lose neutral groups such as H<sub>2</sub>O, H<sub>2</sub>CO or CH<sub>3</sub>OH. Formaldehyde has been detected in the FAB spectrum of glycerol.<sup>26</sup> The loss of water, formaldehyde and methanol from heavier free radical coupling products generate molecules of intermediate molecular weights. The protonation or deprotonation of the newly formed molecules can cause unimolecular rearrangements and condensation reactions. The protonated coupling products can also undergo condensation reactions with glycerol or can form proton bound clusters. The deprotonated (negative) ions cluster with glycerol and other polar molecules also. Gross et al.<sup>25</sup> postulate that the most abundant "background" ions detected in the FAB spectrum of glycerol are protonated or deprotonated free radical coupling products.

The radiation chemistry hypothesis can also explain the detection of background ions with masses as large as 2000 Daltons. The free radicals couple to form higher molecular weight molecules. These less volatile heavier molecules accumulate in the matrix over time. When a subsequent fast atom impact occurs, the heavier molecules may form radicals and couple to form even heavier molecules. It is also possible for the heavier molecules to be ionized, desorbed and detected.

The ions with intermediate masses (100 to 180 Daltons) detected in the FAB spectrum of glycerol are a challenge to the free radical coupling hypothesis. The free radicals formed from glycerol appear to be carbon centered.<sup>25</sup> Carbon centered free radicals are free radicals that have the site of the unpaired electron on a carbon atom. The carbon centered free radicals of glycerol have masses of 31, 61, 75 and 91 Daltons. The simple combinations of the possible carbon centered free radicals form neutrals with atomic Weights of 106, 122, 136, 152, 166 and 182. The neutrals become ions by

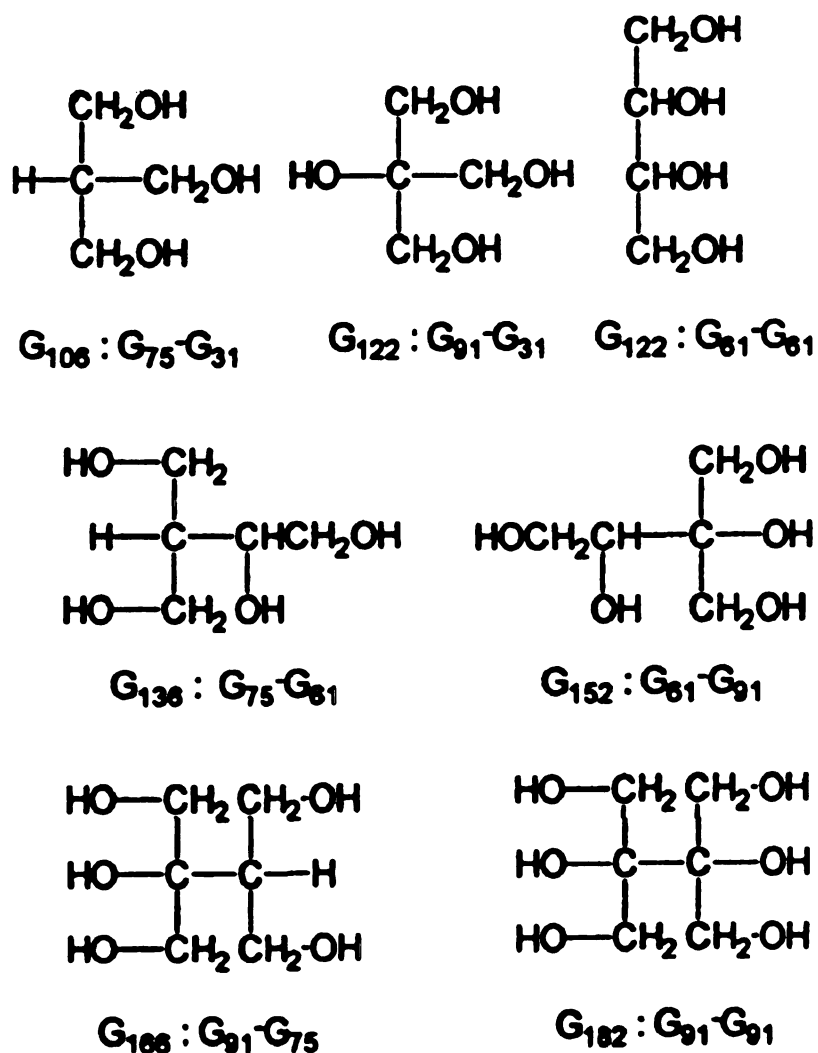


**Figure 1.7: The Neutral Compounds Formed By The Coupling of Glycerol Derived Free Radicals. The free radicals bonded to form each coupling product are listed under each structure.**

protonation or deprotonation. These intermediate mass ions are dehydrated with the possibility of subsequent water, formaldehyde and methanol losses. Gross et al.<sup>25</sup> postulated that the neutral losses are the source of the intermediate mass ions of between 100 and 180 Daltons. There are 24 positive ions of low abundance between 100 and 180 Daltons that are of unexplained origin using Gross et al.'s hypothesis. Though of low relative intensity in the mass spectra, these 24 ions are of similar relative intensity of many of the ions explained by Gross et al.'s hypothesis. The best example of an ion of unexplained origin is the  $m/z = 143$  positive ion. This ion could be formed from the free radicals coupling products of atomic weights of 152, 166 and 182. The loss of five  $H_2$  molecules from the protonated  $G_{152}$  molecule would be needed to form the  $m/z = 143$  ion. The most plausible route from the protonated  $G_{166}$  molecule to the  $m/z = 143$  ion is the loss of water followed by the loss of three  $H_2$  molecules. The protonated  $G_{182}$  molecule would need to lose two water molecules and two  $H_2$  molecules to form the  $m/z = 143$  ion. All of these possible formation routes from the free radical coupling products to the  $m/z = 143$  ion are ruled out by the reported composition of the  $m/z = 143$  ion. The  $m/z = 143$  ion has a composition of  $C_7H_{11}O_3$ . Gross et al.<sup>25</sup> did not publish a fragmentation mechanism for the formation of the  $m/z = 143$  ion. In addition, the positive ion with a 185 Daltons mass has the highest relative intensity in the mass spectra between 100 and 200 Daltons.<sup>25</sup> This ion  $(G_2+H)^+$  is not a protonated free radical coupling product.

A possible source of the  $(G_2+H)^+$  ion is ion-molecule reactions in the selvedge region. The fast atom's impact can fragment and ionize the glycerol molecules. The ions formed and desorbed into the gas phase can undergo ion-molecule reactions with gas phase glycerol. Since the ion-molecule chemistry of glycerol is not known it is not possible to conclude how many of the "background" ions detected by Gross et al.<sup>25</sup> are actually ion-molecule reaction products. The role of ion-molecule chemistry in the

formation of the ions detected in the FAB studies of glycerol was investigated by Allison et al.<sup>27</sup>

Allison et al.<sup>27</sup> performed a study of the time dependence of the relative abundance of the glycerol ions generated in FAB. The FAB spectra of pure glycerol were recorded once each minute until all of the glycerol had evaporated. In this experiment it is possible to vary the extent that gas phase ion-molecule reactions change the ions that have desorbed from the glycerol. When the FAB beam is first turned on, the number of glycerol molecules in the selvedge region is at a minimum. And as the glycerol evaporates to dryness, the number of glycerol molecules in the selvedge region again decreases. These events reduce the number of ion-molecule reactions that occur.

Allison et al.<sup>27</sup> suggest that low mass ions (with masses of 93 Daltons or less) are the primary positive ions produced by the fast atom bombardment of glycerol. These ions are desorbed into the high pressure selvedge region where the ions react with the neutral molecules. The low mass fragment ions of glycerol protonate the glycerol and analyte molecules in the selvedge region. The protonated molecules are then detected by the mass spectrometer. When the fast atom bombardment commences, the protonated glycerol molecules have a high relative abundance (See Scan 1 of Figure 1.8). As the bombardment continues, the density of the gas molecules in the selvedge region increases. The probability of ion-molecule reactions between the protonated molecules of the glycerol and the neutral molecules increases. Further collisions between the protonated glycerol molecules and neutral glycerol form proton bound cluster ions such as  $m/z = 185, 277$  and  $369$  (See scan 10 of Figure 1.8). As the glycerol depletes, the pressure in the selvedge region falls and the primary ions relative intensity increases (See scan 30 of Figure 1.8).

In FAB, negative ions are formed from glycerol by proton loss. The  $(G-H)^-$  anion ( $m/z = 91$ ) can cluster with neutral glycerol molecules to form the anions  $(2G-H)^-$ ,

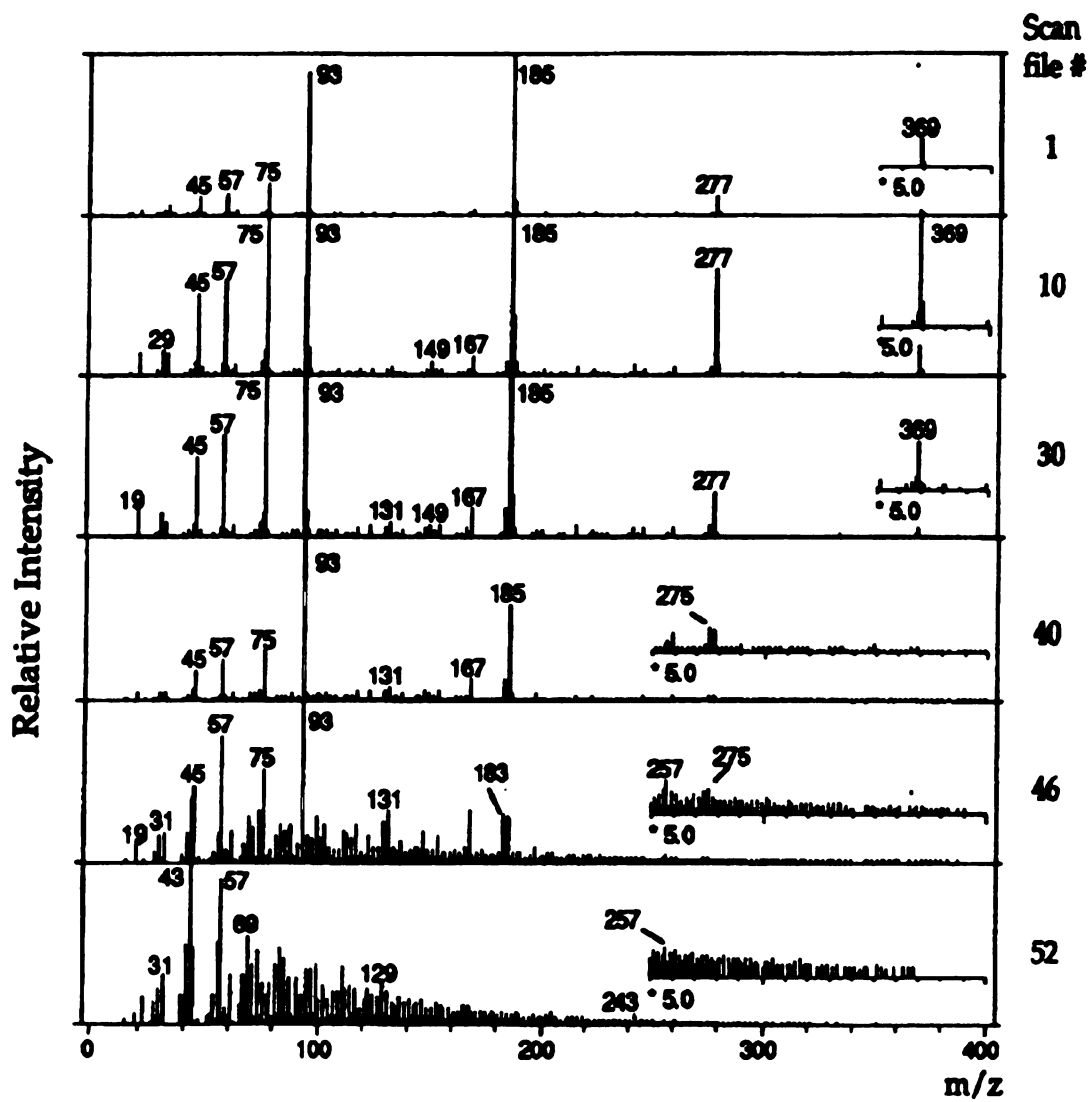


Figure 1.8: The FAB Spectra of Glycerol Taken at 1 Minute Intervals Until All of the Glycerol is Consumed

(3G-H)<sup>-</sup> and (4G-H)<sup>-</sup>.<sup>27</sup> No dehydration products of the glycerol anions were observed. Potential ion-molecule products was reported at  $m/z = 181$  and  $113$ .<sup>27</sup>

The low mass fragment anions of glycerol were observed after a long period of irradiation. These reagent anions have  $m/z$  values of 17, 25, 43, 45, 59, 71 and 91. The anions with mass to charge ratios of 71, 59, 45 and 25 Daltons do not appear in the FAB spectra taken at short irradiation times. These ions could be either the primary reagent anions of negative ion FAB or anions of radiation products.

It is impossible to study the ion-molecule chemistry of glycerol directly in a FAB experiment. Several researchers have alluded to gas phase ion-molecule reactions occurring during fast atom bombardment.<sup>23,27</sup> These postulated ion-molecule reactions will involve both the fragment ions of glycerol and the glycerol neutrals. No complete studies of the ion-molecule chemistry of glycerol are known. The objective of this research is to determine the gas phase ion-molecule reactions of the positive and negative ions of glycerol with neutral glycerol molecules. This research can improve the understanding of the formation of the analyte and background ions detected in FAB.

The ion-molecule chemistry of glycerol was studied using an Ion Cyclotron Resonance (ICR) spectrometer. The ions were generated from gas phase glycerol by electron impact ionization. Both the positive and negative ions of glycerol can be generated by varying the electron energy. Ion cyclotron resonance mass spectrometers are designed to study gas phase ion-molecule reactions. The ion-molecule chemistry of glycerol can be studied up to the ICR's practical upper mass limit of 300 Daltons. This mass range is sufficient to determine the reactivity of the fragment ions of glycerol and to investigate the proposed clustering behavior of glycerol molecules with the ions derived from glycerol.

**References**

- 1) Grove, W. R. *Philos. Mag.* **1853**, 5, 203
- 2) Thomson, J. J. *Philos. Mag.* **1910**, 20, 752
- 3) Barber, M.; Brodoli, R. S.; Elliot, G. J.; Sedgwick, R. D.; Tyler, A. N. *Anal. Chem.* **1982**, 54, 645A
- 4) Mc Neal, C. J. *Anal. Chem.* **1982**, 54, 43A
- 5) Scheifers, S. M.; Hollar, R. C.; Busch, K. L.; Cooks, R. G. *Am. Lab.* **1982**, 19
- 6) Rouse, J. Ph. D. Thesis, Michigan State University, **1993**
- 7) R. C. Weast (ed.), *Handbook of Chemistry and Physics*, 55th Edition, CRC Press, Boca Rotan, **1975**
- 8) R. C. Weast (ed.), *Handbook of Chemistry and Physics*, 68th Edition, CRC Press, Boca Rotan, **1983**
- 9) Sunner, J. *Org. Mass Spectrom.* **1993**, 28, 805
- 10) Perle, J. *Desorption Mass Spectrometry: Are SIMS and FAB the Same?*, ACS Symposium Series, **1985**, 126
- 11) Pachuta, S. J.; Cooks, R. G. *Chem. Rev.* **1987**, 87, 647
- 12) Morales, A. Ph. D. Thesis, Edmonton, Alberta, **1990**
- 13) Sunner, J. A.; Kulatunga, R.; Kebarle, P. *Anal. Chem.* **1986**, 58, 1312
- 14) Calculation by author
- 15) Bojeson, G.; Möller, M. *Int. J. Mass Spec. Ion Proc.* **1986**, 68, 239
- 16) Kathleen Noon, Private Communication
- 17) a) Malorni, A.; Marino, G.; Miloni, A. *Biomed. Environ. Mass Spectrom.* **1986**, 63, 477 b) Gagarly, A.; Van den Heuvel, H.; Claeys, M., *Spectrosc. Int.* **1989**, 7, 133 c) Allmaier, G.; Schmidt, E. R.; *Spectrosc. Int.* **1985**, 4, 297
- 18) Sunner, J. A.; Kulatunga, R.; Kebarle, P. *Anal. Chem.* **1986**, 58, 2009
- 19) Kriger, M. S.; Cook, K. D.; Short, R. T.; Todd, P. J. *Anal. Chem.* **1992**, 64, 3052

- 20) a) Wong, S. S.; Röllegen, F. W. *Nucl. Instrum. Methods Phys. Res.* **1986**, *B14*, 436 b) Jiang, L. F.; Barofsky, E.; Barofsky, D. F., *Proceedings of the 36th ASMS Conference on Mass Spectrometry and Allied Topics*, San Francisco, California, **1988**, 1209 c) Wong, S. S.; Röllegen, F. W.; Manz, I.; Przybyiski, M. *Biomed. Mass Spectrom.* **1985**, *12*, 43 d) Todd, P. J.; Groenwold, G. S. *Anal. Chem.* **1986**, *58*, 895
- 21) a) Puzo, G.; Prome, J. C. *Org. Mass Spectrom.* **1984**, *19*, 448-51 b) Harada, K.; Suzuki, M.; Kimbara, H. *Org. Mass Spectrom.* **1982**, *17*, 386
- 22) a) Tonduer, Y.; Clifford, A.; Deluca, L. M. *Org. Mass Spectrom.* **1985**, *20*, 157 b) Cooks, R. G.; Kruger, T. L. *J. Am. Chem. Soc.* **1977**, *99*, 1279
- 23) Curcuruto, O.; Traldi, P.; Moneti, G.; Corda, L.; Podda, G. *Org. Mass Spectrom.* **1991**, *26*, 713
- 24) Field, F. H. *J. Phys. Chem.* **1982**, *86*, 5115
- 25) Gross, M. L.; Caldwell, K. A. *J. Am. Soc. Mass Spectrom.* **1994**, *5*, 72
- 26) Lehmann, W. D.; Kessler, M.; König, W. A. *Biomed. Mass Spectrom.* **1984**, *11*, 217
- 27) Allison, J.; Szekely, G. *In press*

## Chapter Two: The Results of the Positive Ion Studies of Glycerol

A published electron impact ionization mass spectrum of glycerol reports peaks representing ions with masses of 31, 43, 44, 45 and 61 Daltons.<sup>1</sup> This published EI mass spectrum is typical of the other EI mass spectra of glycerol found in the literature.<sup>1,2,3</sup> When the mass spectrum of glycerol was taken using the Ion Cyclotron Resonance (ICR) spectrometer a different spectrum was obtained. The ICR detected additional ions with  $m/z$  values of 57, 75, 93, 117 and 119. The  $m/z = 93$  ion is the protonated glycerol molecule  $(G+H)^+$  which should be formed by ion-molecule reactions. The appearance of the two spectra are radically different. In the published spectrum the base peak is  $m/z = 61$ . In the ICR spectrum the base peak represents the  $(G+H)^+$  ion. Table 2.1 gives the relative intensities of the ions detected in both spectra. Figure 2.1 shows both mass spectra.<sup>2</sup>

Table 2.1 shows major differences in the relative intensities of the all of the ions with masses from 15 Daltons to 93 Daltons. The most important differences are that the  $m/z = 93$   $(G+H)^+$  ions and the  $m/z = 75$   $((G+H)^+ - 18)$  ions in the ICR mass spectrum do not exist in the EI mass spectrum. Also the  $m/z = 57$  ion is much more abundant in the ICR mass spectrum. The ions of  $m/z = 117$  and 119 are ion-molecule product ions formed in the ICR and are not reported in the published EI mass spectra.

The double resonance ICR studies of the low mass fragment ions of glycerol proved that all of the ions with masses of 75 Daltons or less were not products of ion-molecule reactions. The  $(G+H)^+$  ion could be an ion-molecule product since the ion's

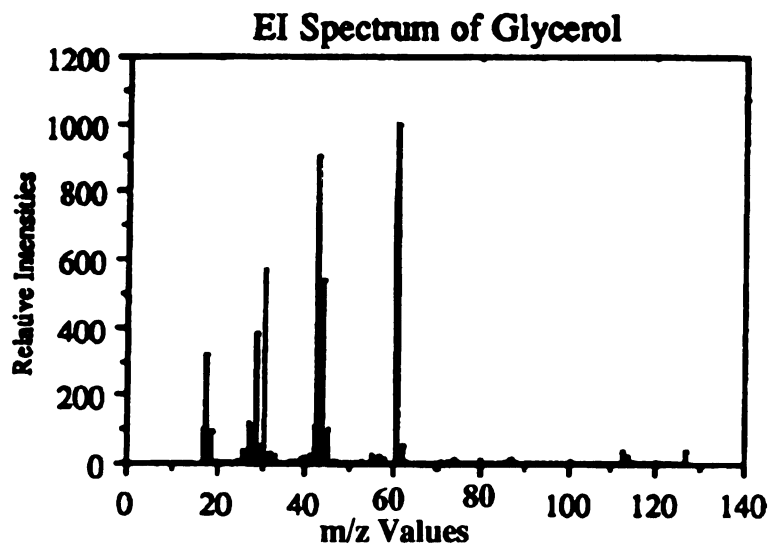
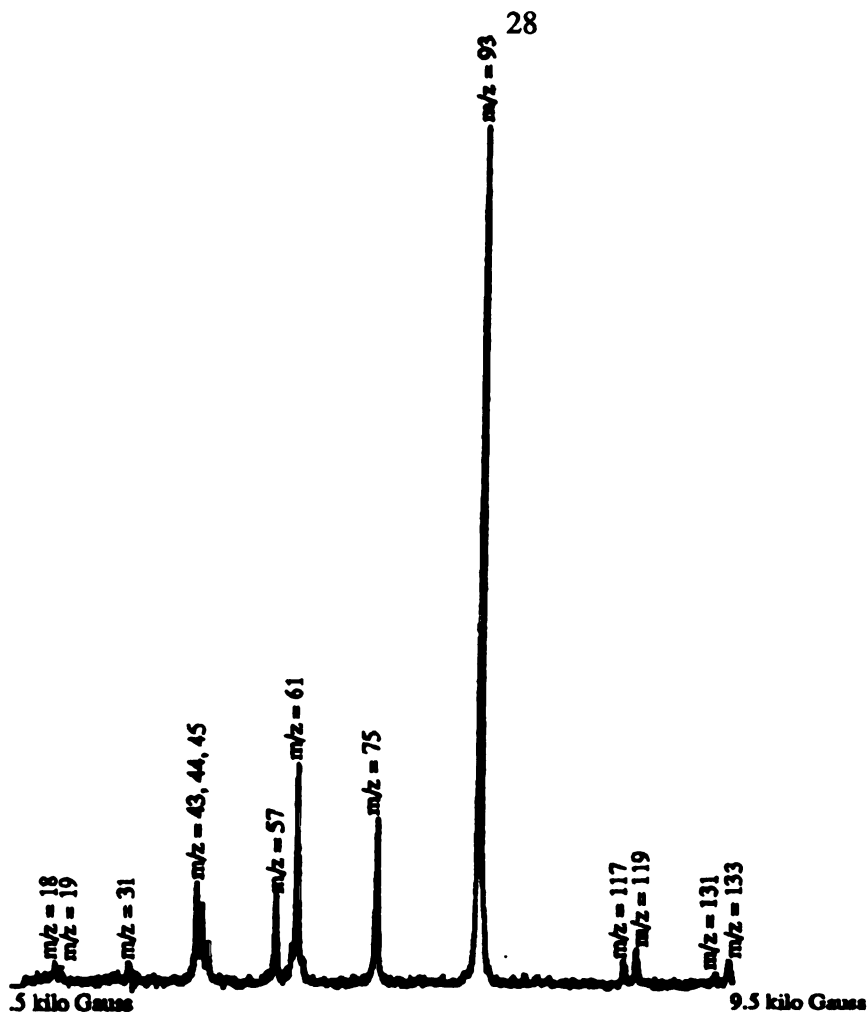


**Figure 2.1: A Comparison of the ICR Mass Spectrum of Glycerol with the EI Mass Spectrum of Glycerol**

mass is greater than that of glycerol. The ICR double resonance studies of the  $(G+H)^+$  ion did not find any ionic precursors when the glycerol sample was first introduced into a clean ICR spectrometer. These results are unexpected. Alcohols do undergo ion-molecule reactions to form the  $(ROH+H)^+$  ion.<sup>4</sup> The fragment ions of glycerol are expected to have lower proton affinities than glycerol and should protonate the glycerol monomers.

Table 2.1: The Relative Intensities of the Low Mass Positive Ions of Glycerol

Ion in the EI Mass Spectra

Ion in the ICR Mass Spectra

Mass in Daltons	Relative Intensity	Mass in Daltons	Relative Intensity
15	206	15	-
18	86	18	118
19	38	19	67
31	226	31	57
43	650	43	247
44	397	44	191
45	45	45	93
57	20	57	164
61	1000	61	382
62	53	62	-
74	14	74	-
75	5	75	234
92	1	92	-
93	3	93	1000
117	-	117	23
119	-	119	32

Glycerol also forms a protonated glycerol dimer  $(G_2+H)^+$  with a mass-to-charge ratio of 185. The  $(G+H)^+$  ion is the principal source of the  $(G_2+H)^+$  ion. Between 51% and 66% fewer of the  $m/z = 185$  ions are detected when the  $(G+H)^+$  ion is ejected. Several of the lower mass fragment ions ( $m/z = 43, 44$  and  $75$ ) also have weak double resonance responses.

The large reduction in the relative intensity of the  $(G_2+H)^+$  ion when the  $(G+H)^+$  ion is ejected is proof that the double resonance experiments work under these experimental conditions. The  $(G_2+H)^+$  ion can be formed from the  $(G+H)^+$  ion by one of three possible mechanisms. Equations 1 to 3 show the mechanisms.



Equation 1 shows a classic ion-molecule mechanism where an ion collides with a neutral forming a new ion and a new neutral. A proton transfer to a glycerol dimer is shown in Equation 2. The last possible mechanism is the formation of a  $(G_2+H)^+$  ion by clustering a  $(G+H)^+$  ion and glycerol and stabilizing the complex by emitting a photon.<sup>5</sup>

An ICR study of deuterium labeled glycerol (glycerol-d<sub>5</sub>) was undertaken to determine the elemental composition and structure of the low mass fragment ions. A 50:50 mixture of glycerol-d<sub>5</sub> and glycerol was studied. The ions detected in the 50:50 mixture are presented in Table 2.2.

Table 2.2: The Positive Ions of Glycerol and Glycerol-d<sub>5</sub>

Ion in Glycerol	Mass in Daltons	Ion in Glycerol-d <sub>5</sub>	Mass in Daltons
CH <sub>3</sub> O <sup>+</sup>	31	CD <sub>2</sub> HO <sup>+</sup>	33
C <sub>2</sub> H <sub>3</sub> O <sup>+</sup>	43	C <sub>2</sub> D <sub>3</sub> O <sup>+</sup>	46
C <sub>2</sub> H <sub>4</sub> O <sup>+</sup>	44	C <sub>2</sub> D <sub>3</sub> HO <sup>+</sup>	47
C <sub>2</sub> H <sub>5</sub> O <sup>+</sup>	45	C <sub>2</sub> D <sub>3</sub> H <sub>2</sub> O <sup>+</sup>	48
		C <sub>2</sub> D <sub>4</sub> HO <sup>+</sup>	49
C <sub>3</sub> H <sub>5</sub> O <sup>+</sup>	57	C <sub>3</sub> D <sub>5</sub> O <sup>+</sup>	62
H <sub>5</sub> C <sub>2</sub> O <sub>2</sub> <sup>+</sup>	61	H <sub>2</sub> C <sub>2</sub> D <sub>3</sub> O <sub>2</sub> <sup>+</sup>	64
C <sub>3</sub> H <sub>7</sub> O <sub>2</sub> <sup>+</sup>	75	C <sub>3</sub> D <sub>5</sub> H <sub>2</sub> O <sub>2</sub> <sup>+</sup>	80
C <sub>3</sub> H <sub>9</sub> O <sub>3</sub> <sup>+</sup>	93	C <sub>3</sub> D <sub>5</sub> H <sub>4</sub> O <sub>3</sub> <sup>+</sup>	98
C <sub>6</sub> H <sub>17</sub> O <sub>6</sub> <sup>+</sup>	185	C <sub>6</sub> D <sub>5</sub> H <sub>12</sub> O <sub>6</sub> <sup>+</sup>	190
		C <sub>6</sub> D <sub>10</sub> H <sub>7</sub> O <sub>6</sub> <sup>+</sup>	195

The glycerol-d<sub>5</sub> that was used has the deuterons attached to the carbon backbone of the glycerol.<sup>6</sup> The compositions of the fragment ions of the glycerol-d<sub>5</sub> can be deduced by comparing the changes in mass between the ions from glycerol and the ions from glycerol-d<sub>5</sub>. The double resonance studies of the fragment ions and the protonated glycerol ions (both deuterated and undeuterated) were completed.

The evidence for the (G+H)<sup>+</sup> ion (m/z=93) being a product of ion-molecule reactions is weak. When the glycerol sample is first inserted into an unexposed ICR, no ionic precursors to the (G+H)<sup>+</sup> ion are detected. Only after the ICR has been exposed to and coated with glycerol are ionic precursors to the (G+H)<sup>+</sup> ion detected.

When a layer of glycerol had been deposited on the stainless steel walls of the ICR spectrometer, the ionic precursors of the (G+H)<sup>+</sup> ions have weak double resonance responses. Higher power double resonance experiments, the m/z = 61 ion and the m/z = 43, 44 and 45 ion cluster are observed to be precursor ions to the (G+H)<sup>+</sup> ions. The double resonance response of the m/z = 43, 44 and 45 ion cluster is strongest for the m/z = 44 ion but could not be resolved for the individual ions. Only 5% fewer (G+H)<sup>+</sup> ions are detected when the m/z = 43, 44 and 45 ions are ejected. The ejection of the m/z = 61 ion reduces by 10% the number of (G+H)<sup>+</sup> ions detected. The double resonance study of the protonated glycerol-d<sub>5</sub> ion (G-d<sub>5</sub>+H)<sup>+</sup> in the 50:50 mixture experiment confirms that C<sub>2</sub>H<sub>4</sub>O<sup>+</sup> (m/z = 44) and the m/z = 61 ions transfer protons to glycerol molecules to a slight extent. The (G-d<sub>5</sub>+H)<sup>+</sup> ion has as ionic precursors the C<sub>2</sub>H<sub>4</sub>O<sup>+</sup>, C<sub>2</sub>D<sub>3</sub>HO<sup>+</sup> (m/z = 47), m/z = 61 and m/z = 64 ions in the 50:50 mixture experiment. The m/z = 47 ion (C<sub>2</sub>D<sub>3</sub>OH)<sup>+</sup> is the companion ion to m/z = 44 (C<sub>2</sub>H<sub>4</sub>O)<sup>+</sup> ion. Likewise H<sub>2</sub>C<sub>2</sub>D<sub>3</sub>O<sub>2</sub><sup>+</sup> (m/z = 64) is the companion ion to the H<sub>5</sub>C<sub>2</sub>O<sub>2</sub><sup>+</sup> ion (m/z = 61). The deuterated ions have similar reactivity to the undeuterated ions.

## Proof of the Existence of Glycerol Dimers

In the 50:50 mixture of glycerol and glycerol-d<sub>5</sub>, three protonated glycerol dimers are detected. These ions are (G<sub>2</sub>+H)<sup>+</sup> (m/z = 185), (G+G-d<sub>5</sub>+H)<sup>+</sup> (m/z = 190) and ((G-d<sub>5</sub>)<sub>2</sub>+H)<sup>+</sup> (m/z = 195). A double resonance study of the precursors of the three protonated dimers proved that glycerol dimers are being protonated.

The ICR double resonance studies of the three proton bound glycerol dimers determined that both (G+H)<sup>+</sup> and (G-d<sub>5</sub>+H)<sup>+</sup> are ionic precursors of all three of the protonated dimers. The (G<sub>2</sub>+H)<sup>+</sup> ion could be formed by the (G+H)<sup>+</sup> ion reacting with a neutral glycerol or a glycerol containing cluster as shown in Equations 1 and 3. The (G+H)<sup>+</sup> ion or the (G-d<sub>5</sub>+H)<sup>+</sup> ion could form the (G<sub>2</sub>+H)<sup>+</sup> ion by transferring a proton to a glycerol dimer. Proton transfer is the only explanation for the (G-d<sub>5</sub>+H)<sup>+</sup> being a precursor to the (G<sub>2</sub>+H)<sup>+</sup> ion.

The (G+G-d<sub>5</sub>+H)<sup>+</sup> ion, (m/z = 190), could be formed by either the (G+H)<sup>+</sup> ion or the (G-d<sub>5</sub>+H)<sup>+</sup> ion combining with either glycerol or glycerol-d<sub>5</sub> or reacting with clusters containing these monomers. A proton transfer to a glycerol-glycerol-d<sub>5</sub> dimer could also explain the double resonance results. None of the reactions shown in Equations 1 to 3 could be ruled out as a source of the m/z = 190 ion.

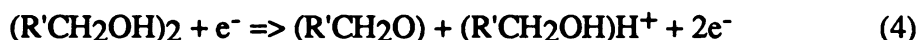
The (G+H)<sup>+</sup> ion has a mass of 93 Daltons and can only form an ion with a mass of 195 Daltons ((G-d<sub>5</sub>)<sub>2</sub>+H)<sup>+</sup> by transferring a proton to a (glycerol-d<sub>5</sub>)<sub>2</sub> dimer. This proton transfer explains how the lower mass fragment ions of glycerol and the (G-d<sub>5</sub>+H)<sup>+</sup> (m/z = 98) ion can be ionic precursors to the m/z = 185 ion and how the (G-d<sub>5</sub>+H)<sup>+</sup> ion (m/z = 98) can be an ionic precursor to the (G<sub>2</sub>+H)<sup>+</sup> ion.

The evidence for the existence of glycerol dimers and the lack of detectable ion-molecule reactions forming the (G+H)<sup>+</sup> ion leads to a logical question: **Do glycerol clusters exist in the gas phase?**

## Evidence for the Existence of Gas Phase Glycerol Clusters

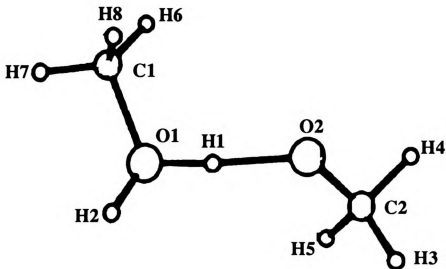
The formation of protonated molecules by electron impact ionization of a neutral clusters has been observed for hydrogen bonded clusters. For example, the  $\text{H}_3\text{O}^+$  ion is formed by the ionization of  $(\text{H}_2\text{O})_2$ .<sup>7</sup> Theoretical calculations suggest that the  $(\text{H}_2\text{O})_2^+$  ion has a proton transferred  $(\text{H}_2\text{OH}^+\cdots\text{OH})$  structure and is represented as a complex between a oxonium ion and an OH radical  $(\text{H}_2\text{OH}^+\cdots\text{OH})$ .<sup>8</sup> The  $(\text{H}_2\text{O})_2^+$  cluster dissociates into  $(\text{H}_3\text{O})^+$  and an OH radical.

In the EI mass spectra of acetone clusters<sup>9</sup>, the ions  $(\text{CH}_3^+$ ,  $\text{CH}_3\text{CO}^+$  and  $\text{CH}_3\text{COCH}_3^+$ ) that are also detected in the EI mass spectrum of acetone are detected. In addition, the protonated and unprotonated acetone cluster ions of the types  $(\text{CH}_3\text{COCH}_3)_n\text{H}^+$  and  $(\text{CH}_3\text{COCH}_3)_n^+$  are present. Shukla et al. studied the ions formed by electron impact ionization of neutral clusters of primary, secondary and tertiary alcohols.<sup>10</sup> The aliphatic alcohols formed the neutral clusters by adiabatic expansion of alcohol vapor through a supersonic jet.<sup>10</sup> When the alcohol clusters are ionized, protonated alcohol cluster ions of the type  $((\text{ROH})_n+\text{H})^+$  are detected. Repeating the experiment with deuterated alcohols of the type ROD, the composition of the protonated molecular clusters formed is  $((\text{ROD})_n+\text{D})^+$ .<sup>10</sup> This result proves that the hydroxyl hydrogen atoms are the source of protons in the formation of the protonated clusters. The exception to this pattern is methanol.  $\text{CH}_3\text{OD}$  clusters form both  $((\text{CH}_3\text{OD})_n+\text{D})^+$  and  $((\text{CH}_3\text{OD})_n+\text{H})^+$  ions.<sup>11</sup> Alcohol clusters exist as proton transfer complexes which dissociate into protonated molecules and alkoxide radicals when ionized. This dissociation is shown in Equation 4.<sup>10</sup>



Methanol is unique in that it also can form proton transfer complexes using both the protons of the methyl group and the hydroxyl protons.<sup>11</sup> The transition states for the hydroxyl proton transfer and the methyl proton transfers are shown in Figure 2.2.<sup>11</sup>

(a)



(b)

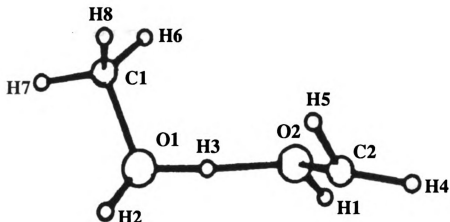


**Figure 2.2: The Proton Transferred Structures of the Methanol Dimer: Computer drawings of the calculated equilibrium geometries of the ionized methanol dimers at MP2/6-31G\*\***

No molecular ions  $((\text{ROH})_n^+)$  are detected in the mass spectra of aliphatic alcohol clusters. Earlier studies have shown that the formation of  $((\text{ROH})_n+\text{H})^+$  ions is always energetically more favorable than the formation of  $(\text{ROH})_n^+$  ions.<sup>11,12</sup> The EI mass spectra of aliphatic alcohol clusters have all of the normal fragment ions detected in the mass spectra of the corresponding alcohol monomers.<sup>10</sup>

If the glycerol molecules exist as clusters in the ICR, the ICR mass spectrum should have similar features to those reported for the EI mass spectra of alcohol clusters. Peaks within the EI mass spectrum of alcohol clusters represent a series of protonated cluster ions of the type  $((\text{ROH})_n+\text{H})^+$ , where  $n$  can have values of up to 4 or 5 or more. The ICR mass spectrum of glycerol has a series of ions of the type  $((\text{G})_n+\text{H})^+$  with  $n$  values of 1, 2 and 3. These ions have  $m/z$  values of 93, 185 and 277. The alcohol clusters do not form  $(\text{ROH})_n^+$  ions. The EI and ICR mass spectra both lack a glycerol molecular ion. This is consistent with the lack of a molecular ion in the EI mass spectra of similar alcohols such as 2-propanol, ethylene glycol and sec-butyl alcohol.<sup>1</sup> The ions of  $m/z = 31, 43, 44, 45, 57$  and  $61$  are the normal fragment ions of glycerol found in the published EI spectra. These fragment ions are also found in the ICR spectrum of glycerol. All of these observations support the possibility that gas phase glycerol clusters exist in the ICR.

The double resonance data from the mixed glycerol ( $d_0$  and  $d_5$ ) experiments proves that gas phase glycerol dimers exist in the ICR. Evidence for the existence of larger glycerol clusters in the ICR comes from the double resonance study of the  $m/z = 277$  ion  $(\text{G}_3+\text{H})^+$ . This ion, a protonated glycerol trimer, has the  $m/z = 185$  ion as its only ionic precursor. The double resonance response to the ejection of the  $(\text{G}_2+\text{H})^+$  ion is not very strong. Only a 12.5% reduction in the number of  $m/z = 277$  ions is observed. The protonated glycerol trimer may be formed by the three reactions shown in Equations 1 to 3. The weak double resonance response of the  $(\text{G}_3+\text{H})^+$  ion may be due to its primary source being the ionization of  $\text{G}_4$  clusters.

## The Source of the Glycerol Clusters

The ICR spectra of glycerol taken at similar pressures have large variations in the relative intensities of the ions. Figure 2.3 shows a pair of glycerol spectra taken at similar pressures. The spectra obtained vary depending on how the glycerol is vaporized. The normal procedure is to insert a direct probe into the inlet arm of the ICR. The glycerol is contained in a capillary tube. Both the inlet arm and the direct probe are heated. The glycerol spectra taken when the glycerol is evaporated from inside the capillary tube all have the  $(G+H)^+$  ion as the base peak. Figure 2.3A shows a typical spectrum.

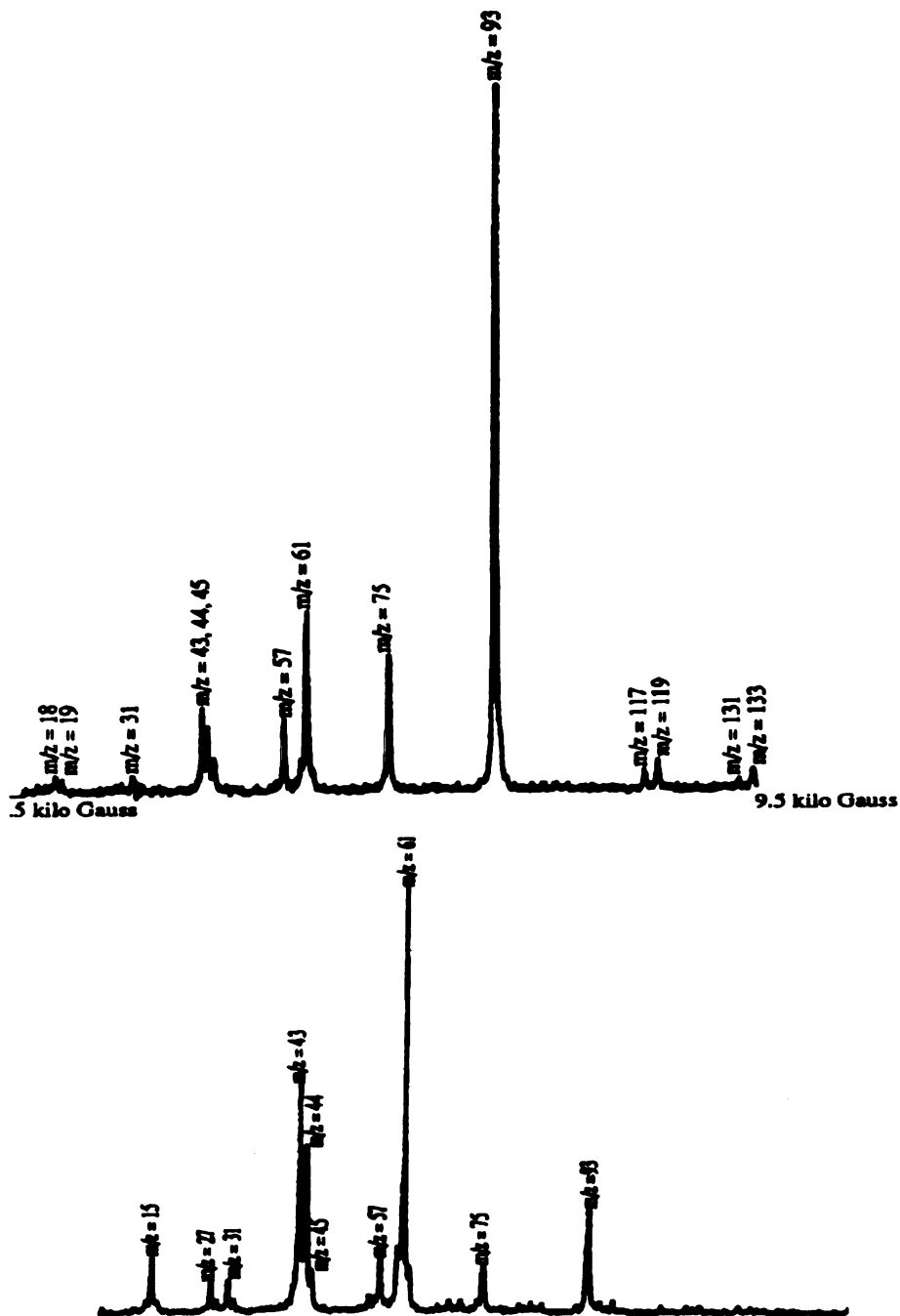
After a series of experiments, enough glycerol coated the walls of the ICR cell and the source inlet to provide a moderate ( $7.0 \times 10^{-6}$  torr) pressure of glycerol without inserting the capillary tube. When the glycerol is evaporated from the glycerol layer inside the ICR the base peak in the spectra is the  $C_2H_5O_2^+$  ( $m/z = 61$ ) ion. The  $(G+H)^+$  ion has a very low relative intensity in these spectra. An example spectrum is shown as Figure 2.3B. Table 2.3 gives the relative intensities of the ions.

Table 2.3: Relative Intensities of the ICR Spectra of Glycerol

Figure 2.3A ( $5.6 \times 10^{-6}$  Torr)

Figure 2.3B ( $7.0 \times 10^{-6}$  Torr)

Mass in Daltons	Relative Intensity	Mass in Daltons	Relative Intensity
18	118	18	440
19	55	19	67
31	57	31	135
33	0	33	138
43	247	43	765
44	191	44	541
45	93	45	134
57	164	57	143
61	382	61	1000
75	234	75	92
93	1000	93	161



**Figure 2.3: A Comparison of the ICR Mass Spectrum of Glycerol Evaporated from a Capillary Tube with the ICR Mass Spectrum of Glycerol Evaporated from the ICR Cell Walls**

The data in Table 2.3 suggests that when the glycerol is evaporated from the walls of the ICR most of the glycerol in the gas phase is in monomeric form. When the capillary tube is also a source of glycerol, the most abundant ion detected is (G+H)<sup>+</sup>. The (G+H)<sup>+</sup> ion is principally an EI fragment ion of a glycerol cluster. The source of the glycerol clusters is the liquid glycerol in the capillary tube or the high pressure region above the glycerol liquid.

### **The Origin, Structure and Chemistry of the Fragment Ions of Glycerol**

Chhabil Dass studied the structure of the fragment ions of protonated glycerol using a Collision Inducted Dissociation (CID)-mass analyzed kinetic energy (MIKES) experiment.<sup>13</sup> In CID, ions are accelerated and collide with monoatomic gas molecules. The collision fragments the heavier ions into smaller ions and neutrals. Dass analyzed the fragment ions using a sector mass spectrometer in the mass analyzed kinetic energy (MIKES) mode. CID-MIKES allows the experimenter to observe the unimolecular and metastable fragmentation of a selected ion. Figure 2.4 shows their proposal for the fragmentation pathways of the protonated glycerol molecule.<sup>13</sup>

The fragmentation of the protonated glycerol molecule is shown in Figures 2.4 and 2.5. The  $m/z = 75$  ion (C<sub>3</sub>H<sub>7</sub>O<sub>2</sub>)<sup>+</sup> ion and the  $m/z = 57$  ion (C<sub>3</sub>H<sub>5</sub>O)<sup>+</sup> ion are formed by successive dehydrations of the protonated glycerol molecule. Several possible structures for the  $m/z = 75$  ion are shown in Figure 2.6. The only ion-molecule reaction of the  $m/z = 75$  (C<sub>3</sub>H<sub>7</sub>O<sub>2</sub>)<sup>+</sup> ion is the transfer of a proton to a glycerol dimer to form the (G<sub>2</sub>+H)<sup>+</sup> ion. The proton transfer is shown in Equation 5.



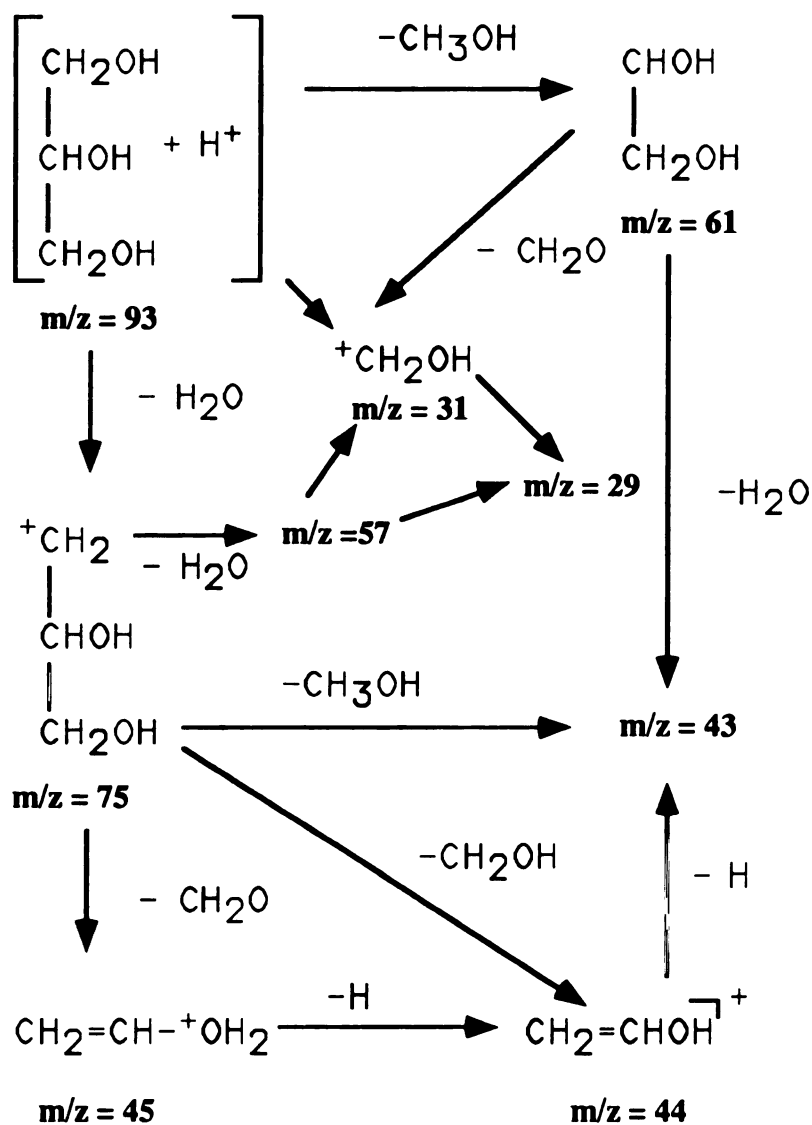


**Figure 2.4: The Fragmentation Pathways of the Protonated Glycerol Molecule**

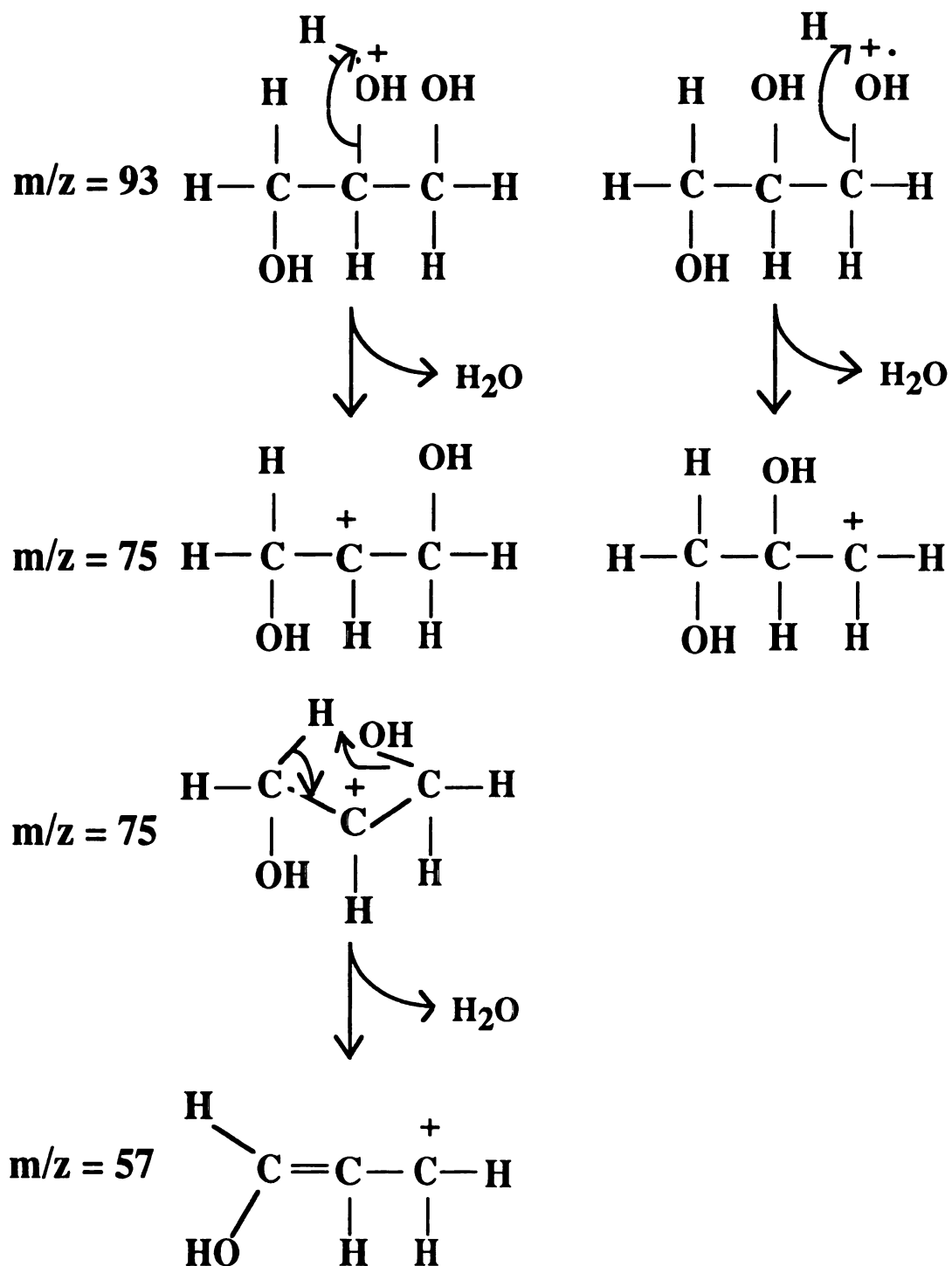


**Figure 2.5: The Dehydration of Protonated Glycerol**

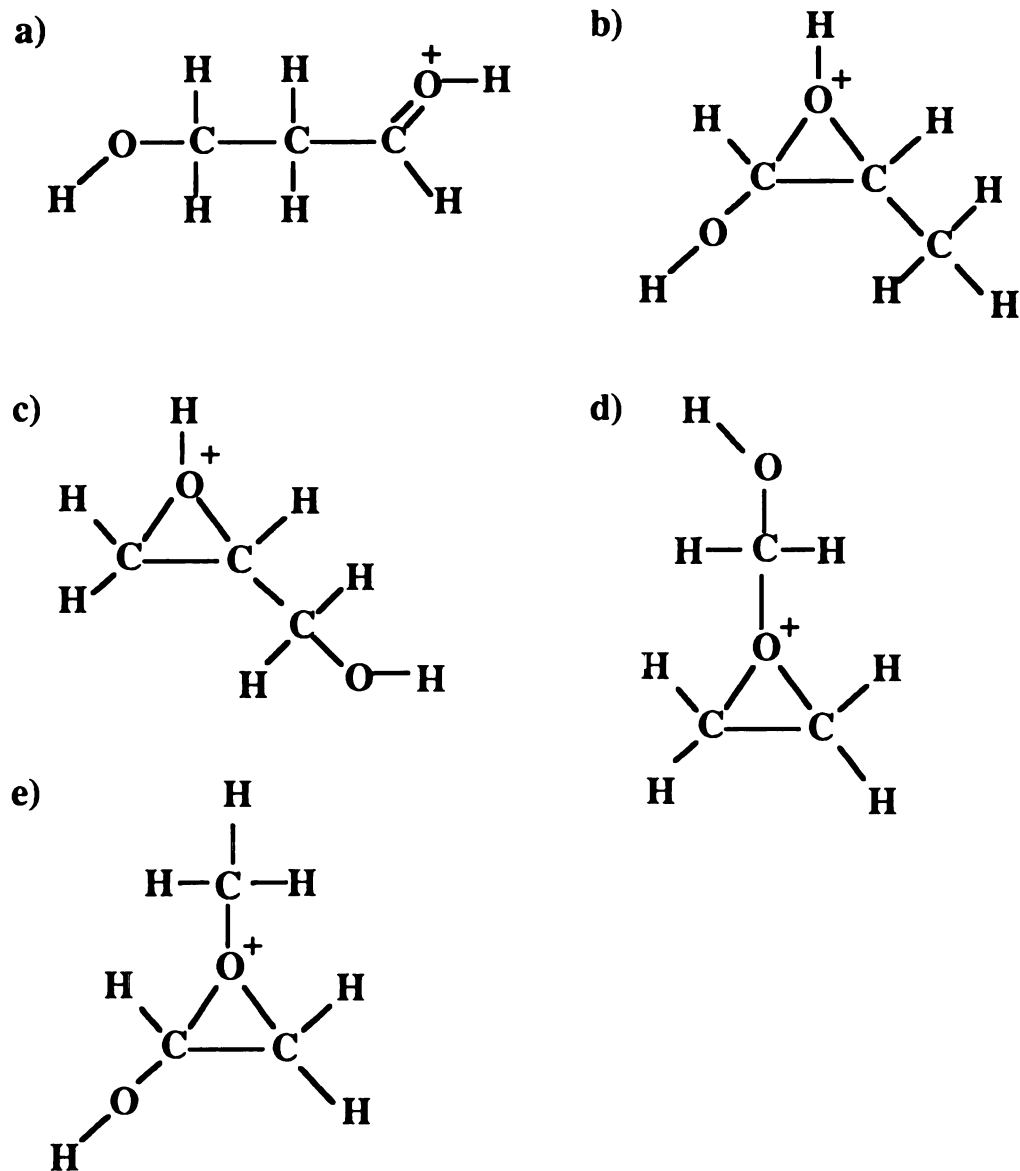


**Figure 2.6: Possible Structures of the  $C_3H_7O_2^+$  Ion**

The  $C_3H_5O^+$  ( $m/z = 57$ ) ion has 9 known structures.<sup>14</sup> The possible structures are presented in Figure 2.7. The  $C_3H_5O^+$  ion has been formed by a wide variety of experimental methods. The experimental methods include the metastable decay of  $C_4H_8O^+$  and  $C_3H_6O^+$  ions as well as EI ionization of precursors such as methyl propionate, but-2-en-1-ol, 1-penten-3-ol and 1-ethylcyclopropanol.<sup>13,14,15</sup> Despite the varied sources of the  $C_3H_5O^+$  ion the researchers report that the  $C_3H_5O^+$  ions are a mixture of two isomers, the acylium ( $CH_3CH_2C=O^+$ ) ion and the hydroxycarbenium ( $CH_2=CHCH=OH^+$ ) ion. The acylium and the hydroxycarbenium isomers of the  $C_3H_5O^+$  ion have been previously reported to be the most stable structures.<sup>14</sup>

The  $C_3H_5O^+$  ion may undergo a condensation reaction with glycerol to form the  $m/z = 131$  ion as shown in Equation 6.



The double resonance response of the  $m/z = 131$  ( $C_6H_{11}O_3$ )<sup>+</sup> ion is very weak so it is possible that the ( $C_6H_{11}O_3$ )<sup>+</sup> ion is a fragment ion of a glycerol dimer. A second possible explanation is the low abundance of the isomer of the  $C_3H_5O^+$  ion which reacts with glycerol resulting in the formation of the ( $C_6H_{11}O_3$ )<sup>+</sup> ion. The  $C_3H_5O^+$  ion does not protonate glycerol or glycerol dimers.

The  $m/z = 57$  ion ( $C_3H_5O^+$ ) reacts with glycerol in an ion-molecule reaction with the loss of formaldehyde to form the  $C_5H_9O_3^+$  ion. This reaction with glycerol to form the  $m/z = 119$  ion and formaldehyde is shown in Equation 7.



One of the known structures of the  $C_3H_5O^+$  ion is protonated acrolein. The proton affinity of acrolein is 811 kJ/mole.<sup>16</sup> Despite the proton affinity of the acrolein being less than the proton affinity of glycerol, and a relative intensity of 164, the

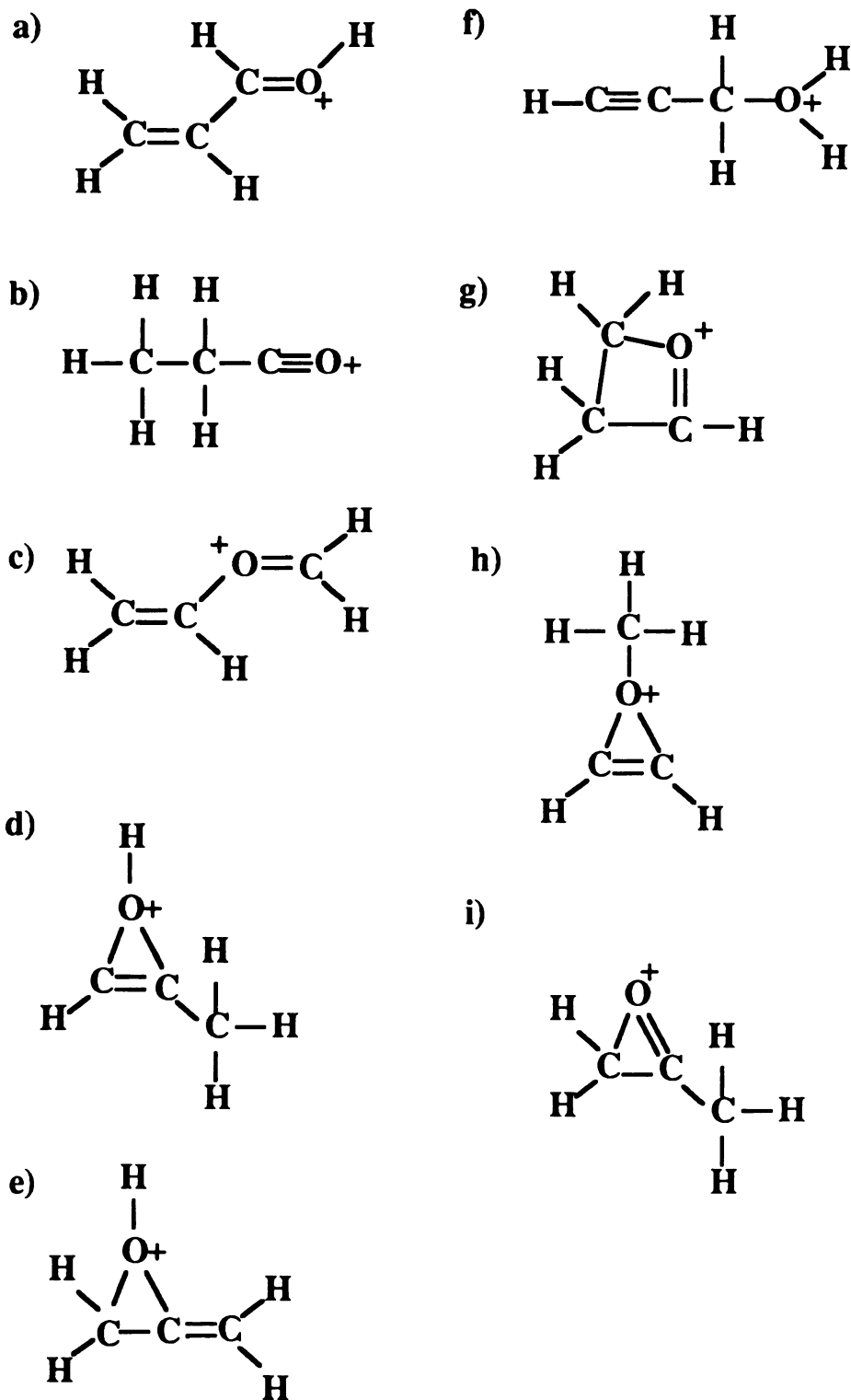


**Figure 2.7: The Possible Structures of the  $C_3H_5O^+$  Ion**

$C_3H_5O^+$  ion does not protonate glycerol or the glycerol dimers. The  $C_3H_5O^+$  ion does not have a protonated acrolein structure in this experiment.

The  $C_2H_5O^+$  ion ( $m/z = 45$ ) is formed by formaldehyde loss by the  $C_3H_7O_2^+$  ion. This ion has four stable structures.<sup>13</sup> The structures are shown in Figure 2.8. The structures are  $(CH_3C=O^+H_2)$ ,  $(^+CH_2OCH_3)$ ,  $(^+CH_2CH_2OH)$ , and a protonated ring structure. The  $C_2H_5O^+$  ion does not react with glycerol.

The  $C_2H_4O^+$  ion ( $m/z = 44$ ) formed by the EI ionization of glycerol has a vinyl alcohol structure  $(CH_2=CHOH)^+$ .<sup>13</sup> The abundant  $C_2H_4O^+$  ion is formed by several fragmentation mechanisms. The  $C_2H_4O^+$  ion is generated by a two step fragmentation from the molecular ion of glycerol. The  $C_2H_4O^+$  ion also is generated by alpha cleavage reaction of the  $C_3H_7O_2^+$  ion and by a H radical loss by the  $m/z = 45$  ion.<sup>13</sup> The  $C_2H_4O^+$  ion protonates glycerol and its dimers. The neutral product formed by the proton loss is acetaldehyde.

Dass<sup>13</sup> and R. G. Cooks et al.<sup>17</sup> studied the possible structures of the  $C_2H_3O^+$  ( $m/z = 43$ ) ion. The five possible structures are shown in Figure 2.9. Both Dass and R. G. Cooks et al. report that the  $C_2H_3O^+$  ion generated by the EI ionization of glycerol is a mixture of two structures. The structures are shown in Figure 2.9 as the acetyl ion (a) and the oxiranyl ion (b). The  $C_2H_3O^+$  ion forms the  $C_5H_9O_3^+$  ( $m/z = 117$ ) ion by a condensation reaction with glycerol as shown in Equation 8.



The  $C_2H_3O^+$  ion has only a slight tendency to transfer a proton to a glycerol dimer. This supports Dass and R. G. Cooks et al.'s conclusion that the  $C_2H_3O^+$  ion is not a protonated ketene (b) or protonated alcohol (e) structure. The lack of a significant proton transfer also supports the conclusion that the  $C_2H_3O^+$  ion does not isomerize upon collision.

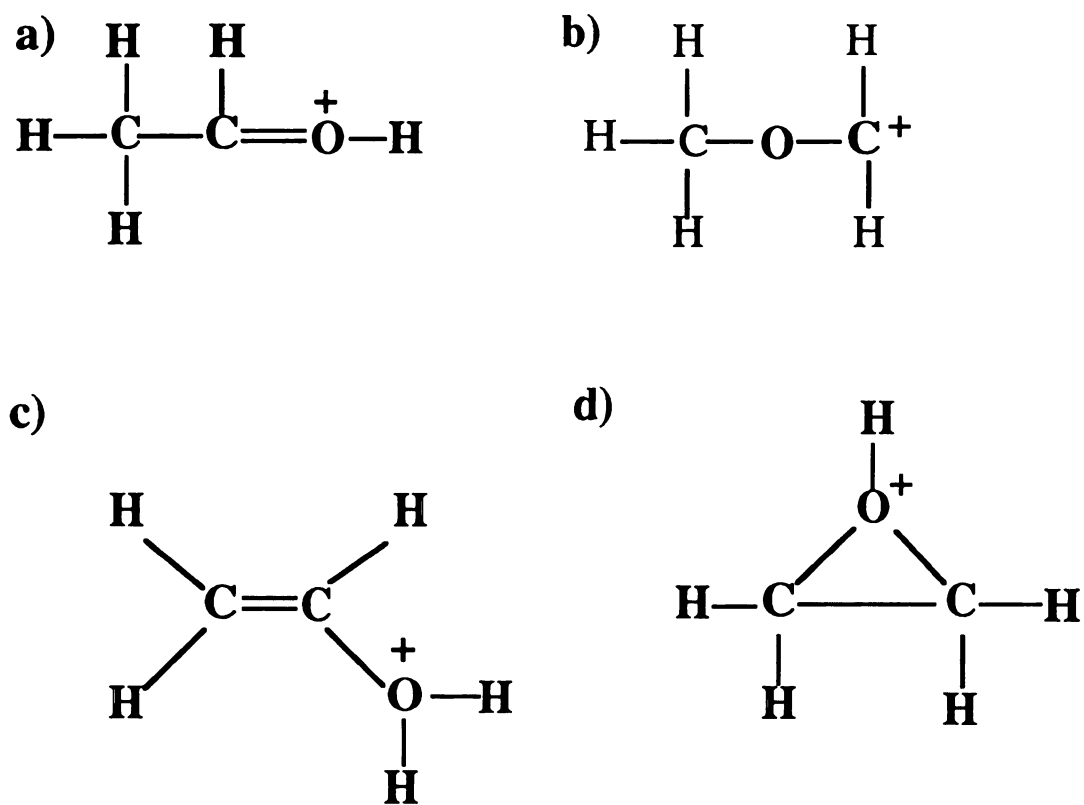
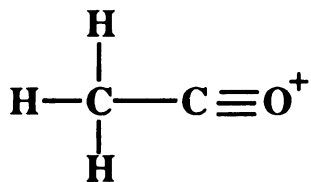
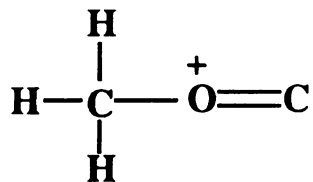


**Figure 2.8: The Structures of the  $C_2H_5O^+$  Ion**

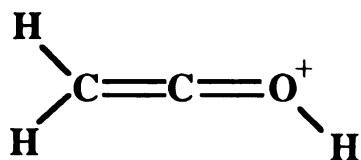
a)



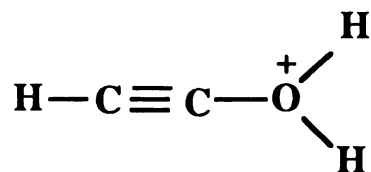
d)



b)



e)



c)

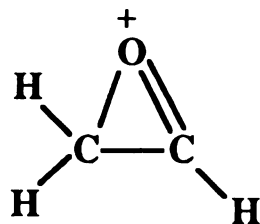


**Figure 2.9: The Structures of the  $\text{C}_2\text{H}_3\text{O}^+$  Ion**

The electron impact ionization of glycerol yields important ions with  $m/z$  values of 31, 43, 44, 61, 62 and 74. The dominant ion fragmentation mechanism in the electron impact (EI) ionization of alcohols is the alpha cleavage reaction.<sup>10</sup> The alpha cleavage reaction of the glycerol molecule forms the abundant  $m/z = 61$  ion and the much less abundant  $m/z = 31$  ion detected in the EI mass spectrum of glycerol. Figure 2.10 shows the alpha cleavage reaction. The loss of water molecules is also an important mechanism in ion formation.<sup>10</sup> The  $m/z = 43$  ion is formed by alpha cleavage of glycerol with the dehydration of the resulting  $m/z = 61$  ion (See Figure 2.11).

The abundant  $m/z = 44$  ion is formed by two fragmentation steps from the molecular ion of glycerol. The first step, shown in Figure 2.12, is the loss of either water or formaldehyde to form the  $m/z = 74$  or  $m/z = 62$  ions respectively. The  $m/z = 74$  ion then loses formaldehyde and the  $m/z = 62$  ion loses water to form the  $m/z = 44$  ion. Figure 2.13 is a diagram of the mechanisms of the 2nd step in the formation of the  $m/z = 44$  ion.

## The High Mass Ions of Glycerol

The high mass ions in the ICR spectrum of glycerol are ions with mass-to-charge ratios greater than 92. Table 2.4 is a list of the ions detected in a typical high mass ICR spectra (Figure 2.14). The relative intensities of the  $m/z = 241$  and 277 ions were calculated using another higher mass ICR spectra that has peaks representing the  $(G_2+H)^+$ ,  $(G_3+H)^+$  and the  $m/z = 241$  ions.

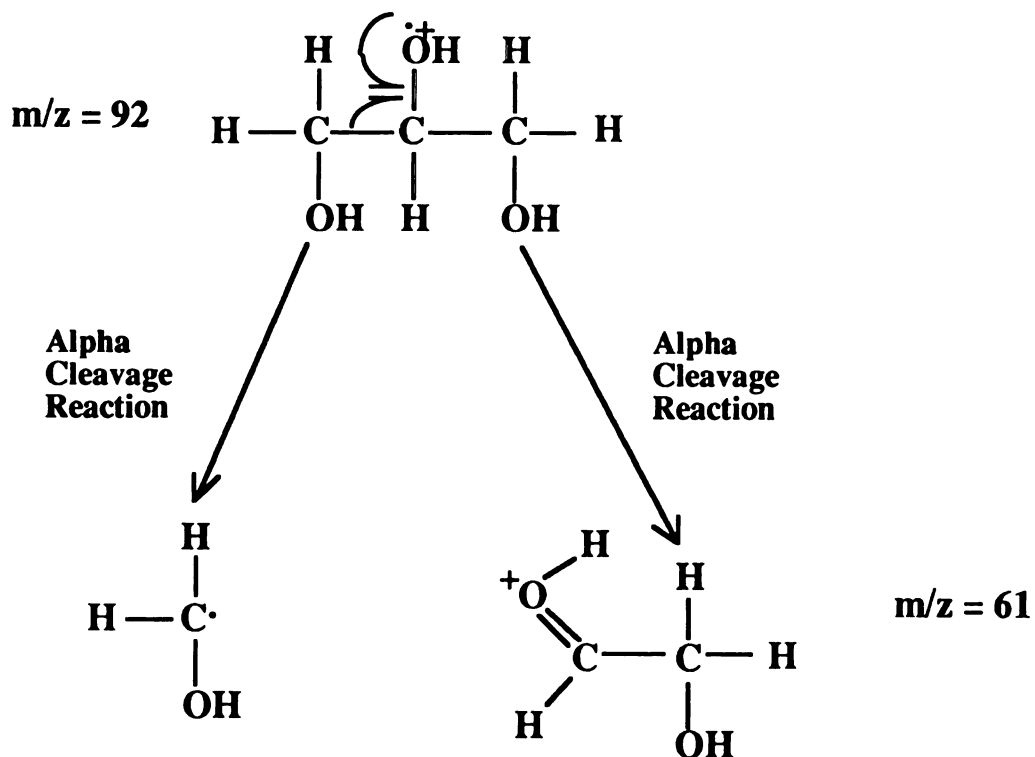
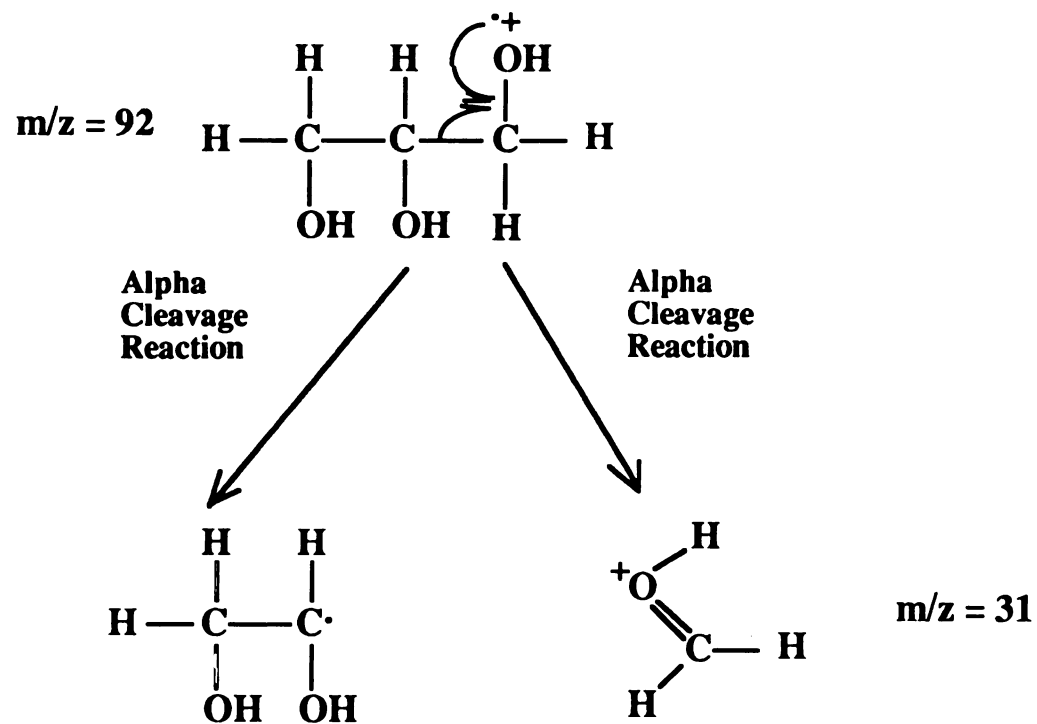


**Figure 2.10: The Fragmentation of Glycerol by Alpha Cleavage**

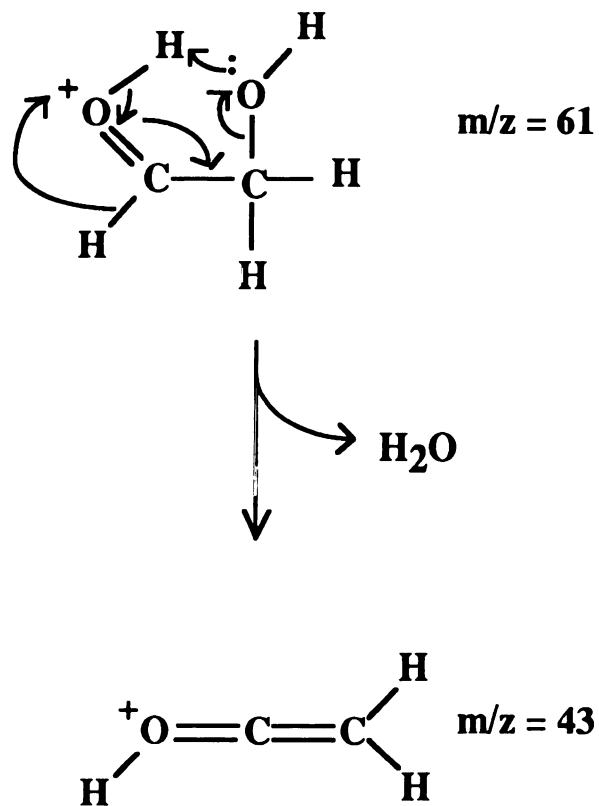


**Figure 2.11: The Formation of the  $\text{C}_2\text{H}_3\text{O}^+$  Ion  
from the  $\text{C}_2\text{H}_5\text{O}_2^+$  Ion**

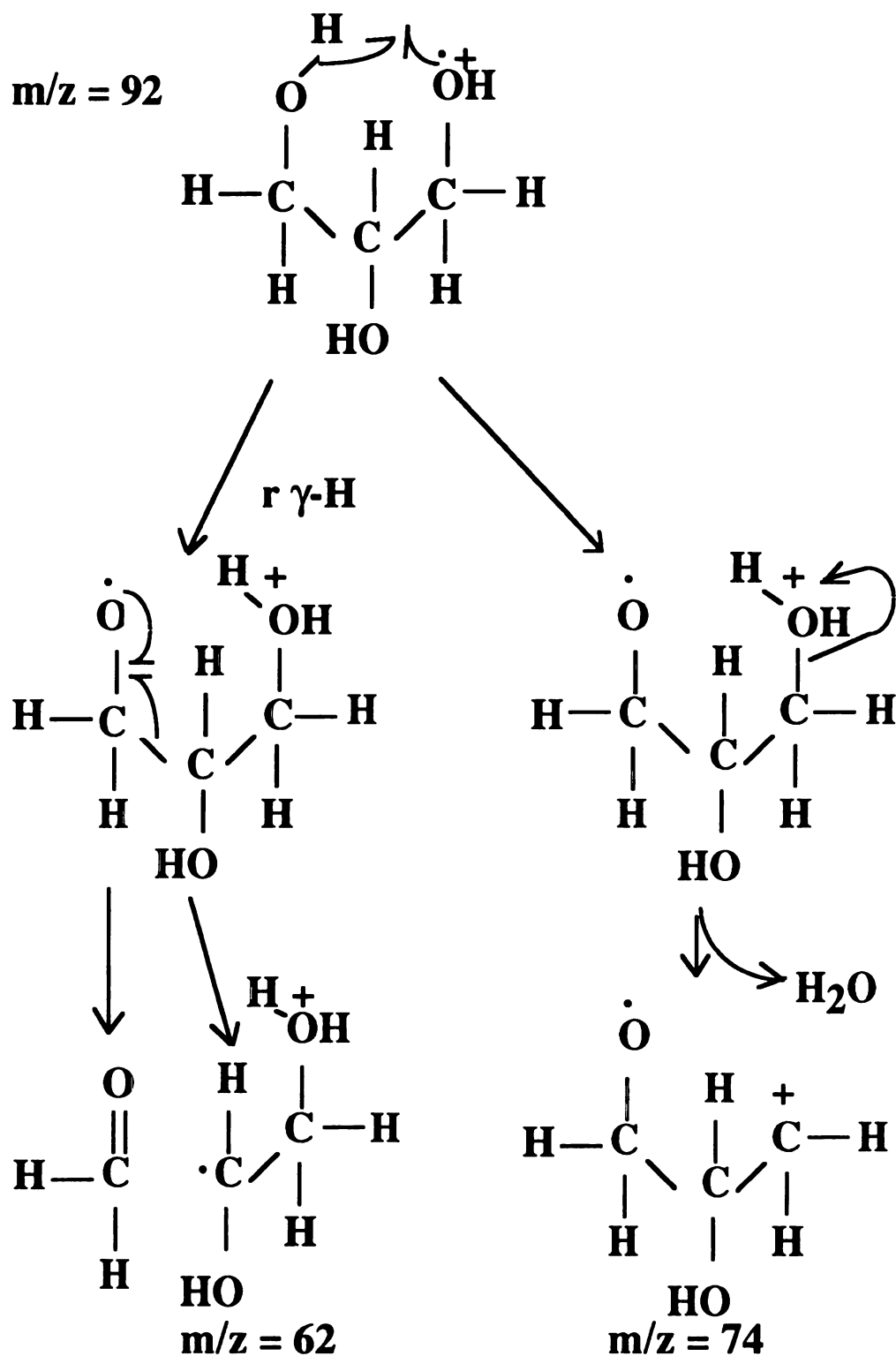


**Figure 2.12: The Formation Mechanisms of the  $m/z = 62$  and  $74$  Ions**

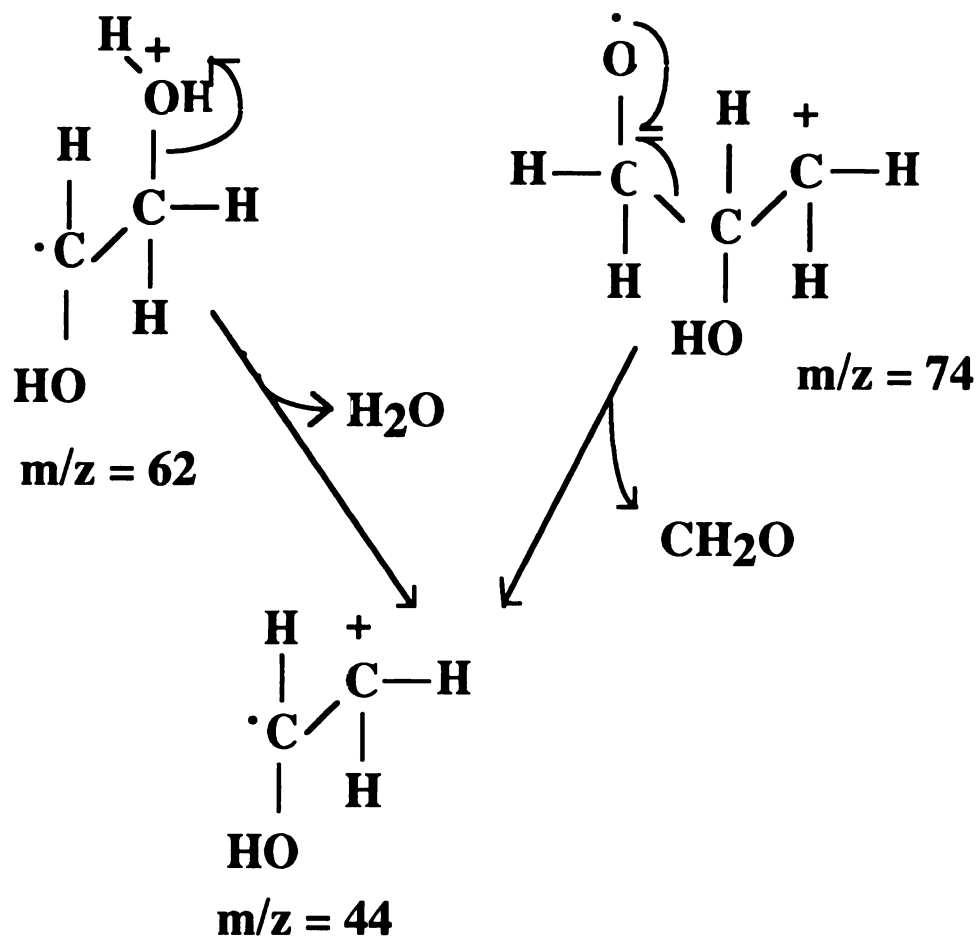


**Figure 2.13: Two Formation Mechanisms for the  $m/z = 44$  Ion**

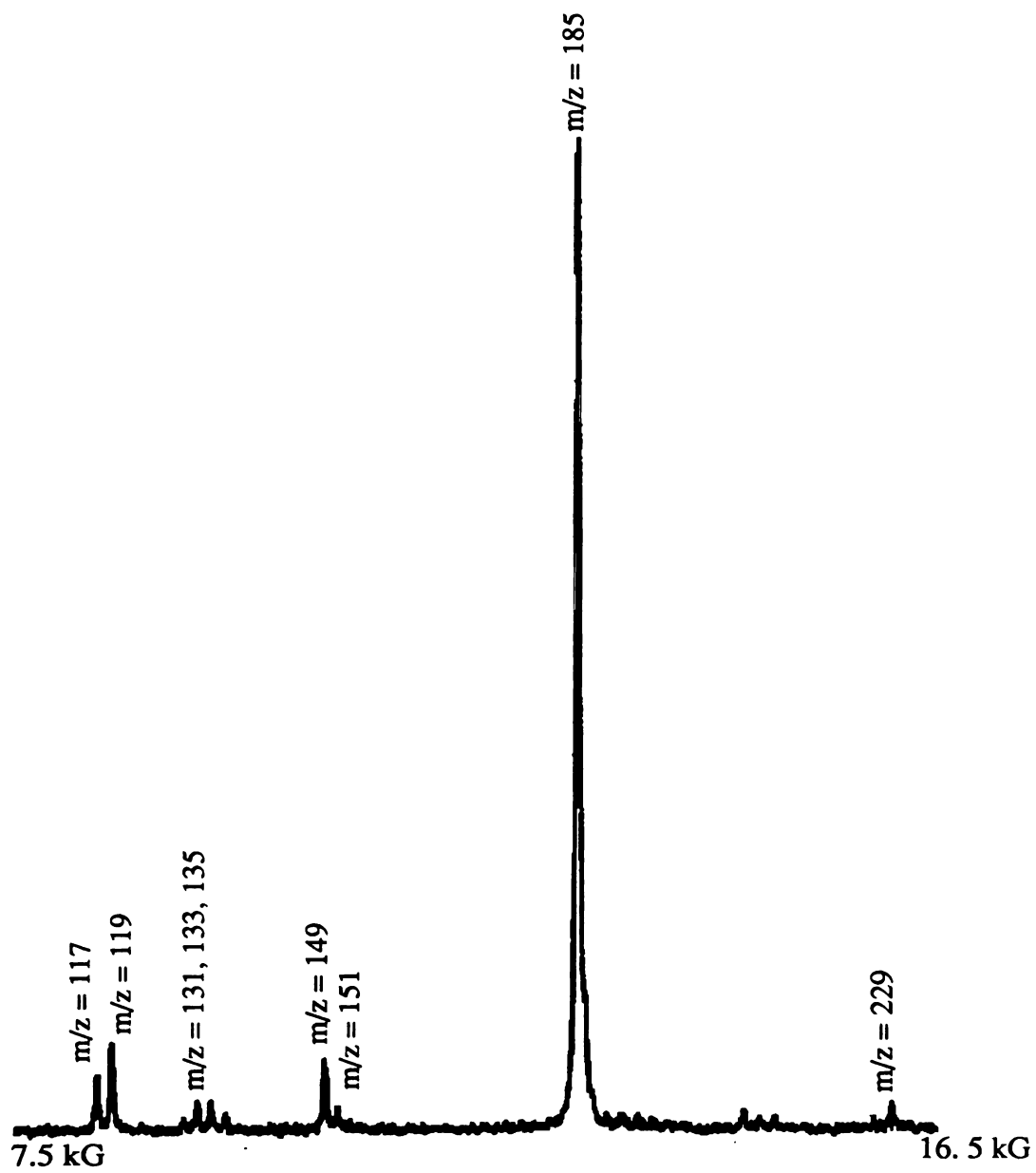


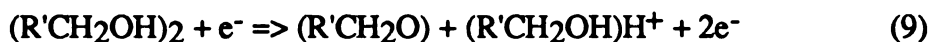
**Figure 2.14: The High Mass Ions of Glycerol**

**Table 2.4: The High Mass Ions in the ICR Mass Spectrum of Glycerol**

Mass in Daltons	Relative Intensity (Corrected for Mass)
117	88
119	115
131	46
133	51
135	22
149	95
151	28
185	1000
241	47
277	34

The double resonance studies of the high mass ions of glycerol proved that all of the ions except  $m/z = 131, 133, 135$  and  $151$  are products of ion-molecule reactions.

Alcohol clusters form protonated alcohol molecules when ionized. The formation of the protonated alcohol molecules occurs as shown in Equation 9.<sup>10</sup>



In the case of glycerol the R' group is  $(HOH_2CCHOH)$ . The 50:50 mixture study of glycerol and deuterated glycerol showed that the proton transferred to form the  $(G+H)^+$  ion did not come from glycerol's carbon skeleton since the ICR mass spectra did not have a peak representing the  $(G+D)^+$  ion ( $m/z = 94$ ). The transfer of the hydroxyl protons of glycerol is the same transfer observed for all of the other alcohols except methanol.<sup>10</sup> The glycerol dimer does not form many fragment ions upon ionization. The fragment ions detected at  $m/z = 93, 131, 133, 135$  and  $151$  are from the glycerol dimer or the protonated glycerol dimer.

The protonated clusters of methanol, ethanol and 1-propanol undergo a condensation reaction shown in Equation 10.<sup>10, 18</sup>



Ethanol can also form  $R_2OH^+$  by an ion-molecule reaction with protonated ethanol. No ions formed by the condensation reaction (Equation 10) of the protonated or unprotonated glycerol dimers were detected.

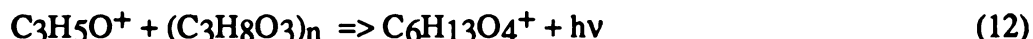
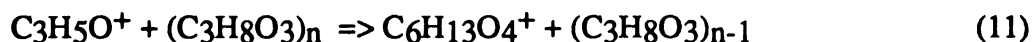
The fragmentation patterns of other alcohol dimers show that fragment ions are formed by the alpha cleavage reaction of one of the alcohol molecules in the dimer. The fragment ion of the alpha cleavage reaction remains bound to the other alcohol molecule. Examples of this type of cluster ion are the fragment ions of 1-propanol, 1-butanol and 1-pentanol. These alcohols form ions of the type  $(ROH)_nCH_2OH^+$ .<sup>10</sup> Secondary alcohols such as 2-propanol and 2-butanol form ions of the type  $(ROH)_nCH_3CHOH^+$ .<sup>10</sup> The cluster ion formed by t-butyl alcohol is  $(ROH)_n(CH_3)_2COH^+$ .<sup>10</sup> The product ions of the alpha cleavage reaction of glycerol are  $m/z = 31$  ( $CH_2OH^+$ ) and  $m/z = 61$  ( $HOCH_2CHOH^+$ ). The cluster ions of a glycerol molecule bound to the  $CH_2OH^+$  or the  $HOCH_2CHOH^+$  fragment ions would have  $m/z$  values of 123 or 153. No ions with these  $m/z$  values were detected. The only possible cluster ion of a known glycerol fragment ion and glycerol is the  $m/z = 135$  ion. The  $m/z = 135$  ion could be a  $G + m/z = 43$  ion.

The lack of fragment ions that are complexed with glycerol molecules may be due to the temperature of the glycerol. In the other alcohol cluster experiments, the alcohol vapor was adiabatically expanded and cooled. In the glycerol experiments, the liquid glycerol is heated to vaporize enough glycerol to maintain a moderate pressure. The heated glycerol dimer or cluster may fall apart upon ionization since its vibrational modes have more energy than the ground state.

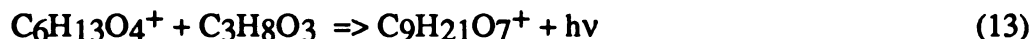
The ion-molecule reactions that form the  $C_5H_9O_3^+$  ( $m/z = 117$ ) ion and the  $C_5H_{11}O_3^+$  ( $m/z = 119$ ) ion have been discussed previously. The ion-molecule reactions discussed in this sections are the formation of higher mass glycerol containing cluster ions.

In the double resonance experiments, no ionic precursors were detected for the  $m/z = 133$  and  $m/z = 135$  ions. The low relative intensities of these ions may explain why no ionic precursors were detected.

The  $m/z = 57$  ion ( $C_3H_5O^+$ ) reacts with glycerol clusters to form the  $m/z = 149$  ion ( $C_6H_{13}O_4^+$ ). The  $C_3H_5O^+$  ion could combine with a glycerol molecule and emit an infra-red photon.<sup>5</sup>



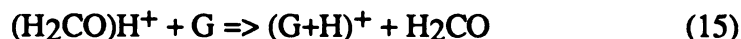
The low relative intensity of the  $m/z = 151$  ion may explain its lack of a detectable ionic precursor. The double resonance study of the  $m/z = 185$  and  $277$  ions has been discussed previously. The  $m/z = 241$  ion is a cluster formed by the reaction of the  $m/z = 149$  ion and glycerol clusters. Equations 13 and 14 show the possible reactions.



The double resonance response is weak. Only 10% fewer of the  $m/z = 241$  ions are detected when the  $m/z = 149$  ions are ejected.

### Proton Transfers from the Fragment Ions

No ion-molecule reactions with glycerol were observed for the  $m/z = 31$  ion. The  $m/z = 31$  ion ( $CH_3O^+$ ) can be viewed as a protonated formaldehyde molecule. The gas phase proton affinity of formaldehyde is 718 kilo Joules/mole.<sup>16</sup> The gas phase proton affinity of glycerol is 874 Kilo joules/mole.<sup>16</sup> The protonated formaldehyde should be able to transfer a proton to the glycerol, Equation 15.



The proton transfer, equation 15, is exothermic by 156 kilo Joules/mole.<sup>16</sup>

The lack of a detectable proton transfer by the  $m/z = 31$  ion may be due to the ion having a  $\text{H}_3\text{C-O}^+$  structure. This ion is 139 kilo Joules/mole higher in energy than the protonated formaldehyde.<sup>19</sup> The  $\text{H}_3\text{CO}^+$  ion should be able to transfer a proton to the glycerol. The reaction is exothermic by 17 kilo Joules/mole.<sup>16</sup> The  $m/z = 31$  ion ( $\text{CH}_3\text{O}^+$ ) does not protonate glycerol. The low relative intensity (57) of the  $\text{CH}_3\text{O}^+$  ion and the weak double resonance responses found for the  $(\text{G+H})^+$  ion may explain why this was not detected. The companion ion  $m/z = 33$  ( $\text{CD}_2\text{HO}^+$ ) did not protonate either glycerol or  $\text{d}_5$ glycerol in the 50:50 mixture experiment. Double resonance studies of the protonated glycerol dimer show that ( $\text{CH}_3\text{O}^+$ ) does not protonate glycerol dimers.

The  $m/z = 43$  ion has an empirical formula of  $\text{C}_2\text{H}_3\text{O}$ . If the  $\text{C}_2\text{H}_3\text{O}^+$  ion transferred a proton to glycerol, the neutral molecule would have a composition of  $\text{C}_2\text{H}_2\text{O}$ . The proposed neutral is a ketene ( $\text{H}_2\text{C}=\text{C}=\text{O}$ ). The proton affinity of the ketene is 825.5 kilo Joules/mole.<sup>16</sup> No proton transfer to glycerol monomers was detected. Proton transfer to the glycerol dimer occurs. The  $\text{C}_2\text{H}_3\text{O}^+$  ion undergoes a condensation reaction with glycerol.

The  $m/z = 44$  ion has a empirical formula of  $\text{C}_2\text{H}_4\text{O}$  and protonates glycerol and glycerol dimers. The proton affinity of the  $\text{CH}_3\text{CO}$  neutral formed upon proton transfer has been estimated to be between 657 and 828 kilo Joules/mole.<sup>16</sup> The proton transfer reaction is exothermic by 46 to 217 kilo Joules/mole.

The  $\text{C}_3\text{H}_5\text{O}^+$  ion ( $m/z = 57$ ) does not transfer a proton to a glycerol molecule or to a glycerol dimer. The proton affinity of the acylium ion ( $\text{CH}_3\text{CH}_2\text{C}=\text{O}^+$ ) is 834 kilo Joules/mole.<sup>16</sup> The other stable structure of the  $\text{C}_3\text{H}_5\text{O}^+$  ion is the hydroxycarbenium ( $\text{CH}_2=\text{CHCH}=\text{OH}^+$ ). The hydroxycarbenium ( $\text{CH}_2=\text{CHCH}=\text{OH}^+$ ) ion has a proton affinity of 811 kilo Joules/mole.<sup>16</sup>

The  $m/z = 61$  ion has a proposed structure of  $(\text{HOCH}_2\text{-CHO})\text{H}^+$ . The  $m/z = 61$  ion has a proton affinity of less than 874 kilo Joules/mole since it can transfer a proton to glycerol. The  $m/z = 61$  ion does not protonate the glycerol dimer. A possible explanation

of this fact is that the irradiating oscillator's frequency is almost exactly 3 times the frequency of the marginal oscillator. The signal detected by the marginal oscillator breaks up at this harmonic frequency. The signal breakup could obscure a weak double resonance response.

The  $m/z = 75$  ion has an empirical formula of  $C_3H_7O_2$ . A proposed structure of this ion is  $(HOCH_2C(OH)=CH_2)H^+$ . This structure is a protonated alcohol. The only ion-molecule reaction observed for the  $m/z = 75$  ( $C_3H_7O_2^+$ ) ion is the transfer of a proton to a glycerol dimer to form the  $(G_2+H)^+$  ion. The proton affinity of the alcohol is less than the proton affinity of the glycerol dimer. The  $m/z = 75$  ion is formed by the dehydration of the  $(G+H)^+$  ion.

## Conclusions

The principal source of the protonated glycerol molecules is the fragmentation of glycerol dimers upon EI ionization. The glycerol dimer exists as a proton transfer complex with a structure  $(HOCH_2CHOHCH_2OH_2^+ \cdots OH_2CCHOHCH_2OH^-)$ . The heated glycerol dimers fall apart upon ionization yielding only minor fragment ions with masses above 93 Daltons. Evidence for the existence of the dimer is the proton transfer from the  $(G+H)^+$  ion to form the  $((G-d_5)_2+H)^+$  ion. The proton transfer from the  $(G-d_5+H)^+$  ion to a glycerol dimer forms the  $(G_2+H)^+$  ion.

The weak double resonance response of the  $(G_3+H)^+$  ion may be due to its primary source being the ionization of  $G_4$  clusters. A more probable explanation of the glycerol data is that the  $(G_3+H)^+$  is the product of successive additions of glycerol to the protonated glycerol molecule. A fraction of the protonated glycerol molecules react to form protonated dimers. Some of the protonated dimer reacts further to form a protonated trimer. The successive additions can explain the monotonic decrease of relative intensity of the  $(G+H)^+$ ,  $(G_2+H)^+$ , and  $(G_3+H)^+$  ions. Setting the relative

intensity of the  $(G+H)^+$  ion as 1000, the  $(G_2+H)^+$  ion has a relative intensity of 610 and the  $(G_3+H)^+$  ion has a relative intensity of 20. The data for the relative intensity of ionized methanol clusters does not show either a rapid or monotonic decrease in ion intensity with increasing cluster size. See Figure 2.15.<sup>11</sup> The weak double resonance response observed for the  $(G_3+H)^+$  ion is due to the very low relative intensity of the ion and not to the existence of  $G_4$  neutral clusters.

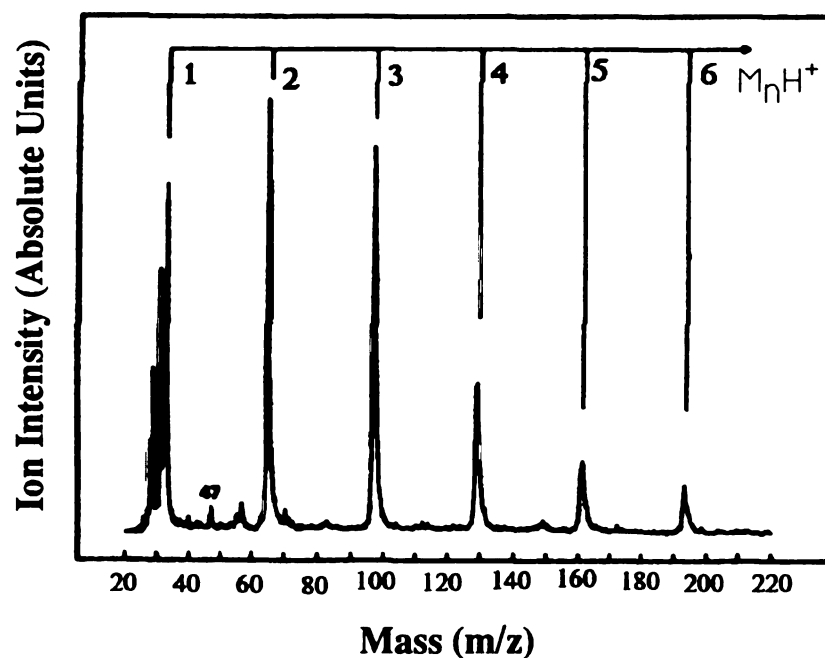


**Figure 2.15: The Relative Intensity of the Cluster Ions of Methanol vs.  $n$ , the number of Methanols ( $M$ ) in the Cluster**

The ions of glycerol undergo few ion-molecule reactions except for the addition to glycerol. A condensation reaction between glycerol and the abundant  $C_2H_3O^+$  ion occurs. The  $C_3H_5O^+$  ion reacts with glycerol to form formaldehyde and the  $C_8H_{11}O_3^+$  ion.

## References

- 1) Stenhagen, E., Abrahamsson, S.; Atlas of Mass Spectral Data, *Volume 1*, John Wiley & Sons, 1969
- 2) a) Stenhagen, E., Abrahamsson, S.; Registry of Mass Spectral Data, *Volume 1*, John Wiley & Sons, 1970
- 3) Bojeson, G., M?ller, M., *Int. J. Mass Spectrom. Ion Processes*, 1986, 68, 239
- 4) McLafferty, F. W., Interpretation of Mass Spectra, 3rd edition, University Science Books, 1980
- 5) Beauchamp, J. L., Caseiro, M. C.; *J. Amer. Chem. Soc.*, 1972, 94, 2638
- 6) The 1,1, 2, 3, 3-d<sub>5</sub> glycerol was obtained from Cambridge Isotope Laboratories. The deuterium content was reported as 98%. The deuterons are reported to be attached to the carbon atoms.
- 7) Fricke, J., Jackson, W. M., Fite, W. L., *J. Chem. Phys.*, 1972, 57, 580
- 8) Shinohara, H., Nishi, N., Washida, N., *J. Chem. Phys.*, 1986, 84, 5561
- 9) Stace, A. J., Shukla, A. K., *J. Phys. Chem.*, 1982, 86, 865
- 10) Stace, A. J., Shukla, A. K., *J. Phys. Chem.*, 1988, 92, 2579
- 11) Lee, S. Y., Shin, D. N., Cho, S. G., Jung, K., Jung, K. W., *J. Mass Spectrom.*, 1995, 30, 969
- 12) Rollgen, F. W., Beckey, H. D. Z., *Naturforsch., A: Phys., Phys. Chem., Kosmophys.*, 1974, 29A, 230
- 13) C. Dass, *Org. Mass Spectrom.*, 1994, 29, 475
- 14) F. W. McLafferty, J. Wachs, C. Koppel, P. P. Dymerski, F. M. Bockhoff, *Adv. Mass Spectrom.*, 1978, 7, 231

- 15) a) Zwinselman, J. J., Harrison, A. G., *Org. Mass Spectrom.*, **1984**, *19*, 573  
b) Bouchoux, G., *Org. Mass Spectrom.*, **1985**, *20*, 154, c) Bouchard, G.,  
Hoppilliard, Y., Flammang, R., Maquestiau, A., Meyrant, P., *Org. Mass  
Spectrom.*, **1983**, *18*, 340, d) Hudson, C. E., McAdoo, D. J., *Org. Mass  
Spectrom.*, **1982**, *17*, 366, e) Turecek, F., Hanus, V., Gumann, T., *Int. J. Mass  
Spec. Ion Proc.*, **1986**, *69*, 217
- 16) Lias, S. G., Bartmess, J. E., Liebman, J. E., Holmes, J. L., Levin, R. D., Marland,  
W. G.; *J. Phys. Chem. Ref. Data*, **1988**, *17*, Suppl. 1
- 17) Eberlin, M., Majumdar, T. K., Cooks, R. G., *J. Am. Chem. Soc.*, **1992**, *114*, 2884
- 18) Stace, A. J., Shukla, A. K., *J. Amer. Chem. Soc.*, **1982**, *104*, 5314-18
- 19) Allison, J., Szekely, G.; *In press*

## **Chapter Three:**

### **The Studies of the Negative Ions of Glycerol**

#### **The Formation of the Negative Ions**

The negative ions of glycerol are formed by bombarding the vaporized glycerol with low energy electrons. The electrons were emitted by the hot rhenium filament and accelerated by a 1.00 to 8.00 volt difference between the filament voltage and the trapping plate voltages. The voltages of the trapping plates were negative to prevent the negative ions formed from being neutralized. The voltages of the drift plates were adjusted to cause the negative ions to drift to the analyzer region.

Negative ions are formed by the interaction of electrons with neutral molecules. Three different classes of mechanisms for negative ion formation are known.<sup>1,2</sup> For electrons of very low kinetic energies (near 0 eV), the electron attaches itself to the molecule. This mechanism is called nondissociative electron capture. The resulting anion may emit a photon to stabilize the electron-molecule complex. Equation 1 shows nondissociative capture of an electron by a molecule (AB).<sup>1</sup>



Equation 2 is the simple radiative attachment of an electron to the AB molecule.<sup>2</sup>



As the kinetic energy of the electrons increases, the mechanism of negative ion formation changes. The higher energy electron is captured by the molecule and the resulting anion fragments. This mechanism is called dissociative electron capture. Dissociative electron capture occurs for electrons with kinetic energies above 0 eV to

approximately 15 eV.<sup>1</sup> Equations 3 and 4 show the dissociative electron capture of an electron by the molecule AB.



As the kinetic energy of the electron increases above approximately 10 eV, the electron is no longer captured by the molecule. The impact of the high energy electron merely excites the molecule AB to an electronic level that leads to the production of a positive ion and a negative ion. This mechanism is called ion pair production. Equations 5 and 6 show a high energy electron making an ion pair from the molecule AB.



The electron energies used in the ICR experiments were large enough so that only the dissociative electron capture and the ion pair production mechanisms formed the anions. The experimental evidence to support this finding is that no molecular ions of glycerol or of a glycerol cluster were detected. The attachment of an electron to a glycerol molecule could occur at several different sites. Attachment of the electron to one of the sigma bonds (C-C, C-H, C-O, O-H) in the glycerol molecule would place the electron in a sigma anti bonding orbital and lead to the formation of a radical and an anion. The oxygen atoms are the most electronegative atoms in the glycerol molecule. The oxygen atom is the preferred site for electron attachment in the glycerol molecule. The electron cannot attach itself to the filled lone pairs of the oxygen atoms. If the electron attached to the C-O bond the glycerol anion could fragment into an OH radicals and an  $m/z = 75$  anion. No  $m/z = 75$  or 17 ( $OH^-$ ) anions were detected. If the electron attaches to the O-H bond, either a alkoxide radical and a hydride anion or a H atom (the radical part) and an alkoxide anion can form. The lower mass limit used in the ICR experiments is too high for a hydride anion to be detected. Only the alkoxide anion of

glycerol ( $m/z = 91$ ) was detected in the ICR mass spectrum of glycerol. Other alcohols such as ethanol, propanol, isopropanol and t-butyl alcohol also form alkoxide anions.<sup>3,4</sup>

### The Negative Ion ICR Mass Spectrum of Glycerol

The fragment anions detected by the ICR are recorded in the negative ion ICR mass spectrum of glycerol. These fragment anions have  $m/z$  values of 91, 89, 88, 87, 72 and 47 Daltons. Table 3.1 shows the possible compositions of these anions.

Table 3.1: The Compositions of the Fragment Anions of Glycerol

Mass in Daltons	Possible Elemental Compositions
91	$C_3H_7O_3^-$
89	$C_3H_5O_3^-$
88	$C_3H_4O_3^-$
87	$C_3H_3O_3^-$
72	$C_2O_3^-$
72	$C_3H_4O_2^-$
47	$C_2H_7O^-$
47	$CH_3O_2^-$

Figure 3.1 shows the low mass ICR spectrum of the anions of glycerol. The  $m/z = 91$  ion,  $(G-H)^-$ , is an alkoxide anion of glycerol. The loss of 2 to 4 more hydrogen atoms yields the  $m/z = 89, 88$  and  $87$  anions. The loss of  $H_2$  from alkoxide anions has been reported by R. N. Hayes et al.<sup>3</sup> The alkoxide anions  $EtO^-$ ,  $PrO^-$ , and  $i-PrO^-$  were observed to eliminate  $H_2$  to form enolate anions. The enolate anions have a

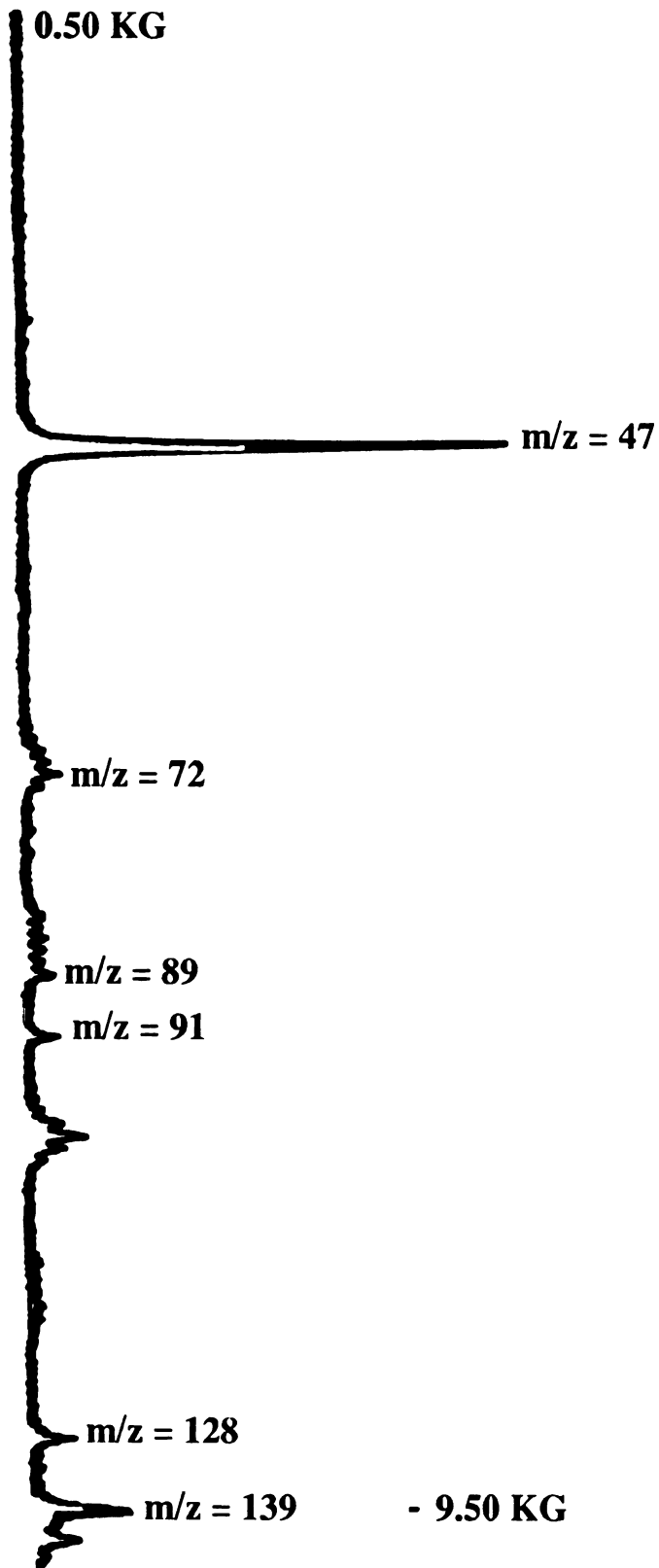


**Figure 3.1: The Low Mass Anions of Glycerol**

R-CH<sub>2</sub>=CHO<sup>-</sup> structure.<sup>3</sup> The proposed structure for the m/z = 89 anion is an enolate structure. The m/z = 89 anion, (M-3)<sup>-</sup>, may arise from the pyrolysis of glycerol by the thoriated iridium ion gauge filament or the rhenium electron beam filament. Caldwell et al.<sup>5</sup> reported the loss of H<sub>2</sub> by primary and secondary alcohols due to the pyrolysis of the alcohols by the hot filaments in their ICR. Most of the pyrolysis occurred at the ion gauge filament since it had a much larger surface area than the surface area of the electron beam filament. The pyrolyzed alcohols were deprotonated by OH<sup>-</sup> Negative Ion Chemical Ionization (NICI) and formed (M-3)<sup>-</sup> anions with enolate structures. Deuterium labeled alcohols revealed that the (M-3)<sup>-</sup> anion is formed by the loss of one hydroxyl proton and one α and one ' hydrogen atom. The hydrogen atom and proton losses reported by Caldwell et al.<sup>5</sup> support the stability of the proposed enolate structure for the m/z = 89 anion of glycerol. The m/z = 87 anions may have an enolate structure. The possible structures of the m/z = 89, 88 and 87 anions are shown in Figure 3.2.

The m/z = 72 anion, (M-20)<sup>-</sup>, has two possible compositions. The possible (C<sub>2</sub>O<sub>3</sub>)<sup>-</sup> anion has not been reported by other researchers. The (C<sub>3</sub>H<sub>4</sub>O<sub>2</sub>)<sup>-</sup> anion was detected by Gross et al.<sup>6</sup> in the study of the anions of glycerol generated by fast atom bombardment. Tandem mass spectrometry was used to identify the m/z = 72 anion as (G-H-H<sub>2</sub>O-H)<sup>-</sup>.<sup>6</sup>

The base peak in the low mass ICR spectrum of glycerol is the m/z = 47 anion, (M-45)<sup>-</sup>. This ion has two possible compositions of (CH<sub>3</sub>O<sub>2</sub>)<sup>-</sup> or (C<sub>2</sub>H<sub>7</sub>O)<sup>-</sup>. The (C<sub>2</sub>H<sub>7</sub>O)<sup>-</sup> anions' structure is CH<sub>3</sub>CH<sub>2</sub>-OH<sub>2</sub><sup>-</sup>. This proposed structure requires the O atom's atomic orbitals to have a dsp<sup>3</sup> configuration. The (CH<sub>3</sub>O<sub>2</sub>)<sup>-</sup> anion has a HO-CH<sub>2</sub>-O<sup>-</sup> structure. The m/z = 47 anion can be formed from the (G-H)<sup>-</sup> ion by the loss of CO<sub>2</sub> or by the loss of C<sub>2</sub>H<sub>4</sub>O. The loss of C<sub>2</sub>H<sub>4</sub>O could occur as the loss of C<sub>2</sub>H<sub>4</sub>O or the loss of H<sub>2</sub>O and acetylene in a concerted fashion. The negative ion ICR spectrum (Figure 3.1) does not have peaks corresponding to the (G-H-H<sub>2</sub>O)<sup>-</sup> or (G-H-C<sub>2</sub>H<sub>2</sub>)<sup>-</sup> anions that would be detected if the losses of H<sub>2</sub>O and acetylene were not

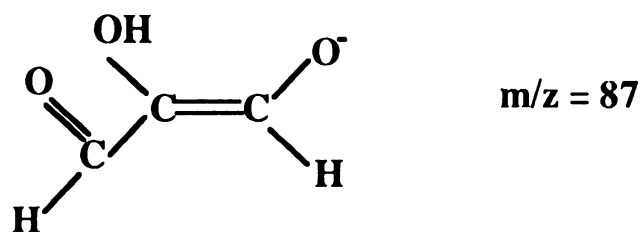
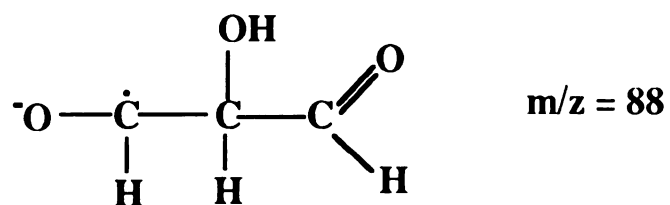
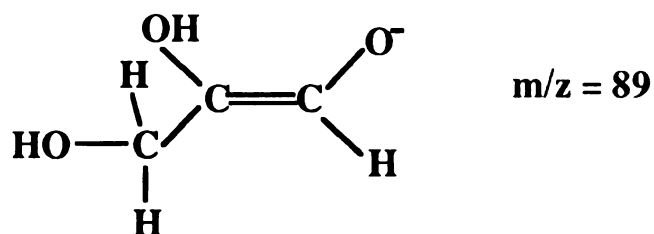


**Figure 3.2: Proposed Structures for the  $(C_3H_5O_3)^-$ ,  $(C_3H_4O_3)^-$ , and  $(C_3H_3O_3)^-$  Ions**

concerted. Figure 3.3 shows a proposed concerted mechanism for the loss of H<sub>2</sub>O and acetylene. The proposed mechanism for the loss of C<sub>2</sub>H<sub>4</sub>O by the (G-H)<sup>-</sup> anion is shown in Figure 3.4.

### A Comparison of the Negative Ion Mass Spectra of Glycerol and Ethylene Glycol

Lloyd et al.<sup>7</sup> studied the ionization reactions and the hydrogen-deuterium exchange reactions in mono- and dialcohol alkoxide anions. Ethylene glycol was first ionized using Negative Ion Chemical Ionization with O<sup>-</sup> as the reagent ion. The "fragment" ions detected are  $m/z = 58$  (C<sub>2</sub>H<sub>2</sub>O<sub>2</sub>)<sup>-</sup> and  $m/z = 45$  (CHO<sub>2</sub>)<sup>-</sup>. The  $m/z = 58$  anion, (M-4), is formed in an ion-molecule reaction. The O<sup>-</sup> ion reacts with ethylene glycol removing two hydrogen atoms to form water. Two more hydrogen atom are lost by the ethylene glycol to form H<sub>2</sub>. The  $m/z = 45$  anion is formed by an ion-molecule reaction between the O<sup>-</sup> ion and ethylene glycol. The mechanism proposed by Lloyd et al.<sup>7</sup> for the ion-molecule reaction is shown in Figure 3.5. The ethylene glycol molecule is cleaved at the C-C bond and the O<sup>-</sup> ion adds to the one half of the molecule. The resulting  $m/z = 47$  anion (CH<sub>3</sub>O<sub>2</sub>)<sup>-</sup> loses H<sub>2</sub> to form the  $m/z = 45$  anion. The fact that the  $m/z = 47$  anion is not detected in the NICI mass spectra of glycerol does not support the idea that the  $m/z = 47$  anion is a stable anion. However, the H<sub>2</sub> loss by the  $m/z = 47$  anion may be due to the ion being formed in an ion-molecule reaction. The  $m/z = 47$  anion may need to release the excess energy from its' formation by eliminating H<sub>2</sub> to form the stable  $m/z = 45$  anion.

Lloyd et al.<sup>7</sup> also ionized ethylene glycol using Negative Ion Chemical Ionization with OH<sup>-</sup> as the reagent ion. The OH<sup>-</sup> ion NICI mass spectrum has peaks representing ions with  $m/z$  values of 61, 59, 58, 45, and 43 Daltons. Lloyd et al.<sup>7</sup> attribute the source the  $m/z = 58$  anions and some of the  $m/z = 45$  anions to the previously described

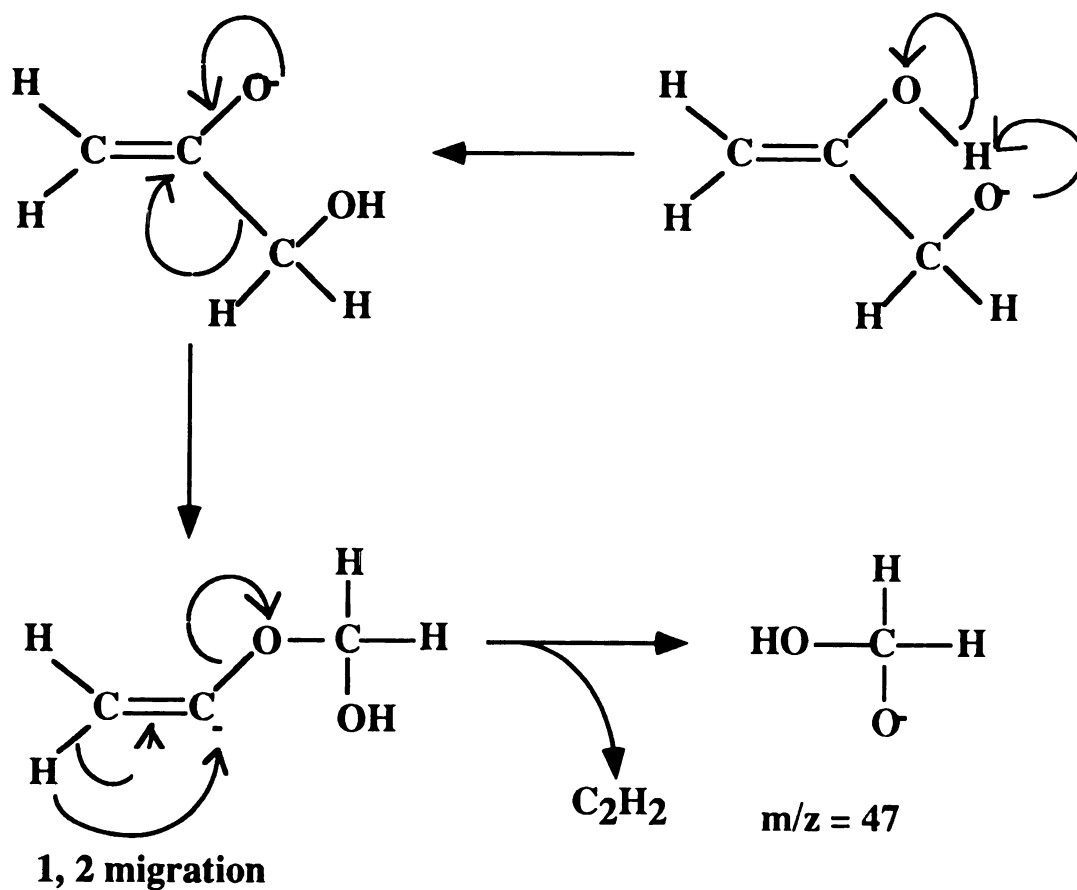
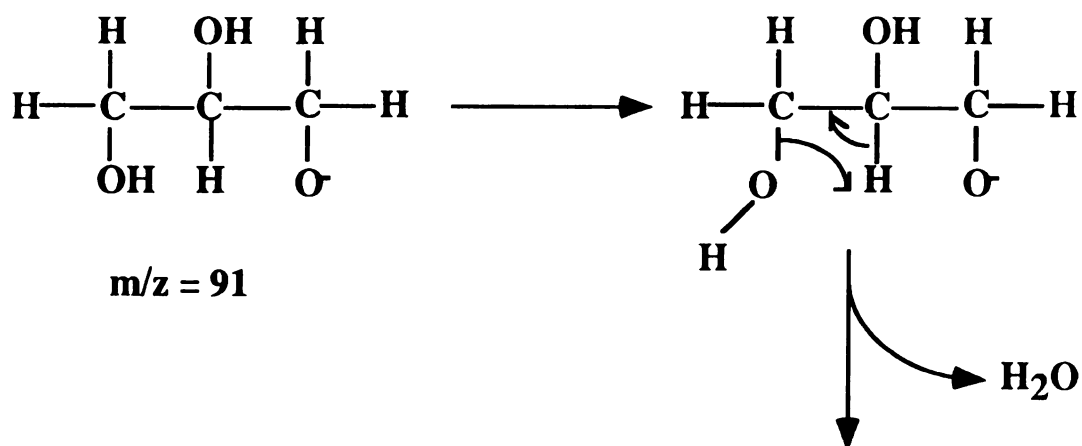


**Figure 3.3: The Proposed Concerted Loss Fragmentation Mechanism**

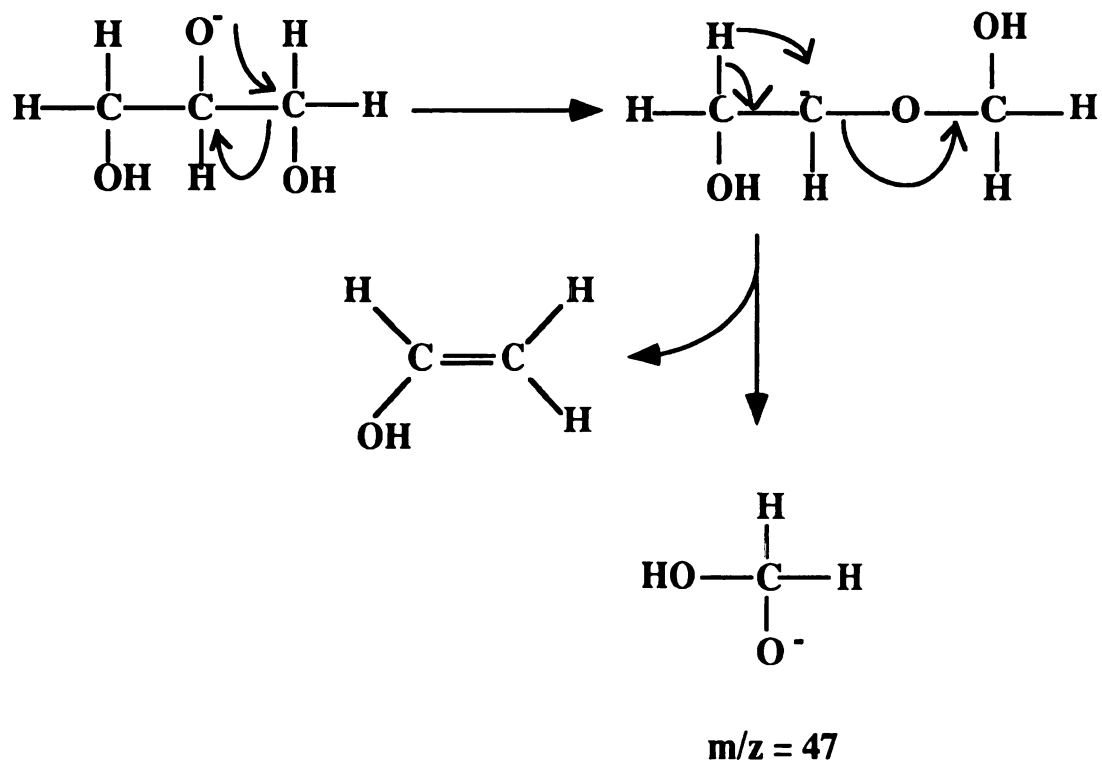


**Figure 3.4: A Proposed Formation Mechanism for the  $m/z = 47$  anion**



ion-molecule reactions with traces of the  $O^{\cdot-}$  ion in the NICI source. The  $OH^-$  reagent ion can also form the  $m/z = 45$  anion by an ion-molecule reaction analogous to that shown in Figure 3.5. The  $m/z = 61$  anion is an alkoxide anion formed by proton abstraction. The  $m/z = 61$  anion can lose  $H_2$  to form the  $m/z = 59$  anion. The  $m/z = 61$  anion can also lose  $H_2O$  to form the  $m/z = 43$  anion.

Neither the  $OH^-$  or the  $O^{\cdot-}$  Negative Ion Chemical Ionization mass spectra of ethylene glycol are similar to the negative ion EI mass spectrum of glycerol. The  $O^{\cdot-}$  ion NICI spectrum lacks the  $(M-1)^-$  and  $(M-3)^-$  anions detected with the other two ionization methods. In addition, the  $(M-4)^-$  ion is of low abundance in the EI mass spectrum of glycerol. The  $m/z = 58$   $(M-4)^-$  anion is the most abundant fragment anion in the  $O^{\cdot-}$  ion NICI mass spectrum. The EI mass spectrum of glycerol lacks anions analogous to the  $m/z = 45$   $(M-17)^-$  and  $m/z = 43$   $(M-19)^-$  anions detected by the NICI of ethylene glycol. The only ion detected in this region of the EI mass spectrum of glycerol is the  $m/z = 72$  ion  $(G-H-H_2O-H)^-$ . There is no corresponding  $m/z = 42$  ion in the NICI mass spectra of ethylene glycol. The  $m/z = 47$  anion  $(CH_3O_2)^-$  of glycerol is a proposed intermediate in the NICI fragmentation mechanisms but is not detected. The comparison of the NICI mass spectra of ethylene glycol with the EI mass spectra of glycerol did not reveal any common fragmentation mechanisms or any unusually stable ion structures. In conclusion, the NICI mass spectra of ethylene glycol have few similarities to the EI mass spectrum of glycerol due to the dominant ionization mechanism in NICI being ion-molecule reactions.

### **The High Mass Anions of Glycerol**

The higher mass negative ions detected in the negative ion ICR spectrum of glycerol are ion-molecule reaction products and fragment ions of glycerol clusters. Figure 3.6 shows the ICR mass spectrum of the high mass anions of glycerol. These

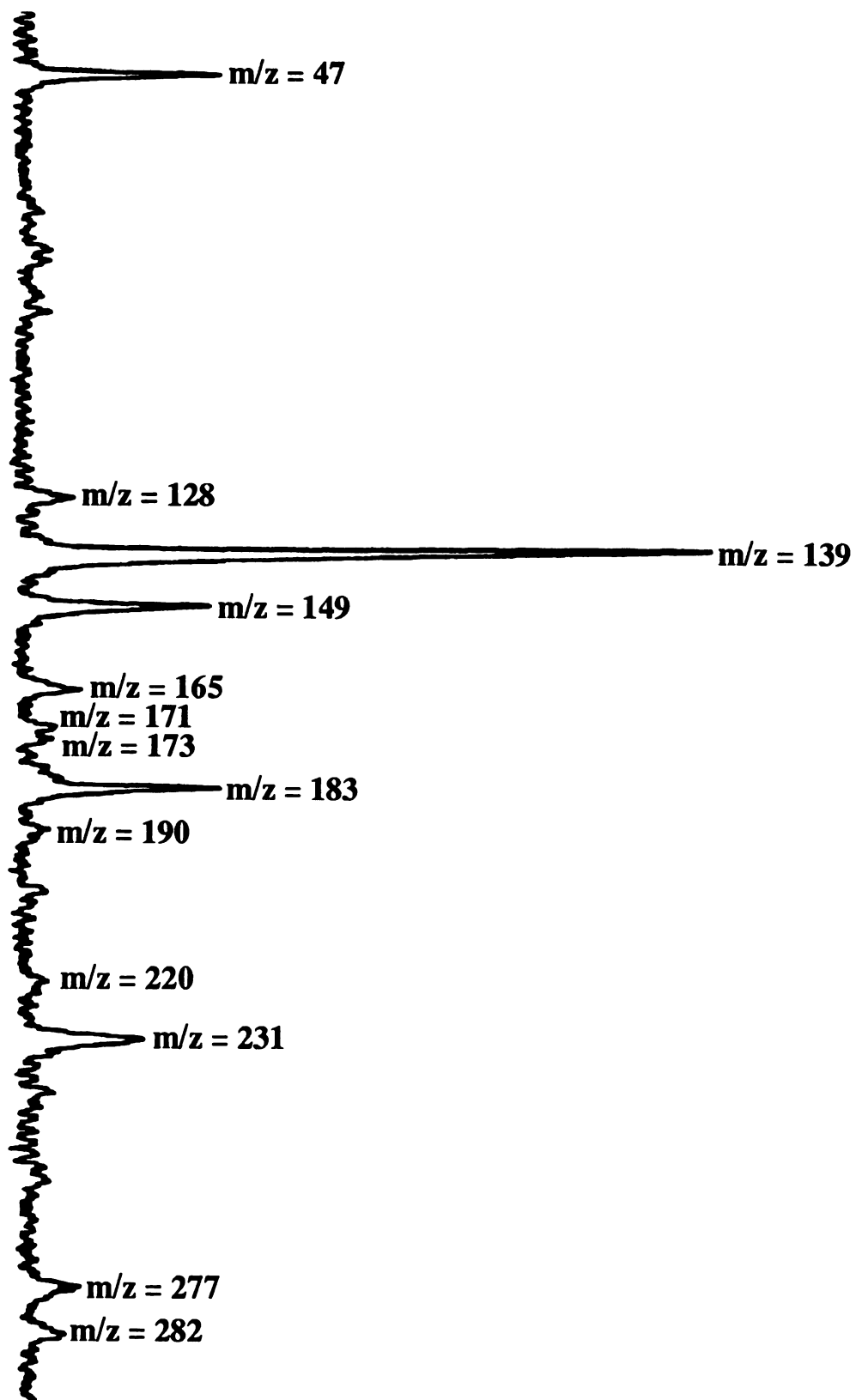


**Figure 3.6 : The High Mass Anions of Glycerol**

anions have  $m/z$  values of 128, 139, 149, 165, 183, 190, 220, 231, 275 and 282. Double resonance studies of these anions determined that the  $m/z = 128$  and  $m/z = 149$  anions are not products of ion-molecule reactions.

### The Evidence for the Existence of Glycerol Clusters

The existence of clusters in the gas phase is demonstrated by the detection of anions of 128 Daltons and 149 Daltons that are not products of ion-molecule reactions. These ions are fragment anions of clustered glycerols which are most likely dimers. Further evidence for the existence of gas phase glycerol clusters are the ion-molecule reactions that form the  $m/z = 165$  and  $m/z = 190$  anions. The  $m/z = 165$  anion could be formed by the  $m/z = 72$  anion reacting with a glycerol dimer and the loss of a neutral or neutrals of mass 91. The  $m/z = 165$  anion is 93 Daltons heavier than its only ionic precursor, the  $m/z = 72$  anion. The ionic precursor to the  $m/z = 190$  anion is the  $m/z = 47$  anion. The only way the  $m/z = 47$  anion can form the  $m/z = 190$  anion in one step is to react with a glycerol dimer or an even larger glycerol cluster.

The glycerol derived anions undergo ion-molecule reactions to cluster with neutral glycerol molecules or glycerol clusters. The anion-glycerol clusters stabilize by emitting a photon or ejecting neutral glycerol molecules. Equations 7 and 8 show the ion-molecule reactions for an arbitrary anion ( $A^-$ ).



Both the  $m/z = 47$  and  $m/z = 91$  anions form glycerol adducts. The resulting adducts are the  $m/z = 139$  anion and the  $m/z = 183$  anion ( $G_2-H$ )<sup>-</sup>. These anions,  $m/z = 139$  and ( $G_2-H$ )<sup>-</sup>, cluster with glycerol to form the  $m/z = 231$  and  $m/z = 275$  ( $G_3-H$ )<sup>-</sup> anions.

The fragment anion  $m/z = 128$  complexes with glycerol to form the  $m/z = 220$  anion. The  $m/z = 190$  ion complexes with glycerol to form the  $m/z = 282$  anion.

### **A Comparison of FAB and EI Mass Spectra of Glycerol**

The EI mass spectrum of the negative ions of glycerol has few similarities to the negative ion FAB mass spectrum. The principal low mass fragment ion,  $m/z = 47$ , was not detected by Gross et al.<sup>6</sup> Only the  $m/z = 91$  and  $89$  anions are generated by both ionization methods. Table 3.2 is a comparison of the composition of the positive ions generated by EI with the negative ions generated by FAB. Some of the fragment ions generated by EI have a similar sequence of  $m/z$  values as the anions generated in FAB. The  $m/z = 91$   $(G-H)^-$  is the negative ion analog to the  $(G+H)^+$  ion. The difference is that the negative ions all have two less hydrogen atoms than their positive ion counterparts. The fragmentation mechanisms of the anions generated in FAB may be similar to the fragmentation mechanisms of the positive ions generated by electron impact ionization.

In the high mass ICR spectrum of glycerol, six anions with  $m/z$  values of 128, 139, 190, 220, 231 and 282 Daltons are detected but are not reported in the FAB mass spectrum. Anions of the type  $(G_n-H)^-$  were detected in both the negative ion FAB mass spectrum and the ICR mass spectrum of glycerol. In conclusion, most of the ions formed by FAB are formed by different mechanisms than the anions generated by the EI ionization of glycerol.

**Table 3.2: A Comparison of the Positive Fragment Ions of Glycerol Generated in EI with the Negative Fragment Ions of Glycerol Generated in FAB**

Positive Ions Generated in EI

Negative Ions Generated in FAB

Mass in Daltons	Compositon	Mass in Daltons	Composition
93	(G+H) <sup>+</sup>	91	(G-H) <sup>-</sup>
		89	(G-3H) <sup>-</sup>
75	C <sub>3</sub> H <sub>7</sub> O <sub>2</sub> <sup>+</sup>	73	C <sub>3</sub> H <sub>5</sub> O <sub>2</sub> <sup>-</sup>
		71	C <sub>3</sub> H <sub>3</sub> O <sub>2</sub> <sup>-</sup>
61	C <sub>2</sub> H <sub>5</sub> O <sub>2</sub> <sup>+</sup>	59	C <sub>2</sub> H <sub>3</sub> O <sub>2</sub> <sup>-</sup>
		58	C <sub>2</sub> H <sub>2</sub> O <sub>2</sub> <sup>-</sup>
45	C <sub>2</sub> H <sub>5</sub> O <sup>+</sup>	43	C <sub>2</sub> H <sub>3</sub> O <sup>-</sup>
43	C <sub>2</sub> H <sub>3</sub> O <sup>+</sup>	41	C <sub>2</sub> HO <sup>-</sup>

### Mass-to-Charge Ratio Verification

The masses of the anions of glycerol were confirmed by mixed carbon tetrachloride/glycerol and carbon tetrabromide/glycerol studies. When a halocarbon such as carbon tetrachloride is bombarded by low energy electrons, chloride anions are formed by dissociative electron capture. Equation 9 shows the reaction to form the chloride anions.



These chloride anions are the only ions detected in the negative ion ICR mass spectrum of carbon tetrachloride. The mass spectrum of carbon tetrabromide is analogous with only bromide anions being formed. The chloride and bromide anions were used as calibration anions to determine the masses of the fragment anions of glycerol.

The chloride and bromide anions complex with gas phase glycerol to form (GCl)<sup>-</sup> and (GBr)<sup>-</sup> anions. No (G<sub>2</sub>Cl)<sup>-</sup> or (G<sub>2</sub>Br)<sup>-</sup> anions were detected. Equations 10 and 11 show the possible ion-molecule reactions for the chloride anion.



The masses of the complexes were confirmed by the double resonance studies of the halide-glycerol adducts. For example, the maximum suppression of the glycerol-chloride<sup>35</sup> anion occurred with a frequency ratio of 0.276 or 35/127. These ion-molecule reactions were used to produce mass marker anions to confirm the masses of the higher mass anions of glycerol.

## References

- 1) Bowie, J. H. *Mass Spectrom. Rev.* **1984**, *3*, 161
- 2) Melton, Charles E., *Principles of Mass Spectrometry and Negative Ions*, Marcel Dekker, Inc., **1970**
- 3) Hayes, R. N.; Sheldon, J. C.; Bowie, J. H.; Lewis, D. E. *J. Chem. Soc., Chem. Comm.* **1984**, 1431
- 4) Brauman, J. I.; Tumas, W.; Foster, R. F.; Pellerite, M. J. *J. Am. Chem. Soc.* **1983**, *105*, 7464
- 5) Caldwell, G.; Bartmess, J. E. *Int. J. Mass Spectrom. Ion Phy.* **1981**, *40*, 269
- 6) Gross, M. L.; Caldwell, K. A. *J. Am. Soc. Mass Spectrom.* **1994**, *5*, 72
- 7) Lloyd, J. R.; Agosta, W. C.; Field, F. H. *J. Org. Chem.* **1980**, *45*, 3483

## **Chapter Four: The Experimental Section**

### **The Theory of Ion Cyclotron Resonance Spectrometry**

#### **Introduction**

Ion cyclotron resonance (ICR) mass spectrometry is a technique well suited to the study of thermal energy ion-molecule reactions. Ion cyclotron resonance spectrometers trap ions in crossed electric and magnetic fields. The trapped ions collide with gas phase molecules and may undergo ion-molecule reactions. The ICR mass spectrometer detects the product ions of the ion-molecule reactions and can be used to determine which of the trapped ions reacted.

Ion trapping in an ICR is based on the phenomenon that a charged particle with a velocity component perpendicular to an uniform magnetic field travels in a circular orbit. The size of the orbit of the charged particle depends on its mass-to-charge ratio, its velocity, and the strength of the magnetic field. This phenomenon was utilized to determine the mass-to-charge ratio of a proton. Hipple, Sommer and Thomas built a specialized mass spectrometer called an omegatron to determine the mass-to-charge ratio of the proton in 1949.<sup>1</sup> The omegatron was the forerunner to the modern ICR mass spectrometer.

The first conventional ICR spectrometer was marketed by Varian and Associates in 1966. An ion cyclotron resonance spectrometer can trap ions for several milliseconds in crossed electric and magnetic fields.<sup>2</sup> The ions react by colliding with gas phase molecules to produce product ions. The ICR technique of double resonance allows the

experimenter to determine which ions are the precursors to the product ions. Ion cyclotron resonance mass spectrometry has been extensively reviewed in the literature.<sup>2,3</sup>

### Ion Motion in an ICR

Ion cyclotron resonance mass spectrometry is based on the behavior of a charged particle in crossed electric(**E**) and magnetic(**B**) fields. A charged particle with a velocity perpendicular to a uniform magnetic field(**B**) is confined to a circular orbit with a cyclotron frequency,  $\omega_c$ , in the plane normal to **B**. The particle is subject to a force that is perpendicular to both the velocity of the particle and the magnetic field. See Figure 4.1.

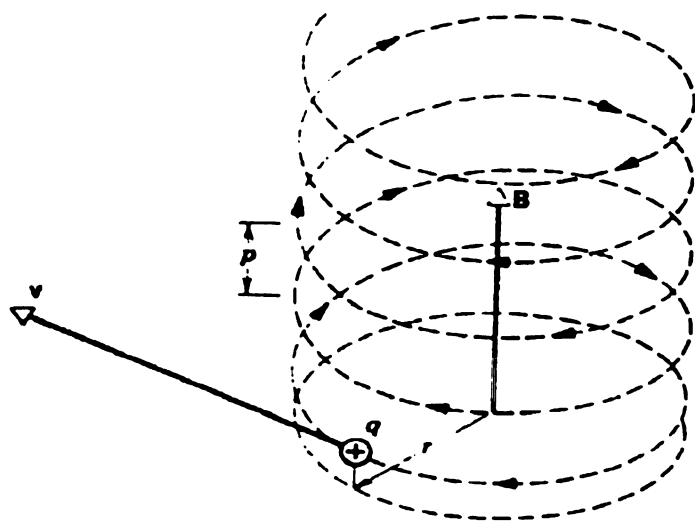


**Figure 4.1: The Path of a Positive Ion in a Uniform Magnetic Field<sup>4</sup>**

Equation 1 shows how the magnitude of the centrifugal force on the particle is proportional to the charge(**q**), the perpendicular velocity(**v**) and the magnetic field.

$$\mathbf{F} = q\mathbf{v}\mathbf{B} \quad (1)$$

The centrifugal force on an object in a circular orbit is given by  $F = mv^2/r$ . The mass of the object is  $m$  and  $r$  is the radius of the orbit. Substitution into Equation 1 yields Equation 2.

$$\frac{mv^2}{r} = qvB \quad (2)$$

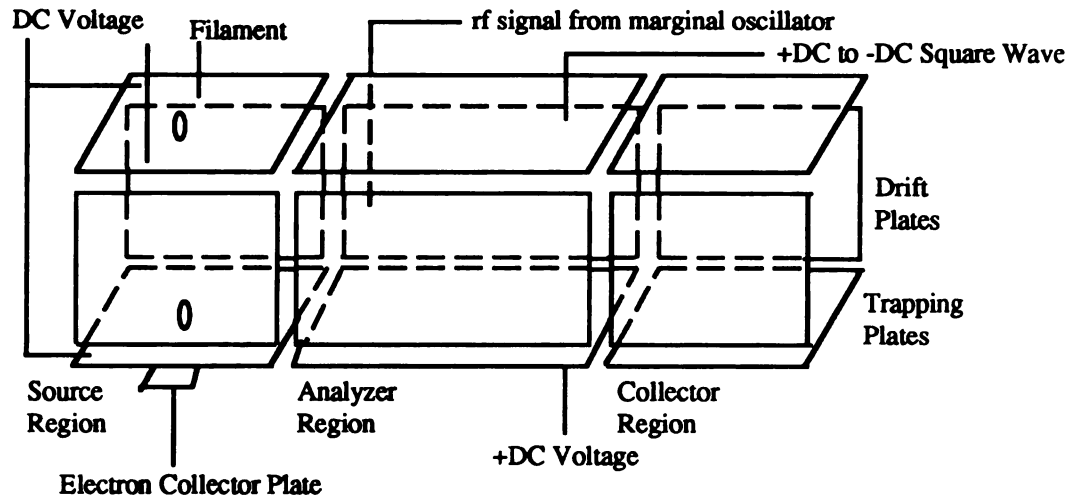
The cyclotron frequency (in radians/sec),  $\omega_c$ , is the ratio of ion velocity divided by the orbit radius ( $v/r$ ). Substitution and rearrangement of Equation 2 yields Equation 3.

$$\omega_c = \frac{v}{r} = \frac{qB}{m} \quad (3)$$

The ICR at MSU has a fixed frequency detector and scans the magnetic field strength to detect various  $m/z$  values. At the correct magnetic field value, the cyclotron frequency,  $\omega_c$ , of some ion and the detector's frequency are the same. This condition is called resonance. Equation 4 illustrates the relationship between the mass-to-charge ratio and the magnetic field.

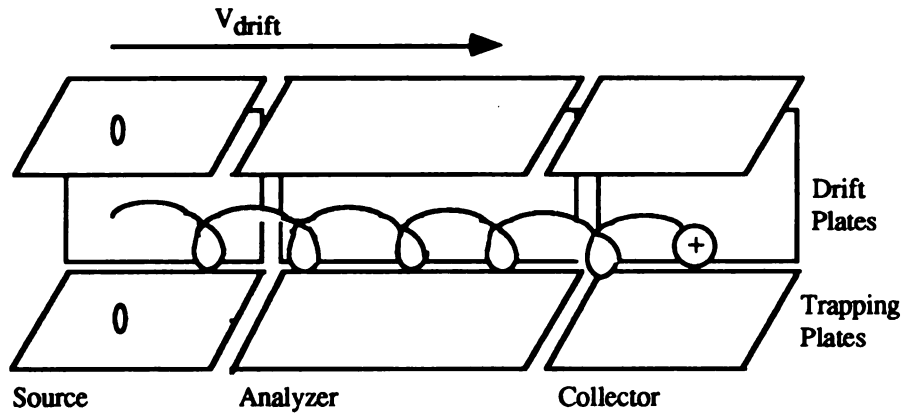
$$B = \frac{m\omega_c}{q} \quad (4)$$

Figure 4.2 shows the ICR cell.



**Figure 4. 2: The ICR Cell**

The ICR cell has three sections. The source is the section where the ions are generated. A beam of electrons is emitted by a rhenium filament and focused into a beam by the magnetic field. The filament is held at a large negative voltage relative to the ground of the ICR cell. This electric field accelerates the electrons before they pass through the source. The ions are generated by electron impact ionization. The trapping plates in the source are held at a dc voltage. The combined electric fields of the four source plates create a potential well to contain the ions generated. After being formed in the source region of the ICR cell, a perpendicular set of electric and magnetic fields superimposes a drift velocity on the orbiting ion. Figure 4.3 shows the cycloid path of a drifting ion in an ICR cell.



**Figure 4.3: The Cycloidal Path of a Drifting Ion in the ICR Cell**

The drift velocity( $v_d$ ) is calculated using Equation 5.

$$v_d = E/B \quad (5)$$

The ions drift through the analyzer section of the ICR cell and then into the collector region.

The ions are generated in the source region of the cell and drift out of the source region continuously. This mode of ICR operation is called the drift mode. The time the drifting ion takes to traverse the cell can be determined.<sup>5</sup>

The analyzer section is where the ions are detected. The ICR's detector is a marginal oscillator. The ions are detected in the analyzer section by measuring the power absorbed by the ions in resonance with the detector. The ac signal from the marginal oscillator is added to the dc voltage applied to a drift plate in the analyzer section.

The trapping plates in the analyzer section have different voltages applied to each plate. The bottom trapping plate is held at a dc voltage. A 20 Hz square wave is applied to the top trapping plate. The voltage of the square wave varies from the -dc to the dc

voltage applied to the bottom trapping plate. The purpose of the square wave is to improve the signal-to-noise ratio by signal modulation.

The last section of the ICR cell is the collector section where the ions are neutralized by a pair of collector plates. The collector plate current is measured to determine the number of ions traversing the cell and is a great help in tuning the ICR.

### **Ions in Resonance**

The basis of ion detection in ICR is the phenomenon of resonance. If an orbiting ion is irradiated with an rf field that has the same frequency as the ion's cyclotron frequency, the ion absorbs energy from the rf field. The resonant ion's kinetic energy and velocity increase. Figure 4.4 shows the path of a resonant ion. The marginal oscillator detects the ions by measuring the amount of energy absorbed by the ions in resonance. The amount of energy a resonant ion can absorb is limited by the dimensions of the ICR cell. As the ion absorbs power, the radius of the ion's orbit must increase in order to maintain the same cyclotron frequency. When the ion strikes the walls of the ICR cell it is neutralized. The amount of energy absorbed by resonant ions is proportional to their number and  $m/z$  value.

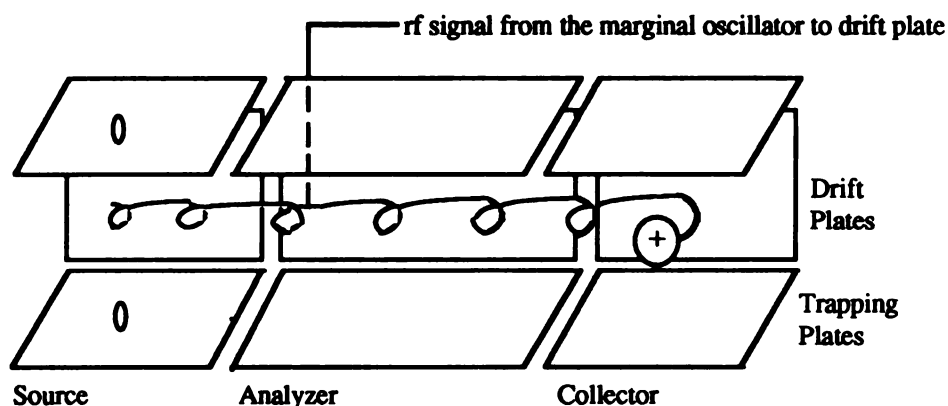


**Figure 4.4: Ion in Resonance in the ICR cell**

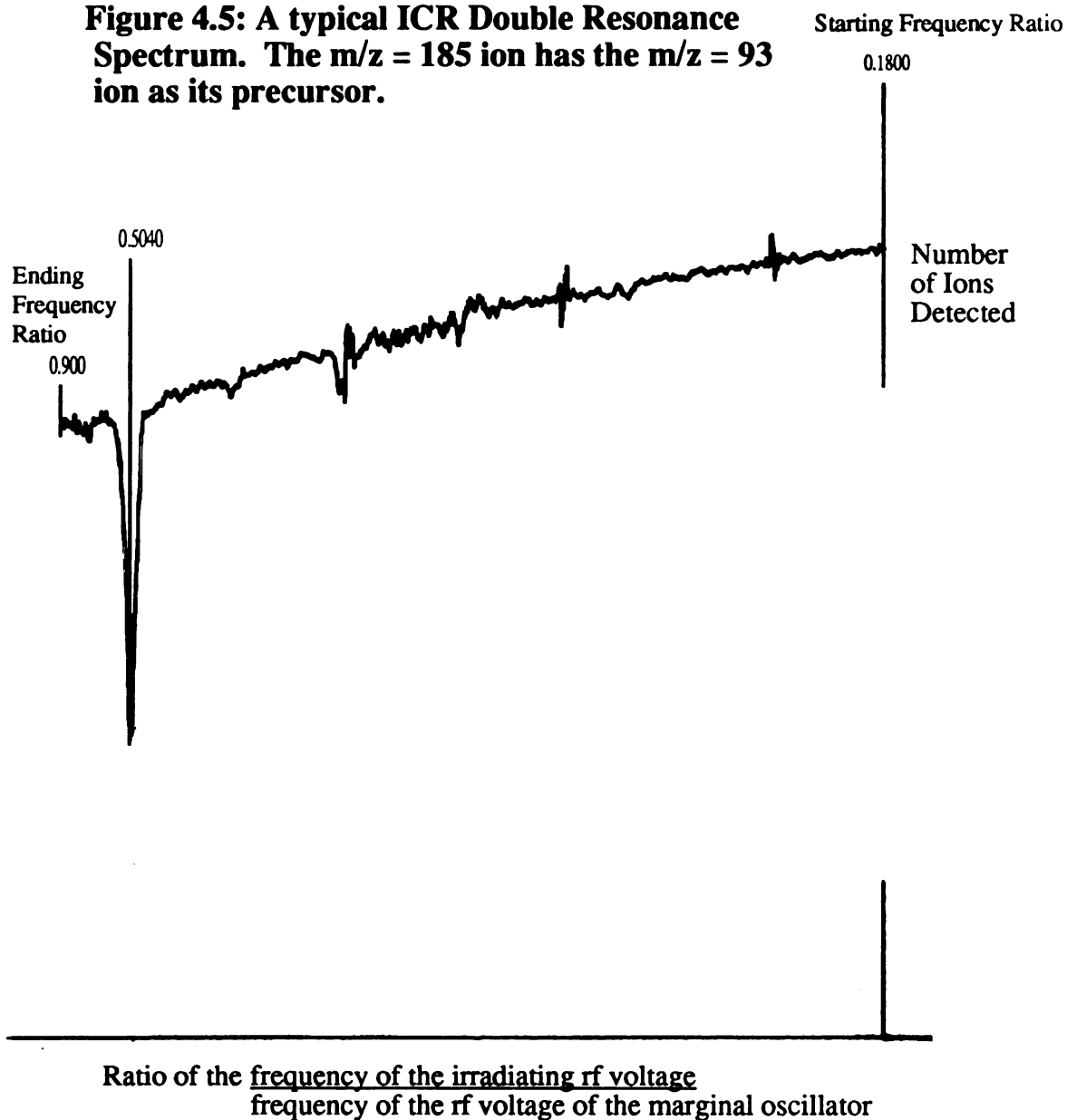
### Double Resonance Experiments

Irradiating a resonant ion until it is neutralized is called ion ejection. Ion ejection is the basis of the double resonance technique for determining the precursors of the product ions. The double resonance technique uses two rf fields to place ions in resonance. The product ion is monitored by the fixed frequency of the marginal oscillator. The frequency of the second rf field is varied, ejecting the potential precursor ions sequentially according to their resonant frequencies. When the precursor ion is ejected, fewer product ions are formed to be detected by the marginal oscillator. The double resonance spectrum shows a decrease in the relative intensity of the product ion when a precursor ion is ejected.

Figure 4.5 is a typical spectrum from a double resonance experiment. Figure 4.5 is a plot of the number of ions detected (the y-axis) vs. the frequency ratio (the x-axis). This frequency ratio is the ratio of the frequency of the irradiating rf voltage divided by the frequency of the rf voltage of the marginal oscillator. When the irradiating oscillator is at the frequency that ejects the precursor ions, the number of product ions detected is reduced. This causes the downward spike seen in Figure 4.5. The frequency ratio at the

minimum of the spike corresponds to the ratio of the  $m/z$  values of the precursor ion divided by the product ion. In Figure 4.5, the precursor ion is  $(G + H)^+$  ( $m/z = 93$ ) and the product ion is  $(G_2 + H)^+$  ( $m/z = 185$ ). The ratio of the  $m/z$  values is  $93/185 = 0.5040$ . This is the frequency ratio measured at the minimum of the double resonance spectrum in Figure 4.5.

**Figure 4.5: A typical ICR Double Resonance Spectrum. The  $m/z = 185$  ion has the  $m/z = 93$  ion as its precursor.**



The typical double resonance experiment starts by ejecting ions with  $m/z$  values of 18% of the  $m/z$  value of the product ion and sequentially ejects heavier ions up to precursor ions with  $m/z$  values of 90% of that of the product ion.

### The Marginal Oscillator

The ions in the ICR cell are detected by a marginal oscillator. To detect the ions, the marginal oscillator creates a rf field of a known radio frequency into the cell. The resonant ions absorb energy from the rf field and the marginal oscillator measures the amount of energy absorbed. The equivalent circuit of the marginal oscillator is shown in Figure 4.6.<sup>6</sup>

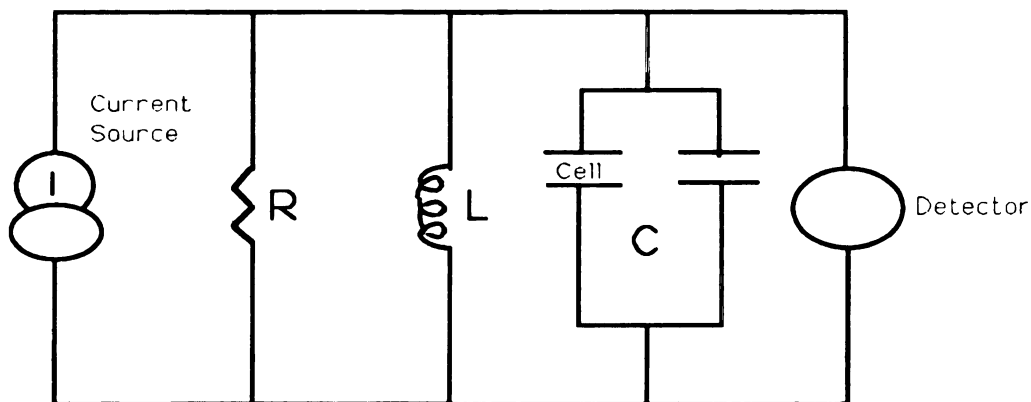


**Figure 4.6: The equivalent circuit of the LC tank circuit used in the Marginal Oscillator Detector**

The constant current generator  $I$  drives a parallel LC tank circuit at its resonant frequency  $\omega_0$ . The plates of the ICR cell form part of the capacitance of the LC circuit. When the ions in the ICR cell are in resonance with the LC circuit a voltage difference is generated across the detector(D). The voltage difference( $\Delta V$ ) is given by equation 6,<sup>5</sup>

$$\Delta V = (QA/V_0) (L/C)^{1/2} \quad (6)$$

where  $A$  is the power absorbed by the ions,  $V_0$  is the voltage of the tank circuit when no ions are present and  $Q$  is the quality factor of the circuit. Equation 7 is the definition of  $Q$  for a parallel LC circuit.<sup>5</sup>

$$Q = R/\omega_0 L = R(C/L)^{1/2} \quad (7)$$

A block diagram of the marginal oscillator detector used in the ICR is shown in Figure 4.7.<sup>5</sup> When ions are in resonance, the demodulator outputs a 20 Hz square wave signal that is observed on the oscilloscope.

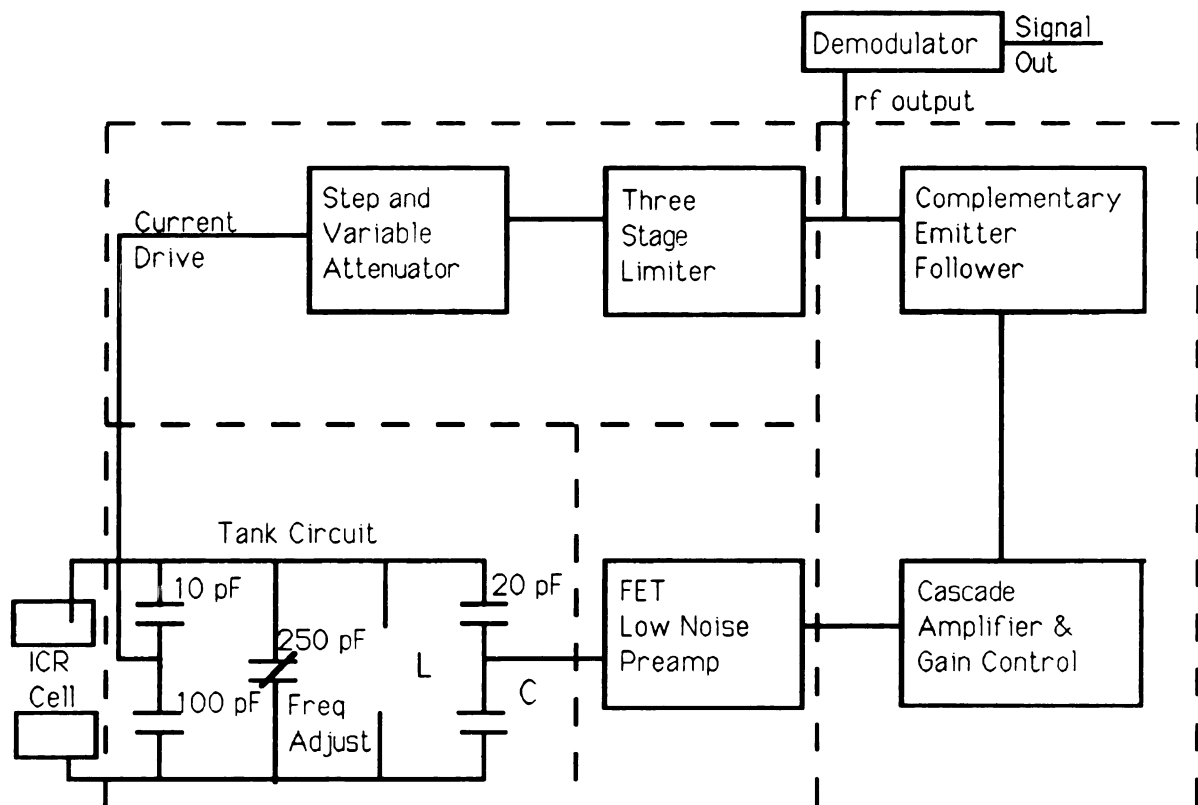


**Figure 4.7: Block Diagram of the Marginal Oscillator**

### Block Diagram of the ICR

Figure 4.8 is the block diagram of the ICR at Michigan State University.

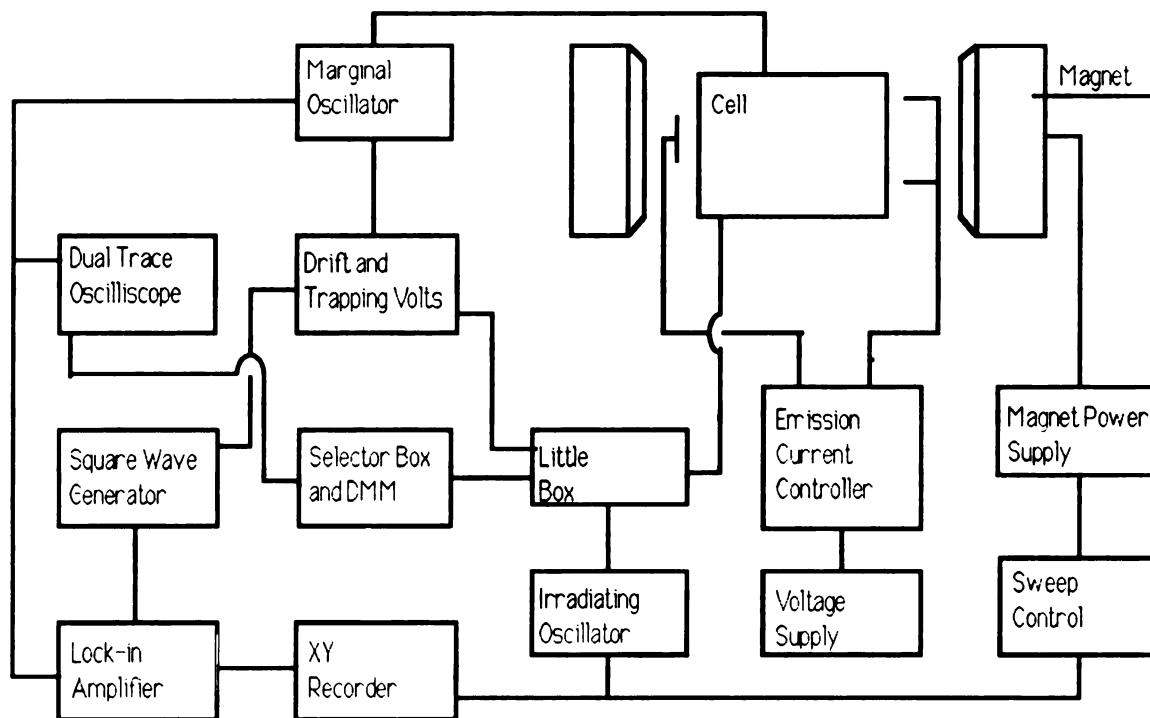


**Figure 4.8: The Block Diagram of the Ion Cyclotron Resonance Spectrometer at Michigan State University**

The ICR has a cell located in a t-shaped vacuum chamber between the poles of the electromagnet. The vacuum chamber is connected to a right angle isolation valve by a 4 inch stainless steel line. A refrigerated trap and a Varian 4 inch diffusion pump is used to pump the chamber down to  $5.0 \times 10^{-7}$  torr. The normal operating pressure of the ICR is  $5.0$  to  $15.0 \times 10^{-6}$  torr. The pressures are monitored using a Bayer-Alpert ionization gauge and a Veeco Instruments model 1000/1002 gauge controller.

A leak valve and a sample vial is attached to the bottom of the vacuum chamber. This leak valve was used to leak chlorobenzene and bromobenzene into the ICR to calibrate the mass scale of the ICR in the negative ion mode. The chlorobenzene and bromobenzene are a source of chloride and bromide anions in the negative ion ICR experiments.

bromobenzene are a source of chloride and bromide anions in the negative ion ICR experiments.

The  $m/z$  values of the positive ions of glycerol were determined by mixing naphthalene with the glycerol. The positive ions of the naphthalene were used as mass markers to calibrate the mass range of the ICR.

The glycerol sample is placed in a capillary tube and spun with a centrifuge. The capillary tube is inserted into the ICR on a direct insertion probe. The probe tip was heated using a TRIAC controller. There was no regulation of the temperature of the probe tip. The TRIAC controller was set to a fixed value determined by the pressure of the glycerol desired in the ICR. The inlet tube to the ICR cell was heated to prevent condensation of the glycerol.

### **Chemicals Used in the Experiments**

The glycerol was reagent grade and manufactured by Matheson, Coleman and Bell. The 1,1, 2, 3, 3- $d_5$  glycerol was obtained from Cambridge Isotope Laboratories. The deuterium content was reported as 98%.

Naphthalene from Mallinckrodt, Inc. was used as a mass marker to calibrate the mass range of the ICR in the positive ion experiments. Chlorobenzene and bromobenzene from Fisher Scientific was used to calibrate the mass range of the ICR in the negative ion experiments.

### **REFERENCES**

- 1) Sommer, H.; Thomas, H. A.; Hipple, J. A. *Phy. Rev.* **1951**, *82*, 697
- 2) Lehman, T. A.; Bursey, M. M. *Ion Cyclotron Resonance Spectrometry*, Wiley, New York, **1976**
- 3) Budzikiewicz, H. *Mass Spectrom. Rev.* **1987**, *6*, 329

- 4) Halliday, D.; Resnick, R. *Fundamentals of Physics*, 3rd Edition, John Wiley & Sons, 1988, 694
- 5) McMahon, T. B.; Beauchamp, J. L. *Rev. Sci. Instrum.* 1971, 42, 1632
- 6) Warrnick, A.; Anders, L. R.; Sharp, T. E. *Rev. Sci. Instrum.* 1974, 45, 929

## **Chapter Five:**

### **The Appendix**

#### **Detailed Description of the ICR Components**

This appendix is a short description of the electronic components that make up the ICR at Michigan State University. The procedure to obtain a typical spectrum is also given.

**Electromagnet** The ICR uses a Varian V7300 12" electromagnet. The electromagnet has a normal operating range from 0 to 23 kilo Gauss. The magnet is controlled by a Varian FIELDIAL magnet controller which senses the magnetic field using a Hall probe. The magnet was calibrated and its true field(y) can be calculated from the field dial setting(x) by  $y = 1.2572 x + 0.005$ .

**Magnet Power Supply** The V 7X00/E-7X00 regulated Magnet Power Supply is designed for spectrometers requiring a stable magnetic field. The power supply can power the electromagnet to field strengths of up to 23 kilo Gauss. The magnet and the power supply are water cooled by a Haskris heat exchanger which exchanges heat with by tap water. The normal operating temperature of the magnet and the power supply is between 16 and 27 degrees centigrade.

**Emission Current Controller** The emission current controller was designed and built by Marty Rabb. The controller regulates either the filament current(filament mode) or the current of the ionizing electrons passing through the ICR cell(feedback mode). The emission current controller maintains a negative bias on the filament with reference to the ICR cell ground. The bias voltage is supplied by a Hewlett-Packard 6299A DC power supply through a BNC connector on the emission current controller.

**Keithley Picoammeter** A Keithley model 480 picoammeter is used to measure the ionizing current passing through the ICR cell. The picoammeter converts the current into a DC voltage used by the emission current controller to regulate the ionizing current.

**Plate Voltage Controls** The voltages applied to the eight plates of the ICR cell are controlled from a panel on the front of the ICR. The four drift plates have dc voltages from -3 to 3 volts supplied from the control panel. The ICR cell source trapping plates are both have the same dc voltage of -10 to 10 volts selected from the control panel. The analyzer section trapping plates have one trapping plate regulated to a dc voltage. The other trapping plate is pulsed with a 20 Hz square wave with an amplitude that varies from the -dc to the dc voltage applied to the other trapping plate.

**Little Box** The "little box" mounts on the 20 pin feedthrough and makes the connections from the control panel to the ICR cell. The rf voltage used to do double resonance experiments is added to one or both of the top drift plate dc voltages through the little box. The filament on/off switch and connections for filament power and for the ionizing current measurement are on the front of the little box. The little box supplies the dc voltage to the marginal oscillator. This dc voltage is added to the rf signal applied to the analyzer section's bottom drift plate. A ribbon cable from the little box to a selector

box on the control panel allows the signals actually applied to the ICR plates to be monitored.

**Digital Multimeter** A Tektronix DM 502A autoranging digital multimeter is used to monitor the signals being sent to the plates of the ICR cell. The plate to be monitored is selected by a set of eight switches in a selector box. The selected plate voltage signals can also be displayed on the oscilloscope.

**Function Generator** A Tektronix CFG 250 was used as a rf voltage generator to supply the variable frequency rf voltage used in double resonance experiments. The CFG 250 has a voltage controlled frequency output. The frequency is swept by applying a dc voltage from the x-axis of the chart recorder to the voltage controlled gain port of the CFG 250. The irradiating rf voltage's amplitude is adjustable.

**Universal Counter** A Tektronix DC 503 Universal Counter is used to determine the frequency of the rf signal generated by the marginal oscillator. The DC 503 is also used to determine the ratio of the frequencies of the rf signal of the marginal oscillator to the rf voltage of the double resonance oscillator.

**Marginal Oscillator** The ICR's detector is a marginal oscillator. The marginal oscillator detector was built by Marty Rabb. The frequency and the amplitude of the sine wave in the marginal oscillator is variable. The normal frequency is 138 kilo Hertz. Lower frequencies are used to detect higher mass ions. The marginal oscillator is attached to the top drift analyzer plate through a BNC connector on the 6 inch flange.

**Function Generator** A Tektronix FG 504 function generator is used to generate the 20 Hz square wave that is used to pulse the trapping plates and to provide the reference signal to the lock-in amplifier.

**Lock-in Amplifier** An EG&G Princeton Applied Research model 128A lock-in amplifier is used to amplify and improve the signal to noise ratio of the signal from the marginal oscillator. The lock-in amplifier uses the same 20 Hz square wave as the trapping plate circuits as a reference signal. The 128A subtracts the signal it receives from the marginal oscillator at the top of the square wave from signal the 128A receives from the marginal oscillator at the bottom of the square wave. The difference in signal intensities is the signal due to the detection of ions. The output of the lock-in amplifier drives the y-axis of the xy chart recorder.

**Chart Recorder** A Soltec xy recorder is used to plot the results of the ICR experiments.

**Oscilloscope** A Tektronix model 455 dual trace oscilloscope is used to display the output of the marginal oscillator. The amplitude of the irradiating rf voltage can also be determined. The voltages and wave forms actually reaching the plates of the ICR cell can also be observed.

**Keithley Electrometer** The Keithley model 610C electrometer is used to monitor the current of the ions that drift through the ICR cell. The electrometer is connected to four ion collector plates at the bottom of the ICR cell through a BNC connector on the 6 inch flange.

**Ionization Gauge Controller** A Veeco RG 1000 ionization gauge controller with a Bayer-Alpert ionization gauge is used to monitor the pressure in the ICR.

## The Procedure for a Typical ICR Experiment with Glycerol

### Positive Ion Spectra

The glycerol sample in a capillary tube is placed on a direct probe and inserted into the heated inlet arm to the ICR cell. Figure 5.1 shows the sample probe and the ICR inlet arm. The TRIAC controller is turned on and adjusted until the desired pressure of glycerol is achieved.

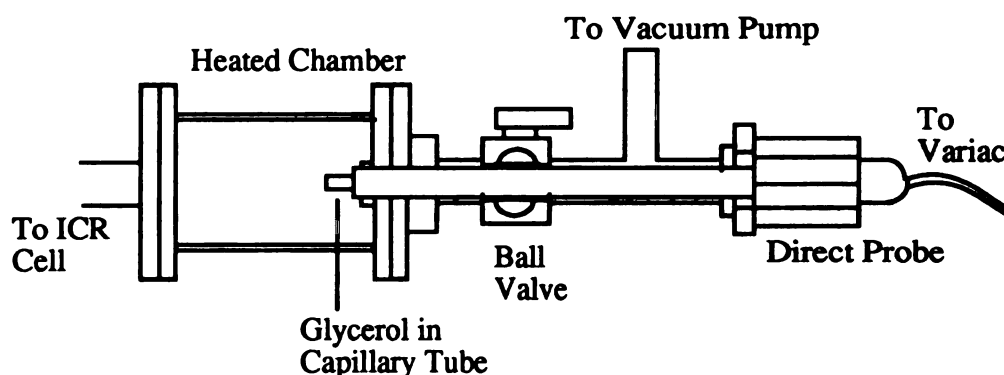


**Figure 5.1: The Sample Inlet to the ICR**

The filament is turned on and the ionizing current begins to flow. The magnet is scanned to the  $m/z$  value of one of the more intense ions and the plate voltages are adjusted to give a large peak height. The filament voltage varies from -50 to -70 volts for positive ions and is adjusted so as to yield the greatest number of ions. The amplitude of the rf signal of the marginal oscillator is adjusted to as small a value as possible to give the best resolution. The amplitude of the rf signal is typically 50 millivolts.

The magnet is set to the starting field strength (normally 0.5 or 7.5 kG) and is scanned from low field to high field (ending at 9.5 or 16.5 kG). A typical scan rate is 1 kG per minute. The ICR mass spectrum is recorded on the chart recorder.

The higher mass ions above 220 Daltons are detected by reducing the frequency of the marginal oscillator from its normal value of 138 kilo Hertz to approximately 100 kilo Hertz. The resolution of the ICR degrades so that unit resolution for ions with  $m/z$  values greater than 300 Daltons is not always possible.

To perform a double resonance experiment the magnetic field is first set to the value corresponding to the product ion being investigated. The sweep controls of the magnet are turned off and the % sweep dial is turned to its highest setting. The CFG 250 is tuned on with normal settings of 450 millivolts and 1 mega Hertz for the rf voltage. After the frequency ratio of the rf voltage from the CFG 250 vs. the rf voltage of the marginal oscillator is measured by the DC 503, the frequency ratio is adjusted to a starting ratio of 0.18. Then the double resonance scan is started. The frequency ratio of the rf voltages of the CFG 250 and the marginal oscillator typically varies between 0.18 and 0.90. The precursor ions that have  $m/z$  values between 18% and 90% of the product ion's  $m/z$  value are detected. When a precursor ion is ejected by the double resonance rf voltage the intensity of the product ion is reduced creating a downward spike on the plot. The starting frequency ratio can be reduced to values as low as 0.10 if needed.

## Negative Ion Spectra

The negative ions of glycerol were formed by resonant and dissociative electron capture. The electrons were emitted by the hot rhenium filament and accelerated by a 1.00 to 8.00 volt difference between the filament voltage and the trapping plate voltages. The voltages of the trapping plates were negative to prevent the negative ions formed from being neutralized. The voltages of the drift plates were adjusted to drift the negative ions to the analyzer region.

At the low acceleration voltages used the electron beam is difficult to control. In the normal negative ion spectra the filament current is set to a constant value. The low

energy electrons are either captured by the glycerol or spread out, hitting the trapping plates. The electron current detected is normally less than 1 nanoamp. All of the other tuning, spectra collection and double resonance experiments are the same as for the positive ions.